REPORT DOCUMENTATION PAGE

Public reporting burden for this collection of information is estimated to average 1 hour per response, including the time for r̶   · $\mathit{0073}$ ·   ̶aintaining the data needed, and completing and reviewing this collection of information. Send comments regarding this burden es̶ma   ·   tions for reducing this burden to Washington Headquarters Services, Directorate for Information Operations and Reports, 1215 Jeffe̶   Office of Management and Budget, Paperwork Reduction Project (0704-0188), Washington, DC 20503

1. AGENCY USE ONLY (Leave blank)	2. REPORT DATE 2-28-00	3. REPORT TYPE AND DATES COVERED Final Report for grant period 9-1-96 to 8-31-99

4. TITLE AND SUBTITLE	5. FUNDING NUMBERS
Lithium Borides - High Energy Materials	AFOSR F49620-91-1-0450

6. AUTHOR(S)
Koop Lammertsma and Tracy P. Hamilton

7. PERFORMING ORGANIZATION NAME(S) AND ADDRESS(ES)	8. PERFORMING ORGANIZATION REPORT NUMBER
Department of Chemistry University of Alabama at Birmingham Birmingham, AL 35294-1240	

9. SPONSORING / MONITORING AGENCY NAME(S) AND ADDRESS(ES)	10. SPONSORING / MONITORING AGENCY REPORT NUMBER
Michael R. Berman AFOSR/NL 801 N. Randolph St., Rm. 732 Arlington VA 22203-1977	

11. SUPPLEMENTARY NOTES
Appendices A-D are reproduced by permission of the American Chemical Society

12a. DISTRIBUTION / AVAILABILITY STATEMENT **DISTRIBUTION STATEMENT A** Approved for Public Release Distribution Unlimited	12b. DISTRIBUTION CODE

13. ABSTRACT (Maximum 200 Words)

A theoretical research investigation of materials that are potential additives for solid hydrogen rocket fuels is investigated. The ab initio calculations show that mixed clusters of boron and lithium prefer to have an electronegative boron atom at the middle, surrounded by positively charged lithiums. The bonding is ionic, and not very directional. There is extensive bridging by the lithium atoms to form nonclassical structures. Upon replacement of boron by aluminum, the clusters are more metallic and quite different. The aluminum stays at the edge of the cluster, more segregated. A great deal of energy will be lost if mixed boron-lithium clusters are formed (relative to the energy of pure lithium clusters), up to around 6 or 7 lithiums. After that, the boron atom is saturated and further lithium addition has the same aggregation energy as pure lithium clusters.

14. SUBJECT TERMS Boron, lithium, clusters, potential energy surface, electron density analysis, HEDM, propellant, nitro compounds	15. NUMBER OF PAGES
	16. PRICE CODE

17. SECURITY CLASSIFICATION OF REPORT Unclassified	18. SECURITY CLASSIFICATION OF THIS PAGE Unclassified	19. SECURITY CLASSIFICATION OF ABSTRACT Unclassified	20. LIMITATION OF ABSTRACT

NSN 7540-01-280-5500

Standard Form 298 (Rev. 2-89)
Prescribed by ANSI Std. Z39-18
298-102

2000324048

Lithium Borides – High Energy Materials

AFOSR F49620-96-1-0450

Program Director: Dr. Michael R. Berman

Final Report:

prepared February 28, 2000

by

Tracy P. Hamilton
Department of Chemistry
University of Alabama at Birmingham

TABLE OF CONTENTS

20000324 048

Lithium Borides – High Energy Materials
AFOSR F49620-96-1-0450

Koop Lammertsma and Tracy P. Hamilton,
Department of Chemistry, University of Alabama at Birmingham

Final Report

Summary

Our research concentrated on ab initio studies of small lithium boride clusters. These have been proposed as additives to boost the I_{sp} of solid hydrogen fuel.[1] They also help to understand the behavior of Li-B alloys.[2] Characterization of the structural properties and stabilities were the main target. In this effort we determined global and local minima, computed harmonic vibrational frequencies, analyzed electron densities, explored structural flexibility, calculated binding energies and atomization energies, and investigated (dis)aggregation trends. Hydrogenation energies were investigated for B_2Li. Other subjects of interest to the Air Force were investigated as opportunity arose, as mentioned below. References are included in the topics which are not yet published.

During the first year efforts concentrated on ab initio studies of the smallest lithium borides to establish a common level of theory by which larger clusters can be studied. To that end we studied in great detail BLi, BLi_2, and BLi_3. We then moved on the larger clusters still containing a single boron atom. To examine the issues that arose when a second boron atom was introduced (would the boron atoms prefer to bond to each other?) we again examined the series with "normal" valence (B_2Li_n, with n=1-4) and then the hypervalent series. By analogy, the analogues where aluminum replaced boron (to give a more metallic cluster) were investigated. The effect was considerably different, with the Al atom(s) not being centrally located. This series was expanded to clusters involving two boron or aluminum atoms in the final year.

Computations were also performed on the diatomic systems formed by all possible combinations of an alkali atom (Li, Na, K) with one of the coinage metal atoms (Cu, Ag, Au). This was in support of experimental work supported by the AFOSR by Michael Duncan at the University of Georgia.[3] A visiting scientist in the third year worked on a proposed chemical mechanism for the initiation of explosions in nitroaromatic compounds, and area of obvious interest to the military. The

mechanism that was investigated was a unimolecular H atom transfer from the (methyl, amino, hydroxyl) group in an *ortho* nitrated toluene (or aniline, or phenol) to form a nitronic acid that then undergoes bond cleavage to form radicals.[4] Finally, after a rather indirect route from 3 membered boron and aluminum rings, we were involved in a collaborative project which examined whether a sandwich compound with 3 membered rings and a "filling" (which included boron and aluminum cations as choices) was feasible. This may be the most important paper (from a fundamental chemistry standpoint) derived from our work, as it predicts that this unique class of compounds is feasible.

Results.

Calculations on BLi, BLi$_2$, and BLi$_3$. Structures and energies for BLi_n (n = 1-3) were investigated with various basis sets and with different levels of theory, including single and multi-reference based correlated methods up to QCISD(T)/6-311+G(3df)//MP2(full)/6-311+G(d), MCQDPT2/6-311+G(2df)// CASSCF/6-31G(d), G2, and G2(MP2) theory. Exhaustive search was possible due to the small size of the system. BLi ($^3\Pi_g$), BLi$_2$ ($^2B_2$) and BLi$_3$ (C_{2v}) are global minima with respective atomization energies of ca. 26, 55, and 95 kcal/mol. This indicates that there will be a large energy loss if boron and lithium form clusters. The energy loss due to boron is a large part of this, as the lithium-lithium interactions are much weaker. To lose a B atom from BLi$_3$ requires an input of 72 kcal/mol, which is close to the sum total of the binding energy (95 kcal/mol)! The structures are not strongly influenced by the size of the basis set nor by the method of electron correlation employed. Energetics for low-lying excited states of BLi and BLi$_2$ were determined. We found that dissociation energies obtained with B3LYP/6-31G(d) theory are in excellent agreement with those obtained with the highest levels of theory. This fact about B3LYP was very useful for the investigation of larger clusters. Of particular concern, even in the smaller clusters, was the high levels of spin contamination present in this study and in the one that followed.

A manuscript describing this work published (K. A. Nguyen and K. Lammertsma, *Structures, bonding, and stability of small boron-lithium clusters*, **J. Phys. Chem. A 1998**, *102*, 1608).

Calculations on BLi$_4$, BLi$_5$, BLi$_6$, BLi$_7$, and BLi$_8$. A full screening of these BLi_n (n = 4-8) systems was conducted. Structures and energetics of BLi_n (n = 4-8) clusters were predicted using

the SCF, MP2, and B3LYP methods with the 6-31G(d) basis set, with final energy evaluations at G2MP2.

For BLi$_4$ we investigated the D$_{4h}$ (^{2}A$_{2u}$), C$_{4v}$ (^{2}A$_1$), and D$_{2h}$ (^{2}B$_2$) forms, for BLi$_5$ the C$_{4v}$ (^{1}A$_1$), D$_{3h}$ (^{1}A$_1$), and C$_{2v}$ (^{1}A$_1$) isomers, for BLi$_6$ the O$_h$ (^{2}A$_{1g}$) structure, for BLi$_7$ the D$_{5h}$ (^{1}A$_1$), C$_{3v}$ (^{1}A$_{1g}$), and C$_{3v}$ (^{1}A$_{1g}$) isomers, and for BLi$_8$ the D$_{4h}$ (^{2}A$_{2u}$), D$_{3h}$ (^{2}A$_{1g}$), and C$_i$ (^{2}A$_g$) structures.

The most stable forms are BLi$_4$ (D$_{2d}$,), BLi$_5$ (C$_{4v}$), BLi$_6$ (O$_h$), BLi$_7$ (D$_{5h}$), and BLi$_8$ (D$_{5h}$). Cohesive energies, defined as the enthalpies of the BLi$_n$ → B + Li$_n$ reactions, and Li and Li$_2$ elimination reaction enthalpies were also estimated at G2MP2. This level of theory predicts the boron cohesive energy to increase up to the BLi$_6$ cluster after which it levels off. This is not a firm boundary, as some levels of theory said that the maximum was at 5 or 7 lithiums around a central boron atom. All BLi$_n$ systems are thermodynamically stable with respect to Li and Li$_2$ dissociations; BLi$_4$ has the largest reaction enthalpies, which means that it has more attraction for lithium since it is less saturated. After the boron has 6 or 7 lithium atoms around it, further Li atom addition only increases the binding energy of the cluster by roughly 10-20 kcal/mol, much the same as in pure lithium clusters. Energetics of the hyperlithiated borides obtained with B3LYP/6-31G(d) are in reasonable agreement with those at G2MP2 but less satisfactory than those of the smaller BLi$_n$ (n =1-3) systems.

We investigated BLi$_4$ in more detail with MCSCF and with QDPT2/MCSCF for the C$_{2v}$ (^{2}A$_1$), D$_{4h}$ (^{2}A$_{2u}$), C$_{4v}$ (^{2}A$_1$), and D$_{2h}$ (^{2}B$_2$) forms. We note that BLi$_4$ was particularly difficult to calculate accurately due to both the flatness of its potential energy surface, and complications due to spin contamination, which indicated the need for multi-reference wavefunctions. However, this further substantiated the reliability of B3LYP for these clusters.

This work was published in K. A. Nguyen, G. N. Srinivas, T.P. Hamilton, and K. Lammertsma, *Stability of hyperlithiated borides,* **J. Phys. Chem. A 1999, 103, 700.**

Calculations on B$_2$Li, B$_2$Li$_2$, B$_2$Li$_3$, B$_2$Li$_4$, and B$_2$Li$_5$. A full screening of these B$_2$Li$_n$ (n = 1-6) systems was conducted. Structures and energetics of B$_2$Li$_n$ (n = 1-4) clusters were predicted using the SCF, MP2, and B3LYP methods with the 6-31G(d) basis set, with final energy evaluations at G2MP2.

For B_2Li we investigated the C_{2v} ($^2B_1$) and C_{2v} ($^2A_1$) forms, for B_2Li_2 (including our earlier work and that of Dr. Jerry Boatz) the C_{2v} ($^1A_1$ and $^3B_2$), D_{2h} (^1A_g and $^3B_{1u}$), and $D_{\infty h}$ ($^1\Pi_u$ and $^3\Sigma g$) forms, for B_2Li_3 the D_{3h} ($^2A'$), C_s ($^2A'$), C_{2v} ($^2A_1$ and $^2B_1$) and $D_{\infty h}$ ($^2\Pi_u$) forms, for B_2Li_4 the D_{4h}, C_{3v}, C_{2v}, D_{2h}, and C_s structures. For B_2Li_5 four C_s isomers were identified. All structures were characterized by obtaining their Hessian indices. Cohesive energies, defined as the enthalpies of the $B_2Li_n \rightarrow B_2 + Li_n$ reactions, and Li and Li_2 elimination reaction enthalpies were also estimated up to G2MP2.

This investigation of B_2Li_n clusters was very tedious due to the unconventional bonding features and the many electronic states to be considered. The problems with spin contamination were so severe for B_2Li_5 that we decided not to publish a manuscript because of the unreliability of the results.

The major conclusion was that the 2 boron atoms definitely prefer to form a true covalent single bond, and then obtain further electron density from coordinated lithium atoms. The lithium atoms prefer to coordinate as bridging around the central B-B bond, although having a lithium with an interaction with a single boron (what we sometimes call a terminal lithium atom). This is clear from Figure 1 in the paper on the normal valent series: G. N. Srinivas, J. Boatz, T. P. Hamilton, K. Lammertsma, *Theoretical Studies on B_2Li_4 (n = 1-4)*, **J. Phys. Chem. A 1999**, 103, 9931 (in the Appendix). It is also clear in the larger B_2Li_6 cluster which we next present results for.

Calculations on B_2Li_6. We explored the B_2Li_6 potential surface to determine the influence of the B_2 dimer on the Li_6 clusters and to evaluate the B-Li versus Li-Li interactions. For B_2Li_6 four C_s, one C_{2h}, and one C_2 symm. equilibrium structures were located on the potential energy surface. None of the structures follows conventional bonding rules. Consequently, their characterization is a very tedious process. However, a few rules are beginning to come out of these studies, referring to the figures on the Pages 6 and 7. Firstly, the B-B forms a strong bond, and is in the middle. Second, the most stable clusters of formula B_2Li_n are made from adding a Li atom to a B_2Li_{n-1} cluster. There are even units identifiable from even smaller B_2Li_n clusters. For example, 3a-3d have a B_2 with 4 lithiums bridging or 3 lithiums bridging and one terminal, as seen for B_2Li_4. The extra Li atom adds either as a bridge to the B-B (up to 4 of them) or as a terminal Li atom or as a cap to a Li_3 unit (as the central B-B gets saturated). If a terminal lithium has an opportunity to bend a little so that it caps a
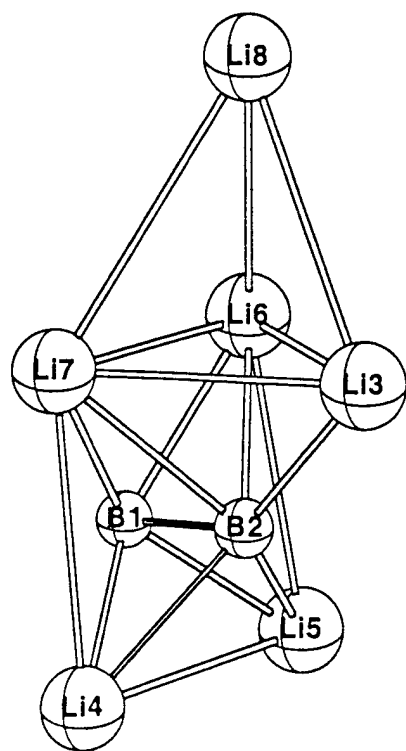
3a C_s
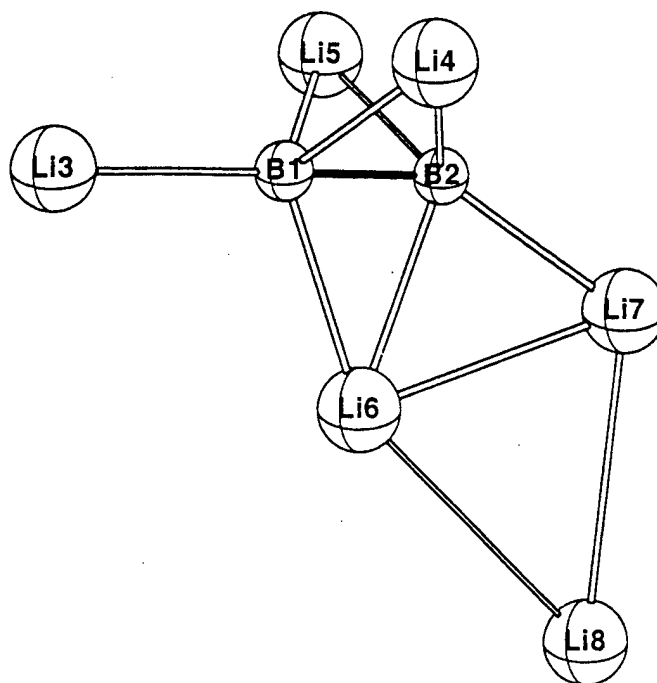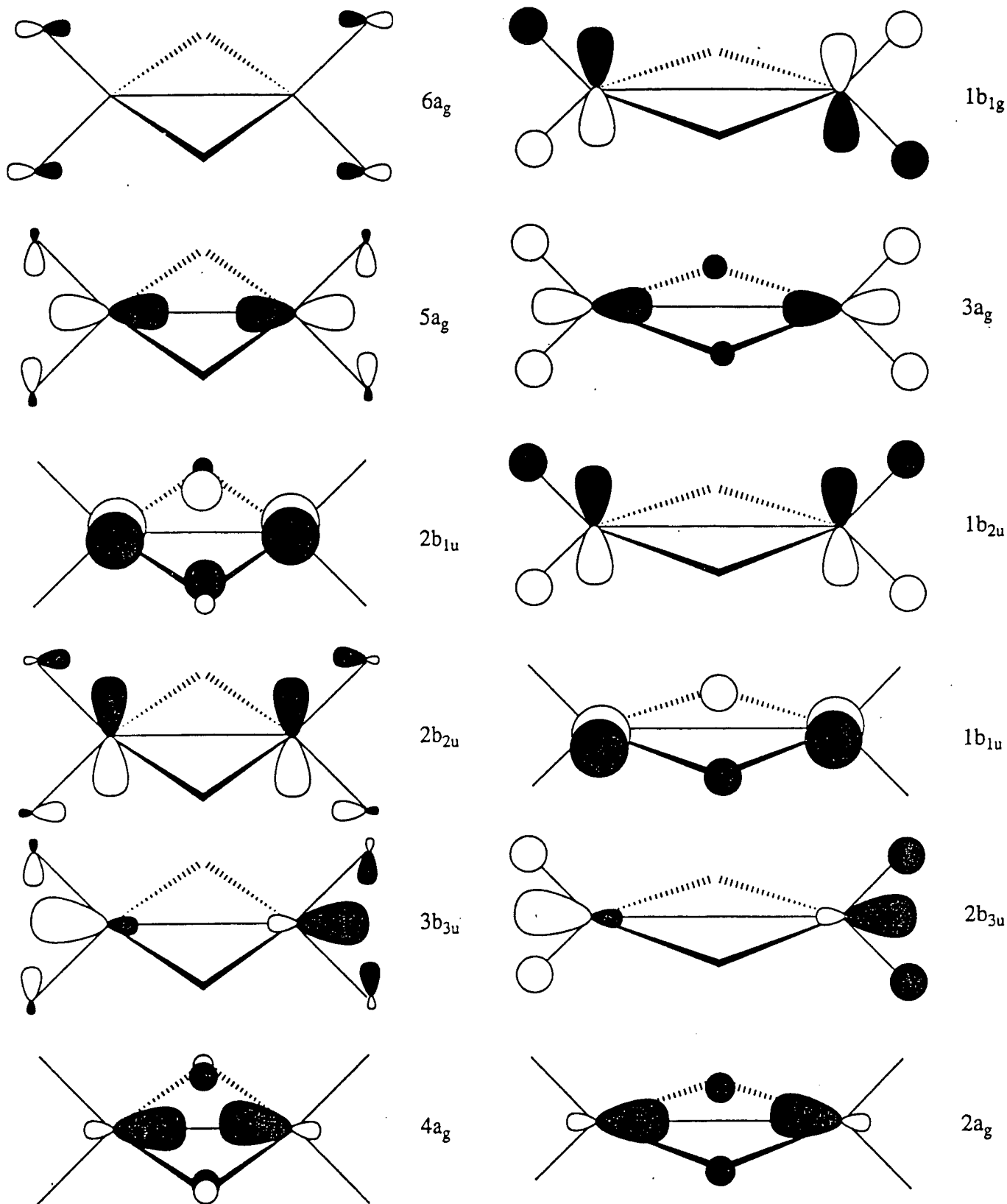
3b C_s
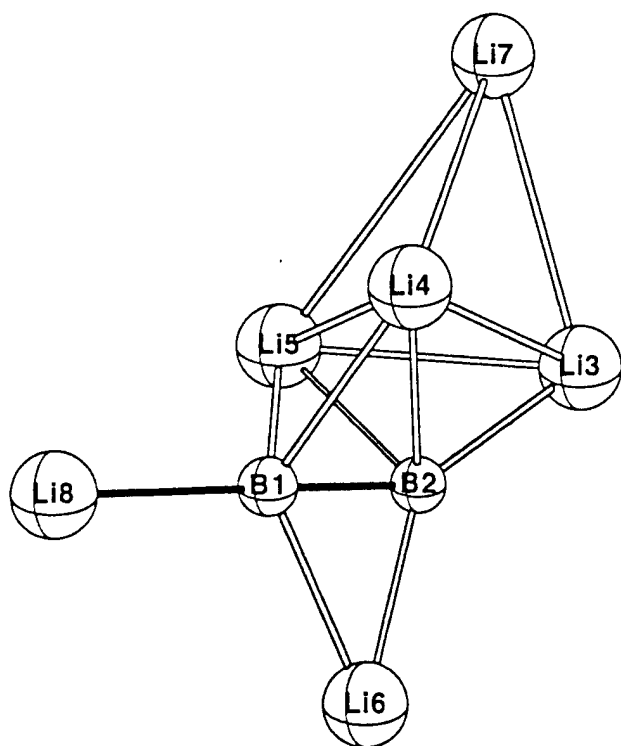
3c C_s
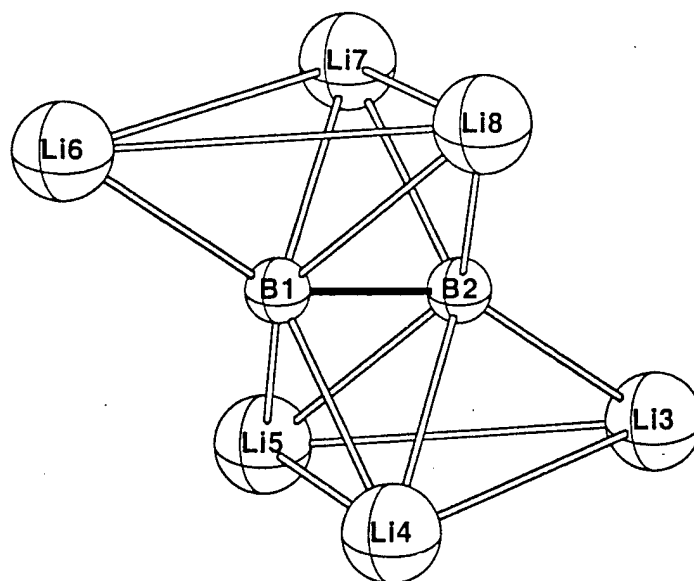
3d C_{2h}
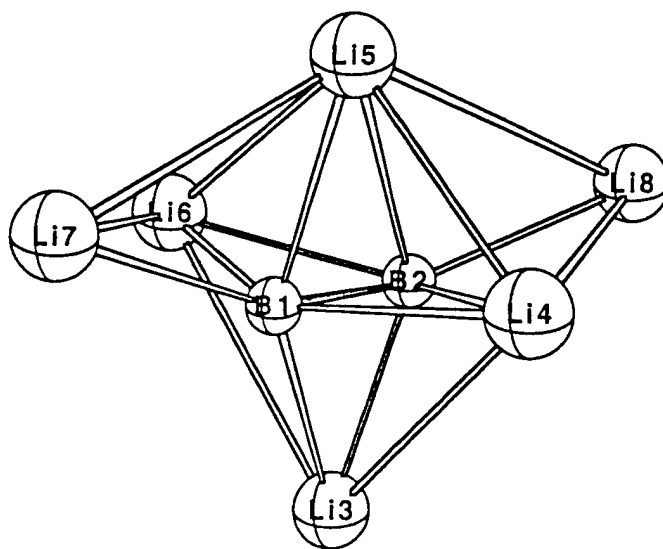
3e C_2
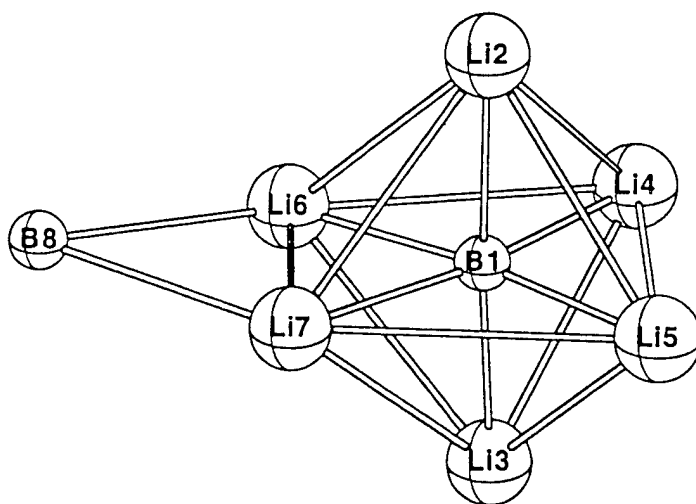
3f C_s

Schematic diagram representing the valence occupied MOs for B_2Li_6 (left side) and B_2H_6 (right side). The MOs $6a_g$ and $1b_{1g}$ are the HOMO of B_2Li_6 and B_2H_6 respectively.

triangular unit with the B as one of the vertices, it will do so. Surprisingly, one can get no more lithium atoms around B_2 than around a single B - six seems to be the maximum again, and that structure is 10 kcal/mol higher in energy than 3 other isomers! The energies of the first 3 structures are very close, and none of them has all of the Li atoms attached to B!

The structure evaluations, including the determination of vibrational frequencies, were conducted at the HF, MP2, and B3LYP levels of theory using the 6-31G* basis set using GAUSSIAN 98.[5]

The figure on Page 8 shows why the B_2Li_6 cluster does not have a diborane isomer - there is no terminal B-Li bonding. Other structures which emphasize increased electron density on the two borons and energy stabilization from arranging positively charged Li atoms around them are energetically favored.

A paper on B_2Li_6 has been submitted to **Chemical Physics Letters**.

Calculations on B_2LiH and B_2LiH_2. A complete screening of two B_2LiH_n (n = 1,2) systems was conducted. Their structures are on the following two pages, with the relative energies in kcal/mol on the figures. Structures and energetics of B_2LiH and B_2LiH_2 were predicted using the SCF, MP2, CBS-Q, and B3LYP methods with the 6-31G(d) basis set, with final energy evaluations at G2MP2. For a more thorough analysis of the various electronic states we employed the MCSCF method, which was augmented with single point QDPT2 calculations, using GAMESS.[6] Enthalpies of hydrogenation of B_2Li are also provided. For B_2LiH we investigated the (two) $C_{\infty v}$ ($^1\Sigma$ and $^3\Sigma$), C_s ($^1A'$ and $^3A''$), and C_{2v} ($^1A_1$ and $^3B_1$) forms, and for B_2LiH_2 five C_{2v} ($^2A_1$), two C_s ($^2A'$ and $^2A''$), and one $D_{\infty h}$ isomer. Calculation of 'proper' electronic states proved to be extremely tedious because of symmetry breaking. The tabulated data is in the Appendix.

The data indicates a slight preference of lithium over hydrogen if there is bridging in the system. The hydrogen would rather form a true sigma bond to boron. Of course, as more hydrogens are added, this will fail to be the case as it approaches its normal valency.

Given the small size of the system, we are currently finishing the search for the transition states so that the kinetics of the process is properly considered. The manuscript will be submitted to **J. Phys. Chem. A**.
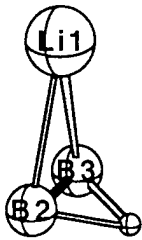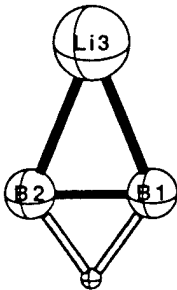
		Relative Energies	
		Triplet	Singlet
$C_{\infty v}$		0.0	20.1
C_s		44.6	28.7
C_{2v} Planar		24.9	32.4
$C_{\infty v}$		83.7	100.5

Figure 1. Optimized structures of B_2LiH molecule and B3LYP/6-31G** Relative Energies.
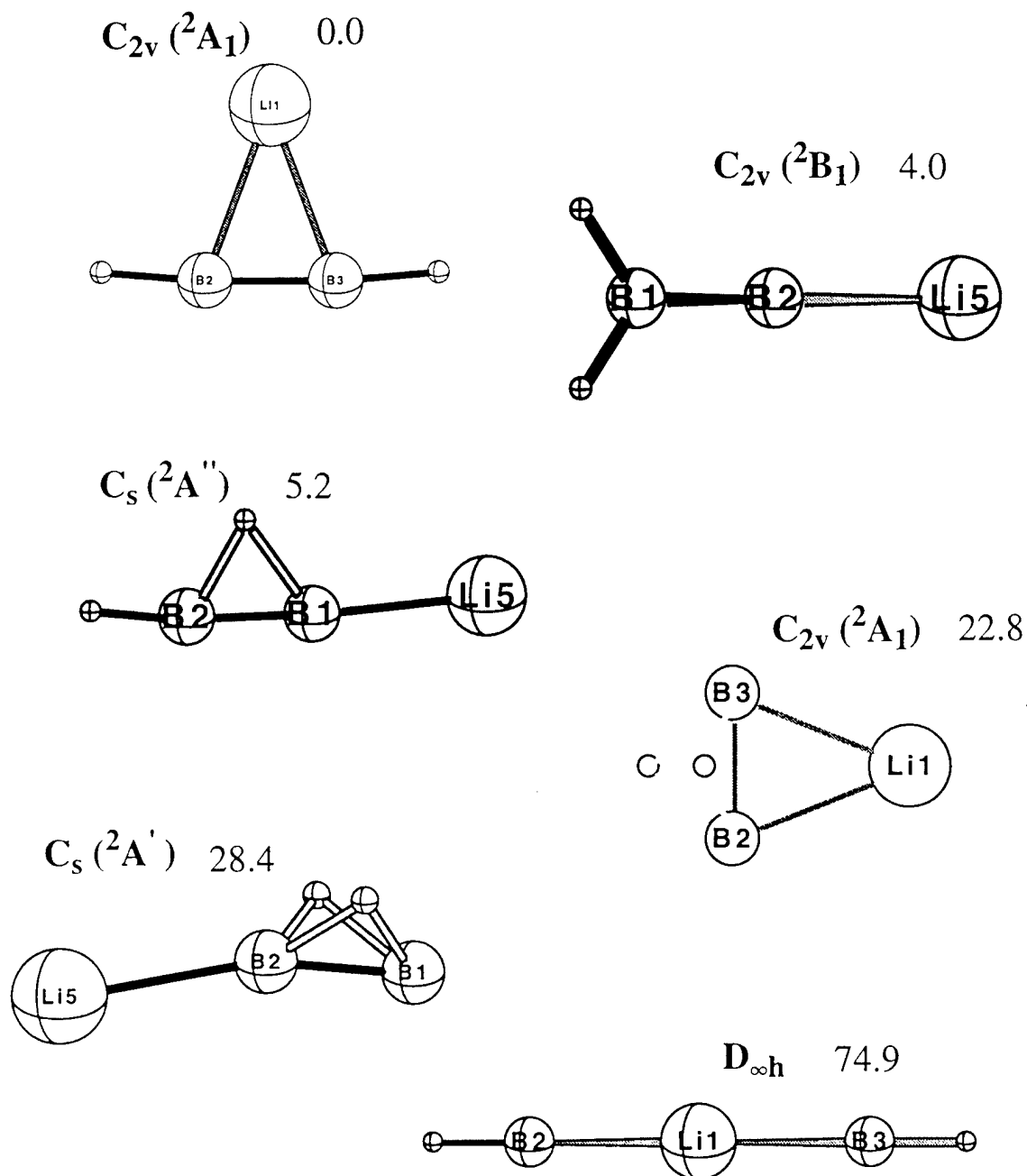
Figure 2. Optimized structure of B_2LiH_2 minima.

Aluminum-Lithium Clusters. A natural thing for a chemist to do is to compare the behavior of two different elements in the same family, to determine commonalities and differences in properties. For this purpose, we decided to examine the lithiated clusters with one Al atom, and to examine Al_2Li_6. It is apparent that the less electronegative element no longer prefers the center of the cluster (see figure on the next page), and that this has the potential of putting more lithiums around it or simply adding more lithium atoms to the side away from aluminum. Work is still in progress on the larger clusters to answer this question. Prior work has looked at clusters up to $AlLi_8$,[7] but these were with the Car-Parinello method,[8] which has terrible energetics because none of the better functionals (without Hartree-Fock exchange) were able to be used. We will use the recent assessment of functionals by Handy's group to determine which functionals to try.[9]

From the enthalpies of reaction in the tables on Page 14, it can be seen that the attraction for aluminum is much less than for boron. This is consistent with the lower electronegativity of Al. Such clusters are more metallic. This lower attraction is also the cause of Al not appearing in the middle of the cluster.

The Al_2Li_6 cluster was investigated to see what the effect of electronegativity differences had on preferences for diborane, completely planar, or other structures. If one takes diborane as the parent, replacing 2 H atoms by Li gives a structure where the bridging hydrogens are relaced and the molecule is **planar**. Since the boron and hydrogen have roughly similar electronegativities, would a closer electronegativity match between Al and Li give a diborane structure? A planar structure as in $B_2Li_2H_4$?[10] The answer is: almost. The figure on Page 15 shows that the geometry where all of the atoms are in one plane is one 2 kcal/mol higher in energy than the minimum. The most stable cluster is _trans_ bent. A profitable way of viewing this cluster is defining a plane containing the six lithiums, and noting that one aluminum caps a very low square based pyramid. A paper on this is still at least 6 months away, but it is being continued as part of Zhi Chen's thesis work. Some of the newer nonhybrid functionals without Hartree-Fock exchange can be incorporated into Car-Parinello codes as part of the research.
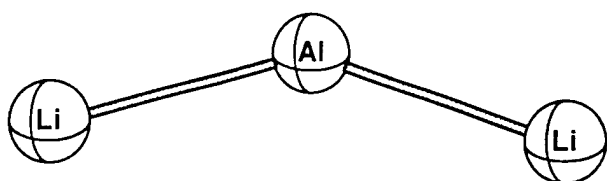
AlLi2-C2v
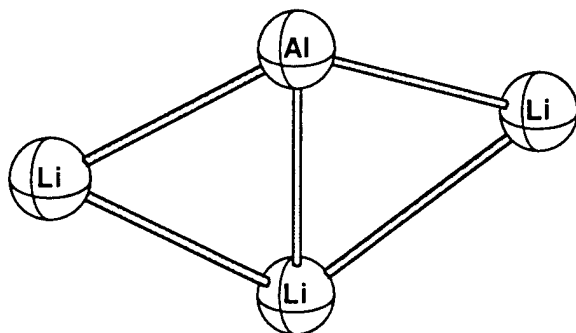
AlLi3-C2v

AlLi-C4v
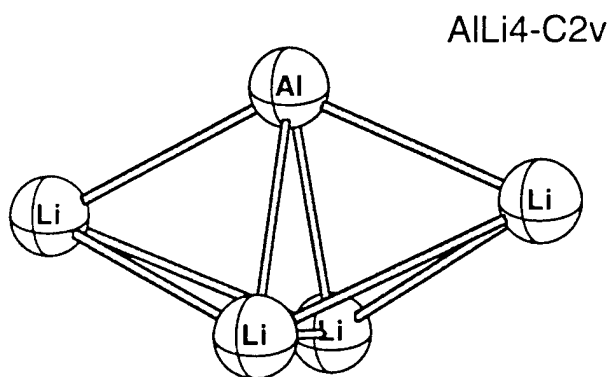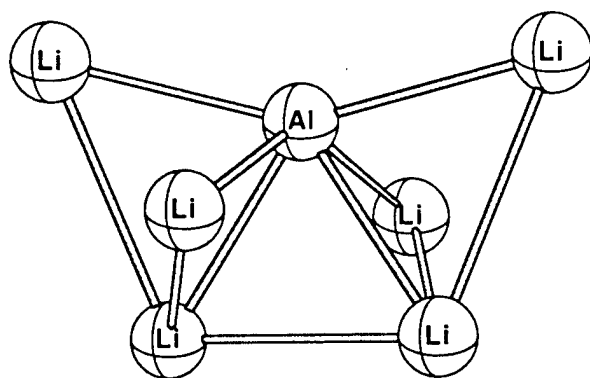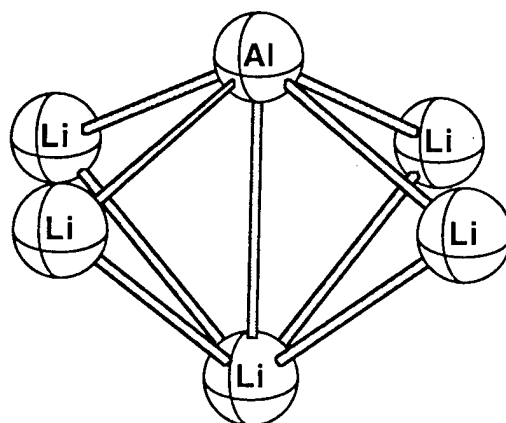
AlLi4-C2v

AlLi6-C2

AlLi$_n$ Energy Minimum Structures

Enthalpies (kcal/mol) of Reaction for $AlLi_n \rightarrow Al + Li_n$

	HF	MP2	B3LYP	
AlLi	1.40	14.6	20.4	
AlLi2-C2v ($^2A_1$)	14.4	20.2	22.8	(36.4)[a]
AlLi3-C2v ($^1A_1$)	15.6	45.1	42.8	(62.0)
AlLi4-C2v ($^2B1$)	38.0	45.9	49.7	(79.9)
AlLi5-C4v ($^1A1$)	27.3	84.9	67.9	(105.0)
AlLi6-**C2** (^2A)	48.2	69.1	62.4	(128.0)

[a] Values in parenthesis are from $BLi_n \rightarrow B + Li_n$ reactions using the same level of theory.

Enthalpies (kcal/mol) of Reaction for $AlLi_n \rightarrow Li + AlLi_{n-1}$

	HF	MP2	B3LYP	
AlLi	1.40	14.6	20.4	
AlLi2-C2v ($^2A_1$)	15.2	19.4	22.1	(28.3)
AlLi3-C2v ($^1A_1$)	10.0	31.4	31.0	(37.0)
AlLi4-C2v ($^2B1$)	26.9	24.0	30.8	(41.5)
AlLi5-C4v ($^1A1$)	10.1	49.4	40.0	(43.1)
AlLi6-**C2** (^2A)	18.3	16.1	20.8	(46.2)

Enthalpies (kcal/mol) of Reaction for $AlLi_n \rightarrow Li_2 + AlLi_{n-2}$

	HF	MP2	B3LYP	
AlLi2-C2v ($^2A_1$)	14.4	20.2	22.8	(36.4)
AlLi3-C2v ($^1A_1$)	23.0	37.1	33.3	(46.0)
AlLi4-C2v ($^2B1$)	34.7	41.6	42.0	(59.1)
AlLi5-C4v ($^1A1$)	34.8	59.6	50.0	(65.2)
AlLi6-**C2** (^2A)	26.2	51.8	37.0	(69.8)

[a] Values in parenthesis are from BLi_n calculation using the same level of theory.

Al$_2$Li$_6$ structures at B3LYP/6-31G(d)

2.631

Al(1)Al(2) : 2.611

Li(7)Al(2)Li(8): 78.74

Angle between Li(6)Al(1)Li(5) and
Al(1)Li(3)Al(2)Li(4) planes is : 136.12

2.637

1 C_i RE=0.0 (0)

2.605

2.590

Al(1)Al(2) : 2.540

2 D_{2h} RE=2.6 (2)

2.675

2.680

Al(1)Al(2) : 2.574
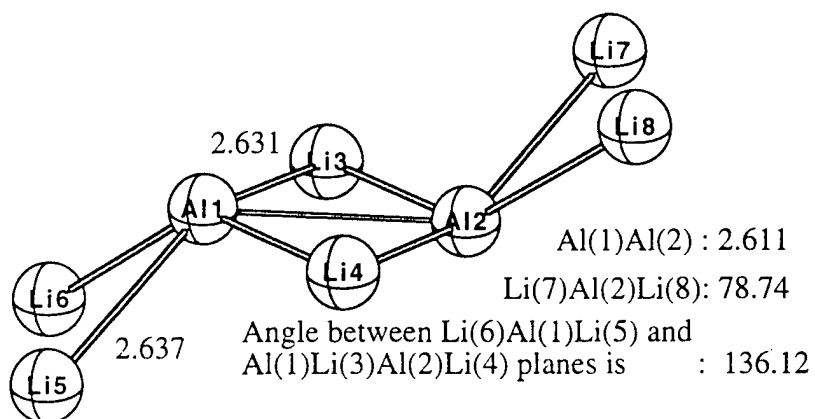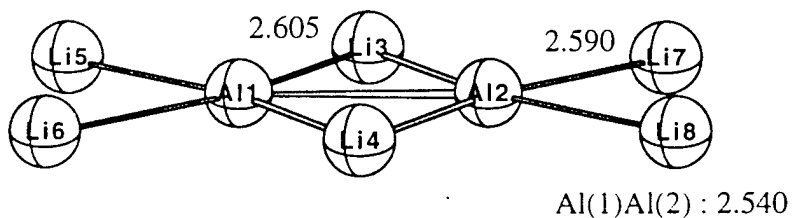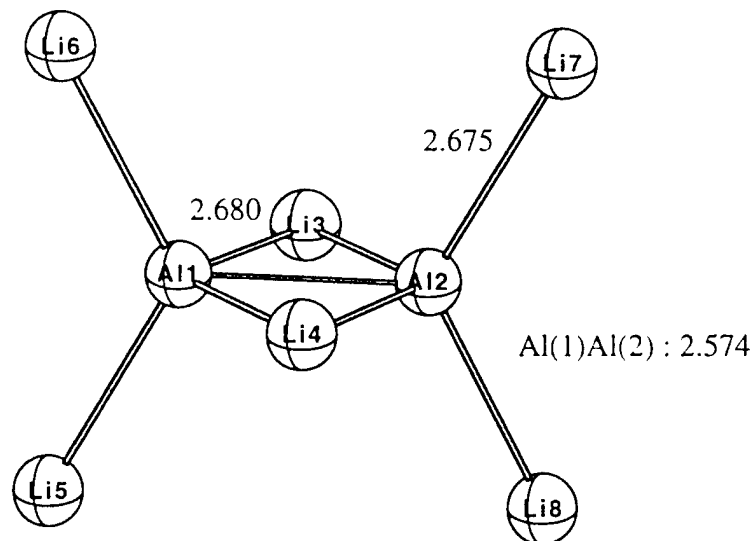
3 D_{2h} RE=19.8 (4)

Alkali Atom - Coinage Metal Diatomics. A diatomic molecule is a small cluster, particularly when both atoms are diatomic. In conversations with Michael A. Duncan at the University of Georgia, we decided to do calculations on systems that Prof. Duncan was performing as part of his AFOSR funded research effort.[3] The ground state potential curve was computed at the SCF, MP2, MCSCF and MCSCF-QDPT2 levels of theory with the effective core potential of Stevens, Basch and Krauss (and Tom Cundari).[11] After a fit to a Morse potential, the theoretical anharmonicity constant was compared to that derived from experimental vibrational progressions. The electronic structure is extremely simple, since there is a single sigma bond formed by overlap of two singly occupied s orbitals. This work will be submitted to **Chem. Phys. Lett.**, after further work is done to make sure that relativistic effects are properly accounted for. This is necessary, as there is uncertainty in the experiments as well. The tabulated data is given in the Appendix.

Agreement between experiment and theory was outstanding for CuLi, there is no experiment for CuNa or CuK. Agreement of theory and experiment for AgLi and AgNa was fair, with theory predicting a shorter bond length (no experimental bond length was reported for AgNa) and higher frequency, yet a lower dissociation energy. We will do some isodesmic reaction computations to determine the theoretical bond dissociation energy more accurately. The experimental AgK number is clearly in error. There is no spectral data reported for AuLi in the literature, and only the dissociation energy of AuNa and AuK. Our theoretical results underestimate the dissociation energy by 15-30% This could be due to the fact that the potential does not fit a Morse potential well.

Some conclusions can be drawn at this point. The dissociation energies of Na-IB is lower than K-IB. The dissociation energies for IA-Ag is lower than for IA-Cu and IA-Au.

Nitro-Aci-nitro Tautomerism. In previous AFOSR funded research, a mechanism for the initiation of explosions in trinitro-toluene (aniline and phenol also) was proposed as coming from H atom transfer to the *ortho* nitro group to form a nitronic acid.[4] Initially, the aromatic ring was modelled by just an ethene, and an exhaustive study was made of many common forms of tautomerism. This is keto-enol, imin-enamine and nitro-aci-nitro tautomerism. 1,5-H atom transfer from the functional group to the nitro group to form the nitronic acid is much easier for 2-nitrovinyl alcohol (5.0 kcal/mol barrier) and 2-nitrovinylamine (13.2 kcal/mol) than for 1-nitropropene (37.8 kcal/mol barrier). Internal hydrogen bonding stabilizes many of the structures. The nitro group stabilizes the ene

structures by 11.4 kcal/mol. relative to the energy difference for the unsubstituted ethene analogues. The ethene study of the more comprehensive picture of tautomerism has been submitted to **J. Org. Chem.** (after receiving favorable reviewers comments on the content of the paper, except for not having a general enough interest).

The nitrated aromatics 2,6-dinitrotoluene, 2,6-dinitroaniline, 2,6-dinitrophenol, 2,4,6-trinitrotoluene, 2,4,6-trinitroaniline, and 2,4,6-trinitrophenol were optimized at the HF/6-31G* and B3LYP/6-31G* levels of theory. Single point energies were computed at the B3LYP/6-311+G** level of theory. The corresponding tautomer from transfer of an H atom from the functional group to the nitro group to form a nitronic acid was also geometry optimized. The transition state for the process was also searched for if the *aci*-nitro tautomer with the H pointing toward the functional group was stable. Figures containing the optimized structures and tables with absolute energies are in the Appendix.

From the figures, it is clear that the *ortho* nitro groups are coplanar with the aromatic ring if they can hydrogen bond with the functional group. Otherwise they twist. The *para* nitro in the trinitro aromatics is coplanar with the ring. The di- and trinitro toluenes have two *ortho* nitro groups twisted, the phenols one, and the anilines zero twisted nitro groups. The aci-nitro tautomers have the H atom pointing away from the functional group. Transition states are very late, meaning that the H atom is nearly completely transferred. This is consistent with the Hammond postulate.[12] The barriers are very close to the endothermic energy difference between the minima for the phenols and anilines. The tautomerization barrier for DNT is very high, at 70 kcal/mol, whereas ΔE is 42 kcal/mol (smaller than ΔE for the anilines!). The order of ΔE is aniline < toluene < phenol, wherease the kinetic barriers follow phenol < aniline < toluene. The tautomerization energies and barriers for the 2,6-dinitro compounds are on Page 18.

The intramolecular hydrogen bonding stabilizes the aromatic compounds, so that they have more energetic stability than they would otherwise. Of course, this is undesirable in an explosive (kinetic stability is desired), and accounts for the pattern of TNA being less powerful than TNT, and TNP in the middle. Additional nitro groups destabilize the compound, making it a more powerful explosive. Isodesmic reactions can be used to factor the energy change from having all of the groups on one aromatic ring compared to many. It is clear from the data in the table on Page 19 that toluene is

Table 6: Isodesmic energies for the removal of all nitro groups. Isodesmic energies are given for the removal of all the nitro groups from the system as in the example equation below. These energies represent the destabilization that results from the presence of the nitro groups on the ring.

2,6 dinitroaniline + 2 Benezene ---> aniline + 2 nitrobenzene
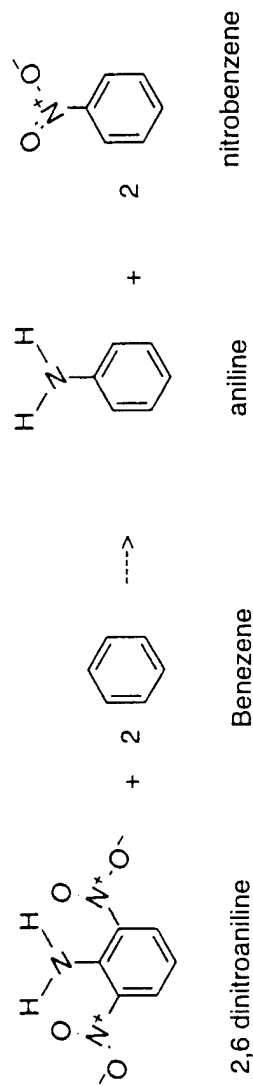
Compound	Isodesmic energy (Hartrees)	Isodesmic Energy (kcal/mol)
o-nitrophenol	0.007049	4.42
o-nitroaniline	0.006464	4.06
o-nitrotoluene	-0.003661	-2.30
2,6-dinitrophenol	-0.009442	-5.92
2,6-dinitroaniline	0.003952	2.48
2,6-dinitrotoluene	-0.015964	-10.02
2,4,6-trinitrophenol	-0.018756	-11.77
2,4,6-trinitroaniline	-0.003150	-1.98
2,4,6-trinitrotoluene	-0.026012	-16.32

Table 3. Tautomerization energies of dinitro systems in kcal/mol

ΔE values	HF/3-21G	HF/6-31G*	B3LYP/6-31G*	B3LYP/6-311+G**
2,6-dinitrophenol	23.50	29.68	26.27	25.71
2,6-dinitroaniline	41.65	46.12	42.62	41.56
2,6-dinitrotoluene	21.48	41.54	35.70	31.01
Tautomerization barriers				
2,6-dinitrophenol	29.00	35.27	31.94	30.26
2,6-dinitroaniline	46.85	50.32	47.24	44.88
2,6-dinitrotoluene	55.71	69.36		

Table 4. Tautomerzation energies of trinitro systems in kcal/mol

ΔE values	HF/3-21G	HF/6-31G*	B3LYP/6-31G*	B3LYP/6-311+G**
2,4,6-trinitrophenol	23.82	29.04	25.45	24.92
2,4,6-trinitroaniline	44.13	47.32	42.67	41.62
2,4,6-trinitrotoluene	20.93	39.83	33.01	29.03

progressively and evenly destabilized by nitro groups. Phenol stabilizes one nitro group through intermolecular hydrogen bonding, with subsequent nitro groups destabilizing the ring. Aniline stabilizes the ring so that even with 2,4,6-TNA the extra energy obtained from having all groups on the same ring is little.

The work dealing with the aromatic systems themselves will be submitted to **J. Am. Chem. Soc.**, given the widespread interest in these well known explosives, and the unknowns about the chemical mechanism behind detonation.

Silicon Sandwich Compounds. $Si_3H_3^+$ has one form that is very much like cyclopropenyl cation, in addition to an isomer that looks much more like a cluster (3 H atoms bridging the 3 Si-Si bonds, all on the same side - this bridging is unique to hydrogen, substituted forms will only be the classical analogue).[13] Ferrocene is a well known sandwich compound which is essentially an iron(II) cation with cyclopentadienyl anion layers. Previous work in the literature has considered the theoretical possibility of cyclopropene as the "bread".[14] This is predicted to be unfeasible, and indeed no compounds of this type have been made. The problem is that the charge transfer is the opposite direction of that required to obtain aromatic character in the rings. What _will_ qualify is a more electropositive ring and electronegative middle. Stabilization is indicated from a qualitative MO analysis, so several structures were investigated, including those that used the nonclassical $Si_3H_3^+$. The central element should have 2 valence electrons (so that it will satisfy the octet rule, the other six electrons coming from 2 η^3 interactions), so Be, Mg, B+, Al+ and C++ were used.

At first the results were discouraging, because the central element inserts into the Si-Si bond to make a 4 membered ring. This was through a transition state that was essentially a form arrived at by rotation of the rings, so expected to have a low barrier. However, with silyl substitution for the H atoms in the model compound to give something that will more closely resemble actual synthons makes the energy differences as small as 10 kcal/mol. This phenomenon is similar to the well known strengthening of pi bonding in disilenes by electropositive substituents.

The manuscript will be published very soon: G. N. Srinivas, T. P. Hamilton, E. D. Jemmis, M. L. McKee and K. Lammertsma, _Will an η^3 - Si_3H_3 Ligand Form Sandwich Compounds with Main Group Elements?_, **J. Am. Chem. Soc.** in press.

Conclusions

The ab initio studies show that mixed boron-lithium clusters are such that if there is a single boron, then lithiums atoms will bond to it quite strongly (up to 6 or possibly 7 Li atoms). The bonding is primarily ionic, with the B atom being quite negatively charged.

If two B atoms are in the cluster, they form a strong bond between them, and the Li atoms are again ionically bound to a very negatively charged core. Up to 4 Li can bridge the B-B bond, and capping of 3 atoms by a Li, or a terminal attachment of Li to a single B is common. Terminal Li atoms will bend up to cap a BLi_2 triangle if possible. The energy of aggregation grows at a slower rate (similar to that of pure Li clusters) once the B atoms are saturated by Li atoms. B_2Li_6 is very unlike diborane, or even the planar $B_2Li_2H_4$ structure.

When aluminum replaces borons in the above types of clusters, they are more metallic and less ionic. The Al is less negatively charged, and does not occupy the center of the cluster. The loss of energy due to aggregation is half that for boron. In Al_2Li_6, the planar structure in a transition state only 2 kcal/mol above a trans bent minimum.

For the alkali - coinage metal diatomics, agreement with experiment for lighter elements is excellent, with disgreement growing for the heavier combinations, particularly IA-Au. There our theoretical results underestimate the dissociation energy by 15-30%. The dissociation energies of Na-IB are lower than K-IB. The dissociation energies for IA-Ag are lower than for IA-Cu and IA-Au.

An exhaustive study was made of many common forms of tautomerism in nitroethenes: keto-enol, imin-enamine and nitro-aci-nitro tautomerism. 1,5-H atom transfer from the functional group to the nitro group to form the nitronic acid has a 5.0 kcal/mol barrier for 2-nitroviny alcohol, 13.2 kcal/mol for 2-nitrovinylamine, and 37.8 kcal/mol for 1-nitropropene.

Studies of nitrated aromatics shows that each nitro group destabilizes the ring, but with results that follow a pattern involving H-bonding with the functional group. The amino group of aniline stabilizes the compound, making it less energetic. Toluene is not able to do this, and pehnol is intermediate. A proposed process for initiation of detonation, H atom transfer from the methyl group in TNT has a very high barrier of 70 kcal/mol and so is unlikely.

Finally, a unique type of sandwich structure has been predicted to be a synthetic target, based on our studies involving $Si_3H_3^+$ rings.

Publications

Papers that have already resulted or are being prepared are:

1. K. A. Nguyen and K. Lammertsma, *Structures, bonding, and stability of small boron-lithium clusters,* **J. Phys. Chem. A 1998,** *102,* 1608.

2. K. A. Nguyen, G. N. Srinivas, T.P. Hamilton, and K. Lammertsma, *Stability of hyperlithiated borides,* **J. Phys. Chem. A 1999,** 103, 700.

3. G. N. Srinivas, J. Boatz, T. P. Hamilton, K. Lammertsma, *Theoretical Studies on B_2Li_4 (n = 1-4),* **J. Phys. Chem. A 1999,** 103, 9931.

4. G. N. Srinivas, T. P. Hamilton, E. D. Jemmis, M. L. McKee and K. Lammertsma, *Will an η^3 - Si_3H_3 Ligand Form Sandwich Compounds with Main Group Elements?,* **J. Am. Chem. Soc.** in press.

5. G. N. Srinivas, Z. Chen, T. P. Hamilton and K. Lammertsma, *A Theoretical Study of B_2Li_6,* **Chem. Phys. Lett.,** submitted.

6. K. Lammertsma and P. V. Bharatam, *Keto - Enol, Imine - Enamine, and Nitro - aci-Nitro Tautomerism and Their Interrelationship in Substituted Nitroethylenes. Keto, Imine, and Vinyl Substituent Effects and the Importance of H-bonding,* **J. Org. Chem.,** submitted.

7. G. N. Srinivas, Z. Chen, T. P. Hamilton, K. Lammertsma, *Theoretical studies of hydrogenation of B_2Li,* **J. Phys. Chem.,** manuscript in preparation.

8. Z. Chen, G. N. Srinivas, T. P. Hamilton and K. Lammertsma, *How Many Lithium Atoms Can Aluminum Coordinate?,* **J. Phys. Chem. A** manuscript in preparation.

9. P. V. Bharatam, H. Hancock, T. P. Hamilton and K. Lammertsma, *Nitro - aci-Nitro Tautomerism in Mono-, Di- and Tri-nitroaromatics: Toluene, Aniline and Phenol.* **J. Am. Chem. Soc.** manuscript in preparation.

10. T. P. Hamilton and C. A. Hixson, *Ab Initio Vibrational Spectra of Alkali-Coinage Metal Diatomics* **Chem. Phys. Lett.** manuscript in preparation.

11. S. A. Davis, J. E. Walker, K. A. Nguyen, and K. Lammertsma, *Ab initio study of the thermal isomerization of tricyclo[3.1.0.0^{2,6}]hexane and bicyclo[2.2.0]hex-2-ene.* **J. Am. Chem. Soc.** in preparation.

The paper on the bicyclobutenes is a collaboration with Prof. S. Davis from the University of Mississippi for which we provided technical expertise. He is responsible for writing up that manuscript. The first 6 papers are included as Appendices, and Data and Tables are included as Appendices for manuscripts 7-10.

Presentations

27th SouthEast Theoretical Chemistry Association (SETCA), Tallahasse, FL, May 28-30, 1998, "Theoretical Studies of Hydrogenation of Boron-Lithium Clusters", Chen, Z., Srinivas, G. N., Hamilton, T. P. (presented by Z. Chen).

13th Canadian Symposium on Theoretical Chemistry, Vancouver, CANADA, Aug. 2-7, 1998, "Theoretical Studies of Boron-Lithium Clusters", G. N. Srinivas, T. P. Hamilton and K. Lammertsma (presented by G. N. Srinivas).

7th Current Trends in Computational Chemistry (CTCC), Vicksburg, MS, Nov. 6-7, 1998, "Ab Initio Studies of Hydrogenation of B_2Li", Z. Chen, G. Naga Srinivas, Koop Lammertsma and Tracy P. Hamilton (presented by Z. Chen).

7th CTCC, Vicksburg, MS, Nov. 6-7, 1998, "Sandwich Compounds $(Si_3H_3)X(Si_3H_3)$, (X=Be, Mg, B+ and Al+)", G. Naga Srinivas, Tracy P. Hamilton, Eluvithingal D. Jemmis, Mike McKee and Koop Lammertsma (presented by G. N. Srinivas).

76th Alabama Academy of Science (AAS) Meeting, Athens, AL, Mar. 24-27, 1999, "Silicon and Carbon - Are They Kissing Cousins?", G. Naga Srinivas, Tracy P. Hamilton, Eluvithingal D. Jemmis, Mike McKee and Koop Lammertsma (presented by G. N. Srinivas).

76th AAS Meeting, Athens, AL, Mar. 24-27, 1999, " How many Lithium Atoms can Aluminum Coordinate?" Z. Chen, G. Naga Srinivas, Koop Lammertsma and Tracy P. Hamilton (presented by Z. Chen).

28th SETCA, Memphis, TN, Apr. 23-24, 1999, "Pyramidal and Sandwich Structures with Si_3H_3+ Ligands", G. Naga Srinivas, Tracy P. Hamilton, Eluvithingal D. Jemmis, Mike McKee and Koop Lammertsma (presented by T. P. Hamilton).

28th SETCA, Memphis, TN, Apr. 23-24, 1999, " How many Lithium Atoms can Aluminum Coordinate?" Z. Chen, G. Naga Srinivas, Koop Lammertsma and Tracy P. Hamilton (presented by Z. Chen).

5th World Congress of Theoretically Oriented Chemists (WATOC), London, UK, Aug 1-Aug 6, 1999, "Theoretical Studies on Boron-Lithium and Aluminum-Lithium Clusters". Gantasala N. Srinivas, Tracy P. Hamilton and Koop Lammertsma (presented by T. P. Hamilton).

5th WATOC, London, UK, Aug 1-Aug 6, 1999, "Ab Initio Vibrational Spectra of Alkali-Coinage Metal Diatomics". Tracy P. Hamilton and Christoper A. Hixson (presented by T. P. Hamilton).

51st ACS Southeast Regional Meeting, Knoxville, TN, Oct. 17-Oct. 20, 1999,"Ab Initio Studies of Mixed Metal Clusters Containing IA Atoms and atoms from Group IB or IIIA. T. P. Hamilton, K. Lammertsma, G. N. Srinivas, Z. Chen, C. A. Hixson. (invited talk by T. P. Hamilton).

Personnel and Facilities

The postdoctoral fellows and graduate student involved in this research project were:

Dr. Kiet A. Nguyen, a Gordon graduate and Truhlar postdoc, has left for Wright-Patterson AFB and taken a position as research scientist in November 1997.

Dr. Gantsala Naga Srinivas, from the University of Hyderabad, joined in June 1997 and has taken another postdoctoral position at the University of North Texas as of Sept. 1999.

Prof. Prasad V. Bharatam was a visiting scientist from Guru Nanak Dev University in Amritsar, India for the five month period of April-Aug. 1999.

Mr. Zhi (Mike) Chen, a Ph.D. student at UAB, worked on the project for the last two years of the grant, with Dr. Hamilton.

Four IBM RISC6000 Model 43P-240 (dual processor) workstations, and a PQS-450 Quantum Workstation were purchased to supplement the four IBM model 3BT workstations, obtained with an earlier AFOSR grant (F49620-93-1-0549DEF). This IBM cluster works to full satisfaction. The PQS machine is particularly good at large calculations of difficult to converge jobs.

Prepared by:

Tracy Hamilton

Tracy P. Hamilton
Associate Professor of Chemistry

Attachments: 1) Manuscripts:
  a) *Structures, bonding, and stability of small boron-lithium clusters*
  b) *Stability of hyperlithiated borides*
  c) *Theoretical Studies on B_2Li_4 (n = 1-4)*
  d) *Will an η^3 - Si_3H_3 Ligand Form Sandwich Compounds with Main Group Elements?*
  e) *A Theoretical Study of B_2Li_6*
  f) *Keto - Enol, Imine - Enamine, and Nitro - aci-Nitro Tautomerism and Their Interrelationship in Substituted Nitroethylenes. Keto, Imine, and Vinyl Substituent Effects and the Importance of H-bonding*

 2) Tables and Figures:
  a) *Energies of B_2LiH and B_2LiH_2 (6 pages)*
  b) *Structures of B_2Li_5 (1 Page)*
  c) *Energies of $AlLi_n$ (n=1-6) (4 pages)*
  d) *Bond lengths and frequencies for IA-IB Diatomics (5 pages)*
  e) *Structures and Energies for Nitrated Aromatics (6 pages)*

References

1. a) J.A. Sheehy, "*Spectroscopy of Lithium Boride, a Candidate HEDM Species*", Proceeding of the HEDM Program, Woods Hole, MA, 1995. b)

2. a) B. Pihlar, V. Pavlovic, S. Pejovnik, S. Spaic, "*Electrochemical Characterization of Lithium-Boron Alloys*", in: *Practical Lithium Batteries*. Y. Matsuda, C. R. Schlaikjer, Eds. JEC Press Inc, Ohio, 1988. b) A. Meden, J. Mavri, M. Bele, S. Pejovnik, *J. Phys. Chem.* **99** (1995) 4252.

3. a) Brock, L.R.; Pilgrim, J.S.; Duncan, M.A., *Chem. Phys. Lett.* **1994**, *230*, 93. b) Berry, K.R.; Duncan, M.A., *Chem. Phys. Lett.* **1997**, *279*, 44. c) Yeh, C.S.; Robbins, D.L.; Pilgrim, J.S.; Duncan, M.A., *Chem. Phys. Lett.* **1993**, *206*, 509. d) Pilgrim, J.S.; Duncan, M.A., *Chem. Phys. Lett.* **1995**, *232*, 355. e) Brock, L.R.; Knight, A.M.; Reddic, J.E.; Pilgrim, J.S.; Duncan, M.A., *J. Chem. Phys.* **1997**, *106*, 6268. f) Stangassinger, A.; Knight, A.M.; Duncan, M.A., *Chem. Phys. Lett.* **1997**, *266*, 189.

4. P. Politzer, M. J. Seminario, P. R. Bolduc, *Chem. Phys. Lett.* **158** (1989) 463.

5. a)GAUSSIAN 98 , M. J. Frisch, G. W. Trucks, H. B. Schlegel, G. E. Scuseria, M. A. Robb, J. R. Cheeseman, V. G. Zakrzewski, J. A. Montgomery, R. E. Stratmann, J. C. Burant, S. Dapprich, J. M. Millam, A. D. Daniels, K. N. Kudin, M. C. Strain, O. Farkas, J. Tomasi, V. Barone, M. Cossi, R. Cammi, B. Mennucci, C. Pomelli, C. Adamo, S. Clifford, J. Ochterski, G. A. Petersson, P. Y. Ayala, Q. Cui, K. Morokuma, D. K. Malik, A. D. Rabuck, K. Raghavachari, J. B. Foresman, J. Cioslowski, J. V. Ortiz, B. B. Stefanov, G. Liu, A. Liashenko, P. Piskorz, I. Komaromi, R. Gomperts, R. L. Martin, D. J. Fox, T. Keith, M. A. Al-Laham, C. Y. Peng, A. Nanayakkara, C. Gonzalez, M. Challacombe, P. M. W. Gill, B. G. Johnson, W. Chen, M. W. Wong, J. L. Andres, M. Head-Gordon, E. S. Replogle and J. A. Pople, Gaussian, Inc., Pittsburgh, PA, 1998   b) GAMESS, "General Atomic and Molecular Electronic Structure System" M.W.Schmidt, K.K.Baldridge, J.A.Boatz, S.T.Elbert, M.S.Gordon, J.H.Jensen, S.Koseki, N.Matsunaga, K.A.Nguyen, S.Su, T.L.Windus, M.Dupuis, J.A.Montgomery, *J. Comput. Chem.* **14**, (1993)1347.

6. a) H.-P. Cheng, R. N. Barnett, U. Landman, *Phys. Rev. B* **48** (1993) 1820. b) C. Majumder, G. P. Das, S. K. Kulshresta, V. Shah, D. G. Kanhere, *Chem. Phys. Lett.* **261** (1996) 515.

7. R. Car, M. Parinello, *Phys. Rev. Lett.* **55** (1985) 685.

8. A. J. Cohen, N. C. Handy, *Chem. Phys. Lett.* **316** (2000) 160.

9. M. Wagner, N. J. R. van Eikema Hommes, H. Noth, P. von R. Schleyer, *Inorg. Chem.* **34** (1995) 607.

10. SBK basis in the GAMESS Program

11. G. S. Hammond, *J. Am. Chem. Soc.* **77** (1955) 334.

12. a) E. D. Jemmis, G. N. Srinivas, *J. Am. Chem. Soc.* **118** (1996) 3738 b) G. N. Srinivas, E. D. Jemmis, *J. Am. Chem. Soc.* **119** (1997) 12968.

13. J. B. Collins, P. v. R. Schleyer, *Inorg. Chem.* **16** (1977) 152.

Structure, Bonding, and Stability of Small Boron—Lithium Clusters

Kiet A. Nguyen[†,§] and Koop Lammertsma*,[†,‡]

*Department of Chemistry, University of Alabama at Birmingham, Chem205, UAB Station,
Birmingham, Alabama 35294-1204, and Department of Chemistry, Vrije Universiteit,
De Boelelaan 1083, 1081 HV Amsterdam, The Netherlands*

Structures and energies for BLi_n ($n = 1–3$) are investigated with various basis sets and with different lev
of theory, including single reference- and multireference-based correlated methods up to QCISD(T)/6-311+
$(3df)//MP2(full)/6-311+G(d)$, MCQDPT2/6-311+G(2df)// CASSCF/6-31G(d), G2, and G2(MP2) theory. E
($^3\Pi_g$), BLi_2 ($^2B_2$), and BLi_3 (C_{2v}) are global minima with respective atomization energies of ~26, 55, and
kcal/mol. Their structures are not strongly influenced by the size of the basis set nor by the method
electron correlation employed. Energetics for low-lying excited states of BLi and BLi_2 were determine
The dissociation energies obtained with B3LYP/6-31G(d) theory are in excellent agreement with those obtain
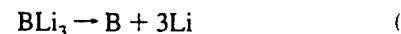with the highest levels of theory.

Introduction

Clusters are of considerable interest in research on materials ranging from ceramics to electronics and because of their impact on phenomena such as chemisorption, catalysis, and crystallization. Theory provides an important means to understand the electronic structures and energetics of clusters, and increasingly contributes toward the development of clusters for practical applications.[1-3] Our attention is focused on binary clusters composed of the elements boron and lithium. Lithium boride has been extensively studied as anode (bulk) material in lithium batteries,[4] whereas its smaller clusters[5-10] are of interest as high-energy additives to cryogenic hydrogen. An understanding of the bonding and energetics of these species is fundamental to the design of fuel additives. We are exploring the properties of the smaller clusters, analogous to the lithium clusters of carbon, oxygen, and sulfur.[11] To investigate such systems by theoretical methods, we found a need to investigate the basic systems because of an apparent lack of comprehensive data. In the present study we therefore report computations on BLi, BLi_2, and BLi_3 at different levels of theory aimed at identifying suitable level(s) of theory for studying larger boron—lithium clusters.

Whereas diatomic lithium boride has already been studied extensively,[4-6,10,12,13] few theoretical studies have addressed larger binary boron—lithium systems.[4,9] We include the diatomic for calibration of BLi_2 and BLi_3. The computed stability of BLi was shown to be rather sensitive to the level of theory employed.[12,13] The first ab initio SCF study by Kaufman and Sachs,[5] and more recently by Meden et al.[4] predicted its $^1\Sigma^+$ state to be unbound, whereas Cade and Huo,[6] using a large Slater basis set, found it to be slightly more stable than the separated atoms. Boldyrev et al.[13] studied BLi at the QCISD(T)/6-311+G(2df)//MP2/6-311+G(d) level and found the ground state to be $^3\Pi_g$ with a binding energy D_e, of 27.2 kcal/mol. The energy differences of $^3\Pi_g$ with the $^1\Sigma^+$ and $^3\Sigma^-$ states were

estimated at 6.4 and 10.9 kcal/mol, respectively. Knowles a Murrell,[8] using MRCI with a moderately large basis set ($10s7p2d/5s5p2d$, Li: $10s4p2d/4s4p2d$), obtained a simi binding energy of 25.5 kcal/mol for the ground state. Recent potential energy curves, spectroscopic constants, and radiati lifetimes of several excited states of the singlet, triplet, a quintet spin states were calculated by Sheehy,[10] using interna contracted MRCI with Dunning's quadruple-ζ basis set, anc D_e of 27.7 kcal/mol for the ground state of BLi was obtaine

The theoretical work on BLi_2 has been limited to UH 6-31G(d) calculations by Meden et al.[4] These authors al examined the electronic structure and stability of BLi_3 and larg BLi_n clusters at SCF/6-31G(d). The most stable BLi_2 structi was predicted to be bent with a B—Li distance of 2.369 Å a a Li—Li distance of 2.510 Å. They reported a planar L structure for BLi_3, with a B—Li distance of 1.836 Å. Earli using CASSCF with a double-ζ basis set, Saxon[9] showed th the D_{3h} and the T-shaped C_{2v} structures of BLi_3 are essentia isoenergetic. However, the planar D_{3h} form has two sm degenerate frequencies at MP2, with imaginary normal moc leading to the C_{2v} isomer.

To shed more light on these small binary clusters and to ass in their gas-phase detection, we examine the structures, energi and thermal stabilities of BLi_n ($n = 1–3$) using ab ini electronic structure theory. To explore their fragmentation, consider all possible dissociation channels (reactions 1–: Enthalpies of reaction for $BLi_n \rightarrow B + Li_n$ reflect the stal lization in the BLi_n clusters due to the boron atom, whereas t thermodynamics for Li and Li_2 elimination is estimated fro the reactions $BLi_n \rightarrow BLi_{n-1} + Li$ and $BLi_n \rightarrow BLi_{n-2}$ Li_2, respectively. Other reactions determine atomization a bond dissociation energies (BDEs), which are useful in estim. ing the stability of clusters of different sizes.

$$BLi_2 \rightarrow B + 2Li \qquad ($$

$$BLi_2 \rightarrow BLi + Li \qquad ($$

$$BLi_2 \rightarrow B + Li_2 \qquad ($$

$$BLi_3 \rightarrow B + 3Li \qquad ($$
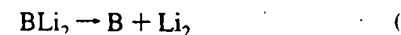
* Author to whom correspondence should be sent to in The Netherlands.
† Department of Chemistry, University of Alabama at Birmingham.
‡ Department of Chemistry, Vrije Universiteit.
§ Current address: Air Force Research Lab, AFAL/MLPJ, Wright
Patterson AFB, OH 45433.

Small Boron–Lithium Clusters

J. Phys. Chem. A, Vol. 102, No. 9, 1998 **1609**

$$BLi_3 \rightarrow BLi_2 + Li \qquad (5)$$

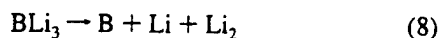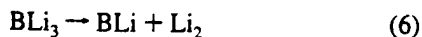$$BLi_3 \rightarrow BLi + Li_2 \qquad (6)$$

$$BLi_3 \rightarrow B + Li_3 \qquad (7)$$

$$BLi_3 \rightarrow B + Li + Li_2 \qquad (8)$$

Our focus is on the ground-state molecules and their adiabatic dissociation channels, but low-lying excited states of BLi and BLi$_2$ are also considered. Because some of these boron–lithium systems possess unusual structures, the atoms in molecules (AIM) one-electron density analysis theory[14-16] is used to address their bonding. The effects of basis set and levels of theory on the structures and energies of these small BLi$_n$ clusters ($n = 1-3$) are evaluated. Because our interest extends to larger clusters, we tested the applicability of the more economical density functional theory (DFT) formulation of Kohn and Sham (KS).[17]

Computational Methods

The structures of all BLi$_n$ isomers are optimized at the Hartree–Fock (HF) Self-Consistent Field (SCF) level,[18,19] Møller–Plesset second-order perturbation theory (MP2),[20,21] and KS theory[17] using the 6-31G(d),[22] 6-311G(d),[23] and 6-311+G-(d)[24] basis sets. Additional sets of d and f functions are used to study the basis set effect further. DFT calculations were carried out using the Becke's three-parameter hybrid functional,[25-27] hereafter referred to as B3LYP. Because BLi$_n$ may have significant configurational mixing and low-lying excited states, requiring a multiconfigurational description, geometries are also evaluated with the Complete Active Space SCF (CASSCF) wave functions.[28]

All structures were verified to be either minima or transition states by evaluation of the force constant matrixes, obtained analytically or from finite differences of the analytically determined gradients. Enthalpies of formation for the single-configurational-based wave functions are reported at G2[29] and G2-(MP2).[30] These methods employ MP2/6-31G(d) optimized geometries. G2 energies are obtained from quadratic configuration interaction (QCISD(T))[31] using the 6-311G(d,p) basis set with various basis set additivity corrections (diffuse and polarization functions) at the frozen core full fourth order perturbation theory (MP4(SDTQ)) and at the MP2 level, an empirical correction, and a 0.8929 scaled SCF/6-31G(d) zero-point vibrational energy (ZPE) correction. The empirical correction of $(-0.19n_\alpha - 4.81n_\beta) \times 10^{-3}$ au is denoted as E(HLC). The G2(MP2) energy expression is simpler. It uses the QCISD(T)/6-311G(d,p) energy with basis set additivity corrections at MP2 and the same empirical and ZPE corrections as for G2. Both expressions are shown later. The G2 and G2-(MP2) methods have been reported to give a mean absolute deviation from 125 experimental energies of 1.21 and 1.58 kcal/mol, respectively[29,30]:

$$E(G2) = E(QCISD(T)/6\text{-}311G(d,p)) +$$
$$E(MP4/6\text{-}311+G(d,p)) - E(MP4/6\text{-}311G(d,p)) +$$
$$E(MP4/6\text{-}311G(2df,p)) - E(MP4/6\text{-}311G(d,p)) +$$
$$E(MP2/6\text{-}311G(3df,2p)) - E(MP2/6\text{-}311G(2df,p)) -$$
$$E(MP2/6\text{-}311+G(d,p)) + E(MP2/6\text{-}311G(d,p)) +$$
$$E(HLC) + E(ZPE) \quad (9)$$

$$E(G2(MP2)) = E(QCISD(T)/6\text{-}311G(d,p)) +$$
$$E(MP2/6\text{-}311+G(3df,2p)) - E(MP2/6\text{-}311G(d,p)) +$$
$$E(HLC) + E(ZPE) \quad (10)$$

Energies for multiconfigurational-based wave functions were obtained by the second-order multiconfigurational quasi-degenerate perturbation theory[32] (MCQDPT2) using CASSCF/6-31G(d) structures. All electronic structure calculations were carried out using the GAUSSIAN 94[33] and GAMESS[34] programs.

Results and Discussion

We investigated the $^3\Pi_g$ and $^1\Sigma^+$ states of BLi, the $^2B_2$ and $^2B_1$ states of BLi$_2$ and the C_{2v} and D_{3h} symmetry forms of BLi$_3$. As part of this investigation, the $^1\Sigma_g$ state of Li$_2$ and the $^2B_2$ and $^2A_1$ states of Li$_3$ are included. Structural parameters, total energies, harmonic vibrational frequencies, and bond critical point data are tabulated for BLi, BLi$_2$, and BLi$_3$, and their fragments Li$_2$ and Li$_3$ (except for critical point data) in Tables 1–8; the total energies for the atomic boron and lithium are included for convenience (Tables 4 and 6). Computer-generated structures of BLi$_3$ and Li$_3$ are displayed in Figure 1. We discuss first the influence of the various theoretical methods on the optimized BLi$_n$ clusters, then some bonding characteristics, and finally their energies.

A. Analysis of Theoretical Methods. The SCF, MP2, QCISD, and B3LYP structures were optimized first with the 6-31G(d) basis set and then with the valence triple-ζ series expanded with different types of polarization and diffuse functions to give the following basis sets: 6-311G(d), 6-311+G-(d), and 6-311+G($2df$). Analysis of the basis set effect on the QCISD and B3LYP geometries was limited to BLi and BLi$_3$ isomers. Only the smaller 6-31G(d) basis set was used for the CASSCF geometry optimizations.

Basis Set Effect. We start with some general observations. Within each selected theoretical method, using different basis sets, changes in geometrical parameters of all systems are <0.05 Å for bond lengths and <1° for bond angles. The exception is the $^2B_2$ state of Li$_3$ for which the largest difference in the Li–Li distance is found to be 0.08 Å at MP2 between the 6-31G-(d) and 6-311+G(d) basis sets; this Li–Li interaction is strongly coupled with a flat Li–Li'-Li bend potential. As we increase from the double to the triple-ζ split valence basis set, all systems show a shortening of bond distances, as expected. However, the effects of additional diffuse and polarization functions on the geometrical parameters are negligible and in some cases nonexistent. Because the basis set effect is small for both the SCF and (single-configurational based) correlated structures, the use of the more economical 6-31G(d) basis set seems adequate for geometry optimizations of larger BLi$_n$ clusters. We note that the SCF-based correlated methods give reasonable geometries and energies (vide infra) for open shell systems even in cases with significant spin contamination.[35]

Electron Correlation. Next, we examine the effects of different electron correlation methods on the geometries. With each of the basis sets considered, the BLi bond lengths at MP2 and B3LYP are slightly shorter, whereas those at QCISD and particularly CASSCF are slightly longer than the SCF bond lengths. However, the various correlated methods give similar optimized structures when the same basis set is used. The most pronounced differences are found for BLi$_3$ (C_{2v}) with differences in BLi bond lengths of -0.04 Å between the SCF and B3LYP methods, of $+0.07$ Å between the SCF and CISD methods, and of $+0.12$ Å between the MP2 and QCISD methods (all with

TABLE 1: Structural Parameters and Total and Relative Energies for BLi Isomers[a]

	BLi ($^3\Pi_g$)			BLi ($^1\Sigma^+$)			
level	energy	B−Li	freq.	energy	B−Li	freq.	ΔE
B3LYP/A	32.19043	2.141	539	32.17774	2.416	425	8.0
B3LYP/B	32.19976	2.128	539	32.18573	2.399	431	8.8
B3LYP/C	32.20061	2.131	538	32.18702	2.398	432	8.5
B3LYP/D	32.20124	2.130	537	32.18742	2.397	430	8.7
(U)HF/A	31.97912	2.143	573	31.94303	2.426	450	22.6
(U)HF/B	31.98993	2.131	570	31.95314	2.403	458	23.1
(U)HF/C	31.99077	2.134	568	31.95496	2.401	459	22.5
MP2(full)/A	32.03079	2.138	564	32.01134	2.426	437	12.2
MP2(full)/B	32.07087	2.126	566	32.04997	2.406	443	13.1
MP2(full)/C	32.07222	2.130	562	32.05213	2.404	445	12.6
QCISD/A	32.04416	2.151	548	32.03603	2.459	392	5.1
QCISD/B	32.06064	2.137	549	32.04927	2.425	409	7.1
QCISD/C	32.06189	2.141	548	32.05089	2.420	414	6.9
CASSCF(4,8)/A	32.02309	2.172	533	32.02433	2.474	348	−0.8

[a] Total energies in −au, relative energies (ΔE) for the two isomers in kcal/mol, bond lengths in Å, and frequencies in cm^{-1}. [b] A: 6-31G-(d), B: 6-311G(d), C: 6-311+G(d), and D: 6-311+G(2df).

the 6-31G(d) basis set). Notable differences are also found for Li$_2$ and Li$_3$; interestingly their CASSCF/6-31G(d) geometries are more compact than the SCF counterparts. For Li$_3$ ($^2A_1$), the largest variation in the Li−Li distance of 0.02 Å between B3LYP/6-31G(d) and CASSCF(3,3)/6-31G(d) can be attributed to the flatness of the Li−Li'-Li bend potential. We note that B3LYP predicts a $^2B_2$ ground state for Li$_3$ and characterizes the $^2A_1$ structure as a saddle point. All other methods identify both structures as minima.

B. Structures and Bonding. The properties of the BLi$_n$ ($n = 1-3$) global minima are discussed with emphasis on bonding, bond lengths, and vibrational frequencies. We use the 'atoms in molecules' topological one-electron density analysis to evaluate the bonding properties. Details of this method have been described elsewhere.[16,18] We concentrate on the properties of critical points where the gradient of the charge density $\rho(\mathbf{r})$ vanishes. Bond critical points are characterized by a Hessian of $\rho(\mathbf{r})$ with one positive eigenvalue along the bond axis and two negative eigenvalues orthogonal to the bond axis. The Laplacian of the electron density at a critical point $\nabla^2\rho(\mathbf{r})$ determines the region in space wherein the electron charge is concentrated or depleted. The $\rho(\mathbf{r})$ and $\nabla^2\rho(\mathbf{r})$ values are summarized in Table 8.

The BLi and BLi$_2$ Structures. The average bond lengths of BLi ($^3\Pi_g$) using all theoretical levels in Table 1 (except that of the CASSCF structure) is 2.135 Å with a standard deviation (σ) of 0.007 Å. The corresponding average harmonic frequency of 554 cm^{-1} ($\sigma = 14$) show BLi to be a well-defined minimum energy structure. The BLi bond critical point is located in close proximity of the Li-nucleus, which reflects the difference in electronegativity between the boron and lithium atoms.

The average bond length of BLi$_2$ ($^2B_2$) of 2.324 Å ($\sigma = 0.014$, Table 2) is longer than that of BLi, and the smallest of its three frequencies of 291 cm^{-1} ($\sigma = 11$) is correspondingly smaller. The difference in these BLi bond lengths (8%) is also reflected in the electron densities of their critical points (Table 8). For example, the MP2/6-31G(d) $\rho(\mathbf{r})$ value of 2.07 × 10^{-2} au for BLi$_2$ is significantly smaller than the 2.90 × 10^{-2} au for BLi. Still, the electron density at all BLi bond critical points is small. Their Laplacian values indicate that the electron density distribution around the bond critical points is rather flat, which suggests that BLi$_2$ is easily deformed from its ideal geometry.

The BLi$_3$ Structure. All levels of theory predict the C_{2v} structure of BLi$_3$ to be a minimum, whereas the D_{3h} isomer is also a minimum at the SCF and CASSCF levels (Table 3). Force

field calculations at the MP2, QCISD, and B3LYP correla levels of theory reveal two small degenerate imaginary frequ cies leading to the C_{2v} structure. These results are in agreeme with the MP2 and CASSCF data reported earlier by Saxo Our CASSCF calculations for BLi$_3$ (D_{3h}) show very lit configurational mixing − all the natural orbital occupati numbers (NOONs) for the bonding and antibonding orbitals close to 2 and 0, respectively (see Figure 2). We next includ the effect of dynamic electron correlation and, because gradie at MCQDPT2/6-31G(d) are not available, the BLi$_3$ potent energy surface was mapped around the CASSCF(6,6) structu to evaluated the $D_{3h} \rightarrow C_{2v}$ relationship. The grid, using points obtained by varying the B−Li distance between 2.0 a 2.4 Å and the Li−B−Li angle between 110° and 130° (s Figure 3), shows that bending the Li−B−Li angle from 12 (D_{3h}) to 130° (with a BLi distance of 2.2 Å) results in an ener gain of 0.15 kcal/mol. Thus, it appears that the shallc minimum obtained at CASSCF(6,6)/6-31G(d) disappears up including the effects of dynamic electron correlation! Only t C_{2v} form of BLi$_3$ is a minimum energy structure.

The average B−Li bond lengths (Table 3, except CASSC are 2.174 Å ($\sigma = 0.023$) and 2.282 Å ($\sigma = 0.047$). The distances are slightly longer than that of diatomic BLi a slightly shorter than that of BLi$_2$. The magnitude of the electr densities at the bond critical points (Table 8) are in line w: these bond length variations. The low values of the electr densities at all levels of theory underscore the high degree structural flexibility for BLi$_3$ (C_{2v}), which is also in line wi the small average value of 109 cm^{-1} ($\sigma = 40$) for its smallc harmonic frequency. From these analyses it appears that bc MP2 and B3LYP/6-31G(d) provide reasonable geometries f the three global minima of BLi$_{1-3}$.

C. Energies. In this section we discuss the relative energic the atomization energies, and the dissociation energies for BI BLi$_2$, and BLi$_3$. Emphasis is placed on the various theoretic methods and basis sets employed. Relative energies are list in Table 5, and the atomization energies for BLi and those f the dissociation reactions 1−8 are given in Table 7. Table also lists Li$_2$ and Li$_3$ atomization energies and the Li-dissociati energy for Li$_3$ (listed as reaction 9). For simplicity, v abbreviate QCISD(T)/6-311+G(3df) as QCI and MCQDPT 6-311+G(2df) as MCQDPT2.

BLi. The energetic preference ΔE of the $^3\Pi_g$ ground sta over the $^1\Sigma^+$ state varies strongly with the theoretical methc employed, but little with the size of the basis set (see Tables and 5). At our highest levels, ΔE ranges between 6.4 kcal/m (QCI), also reported by Boldyrev,[13] and 2.3 kcal/mol (G (MP2)). This is a surprising result because the G2 method calibrated largely on diatomics to approximate the QCISD(1 6-311+G(3df)//MP2/6-31G(d) level.[31] Excluding the G2 er pirical correction, ΔE(HLC) gives an energy difference of 5 kcal/mol for the two spin states. Because no significa: configurational mixing occurs, electron correlation correctio with single reference-based methods, such as MPn and QCISI (T), are expected to be adequate. Evidently, MCQDPT2 predic ΔE of 6.1 kcal/mol, a mere 0.3 kcal/mol smaller than QCI. T modest MP2 and particularly UHF give much larger energ differences, whereas B3LYP/6-31G(d) seems to perform rath well with a ΔE of 8.0 kcal/mol. The basis set effect on goir from the modest 6-31G(d) to the much larger 6-311+G(2df) evident for the CASSCF(4,8) and MCQDPT2 methods wi respective increases in ΔE of 4.3 and 1.5 kcal/mol.

BLi ($^3\Pi_g$) has a bond dissociation energy D_0 of 26.6 kc: mol at QCI. A nearly identical value of 26.5 kcal/mol

Small Boron–Lithium Clusters

J. Phys. Chem. A, Vol. 102, No. 9, 1998 **1611**

A-4

TABLE 2: Structural Parameters and Total and Relative Energies for BLi_2 Isomers[a]

level	BLi_2 ($^2B_2$)					BLi_2 ($^2B_1$)					ΔE
	energy	$\langle s^2 \rangle$	B–Li	Li–Li	freq. (a_1, b_2, a_1)	energy	$\langle s^2 \rangle$	B–Li	Li–Li	freq. (b_2, a_1, a_1)	
B3LYP/A	39.72749	1.242	2.317	2.779	269, 288, 430	39.70783	1.305	2.345	2.546	165, 327, 418	12.3
UHF/A	39.44474	1.647	2.349	2.706	303, 329, 451	39.42488	1.664	2.369	2.509	224, 360, 432	12.5
UHF/B	39.45541	1.654	2.326	2.677	297, 332, 449	39.43748	1.672	2.356	2.475	230, 363, 422	11.3
UHF/C	39.45588	1.653	2.327	2.679	296, 332, 448	39.43808	1.671	2.362	2.477	226, 361, 418	11.2
MP2(full)/A	39.50306	1.646	2.333	2.734	292, 334, 452	39.48317	1.664	2.349	2.524	305, 346, 429	12.5
MP2(full)/B	39.55540	1.653	2.309	2.705	289, 338, 450	39.53753	1.671	2.333	2.496	336, 353, 426	11.2
MP2(full)/C	39.55632	1.652	2.309	2.705	289, 338, 450	39.53877	1.671	2.340	2.500	332, 350, 421	11.0
CASSCF(5,5)/A	39.46255	0.750	2.365	2.760	301, 312, 434	39.44271	0.750	2.383	2.574	206, 340, 419	12.5

[a] Total energies in −au, relative energies (ΔE) for the two isomers in kcal/mol, bond lengths in Å, and frequencies in cm^{-1}. [b] A: 6-31G(d), B: 6-311G(d), and C: 6-311+G(d).

TABLE 3: Structural Parameters and Total and Relative Energies for BLi_3 Isomers[a]

level	BLi_3 (C_{2v})					BLi_3 (D_{3h})			ΔE
	energy	B–Li	B–Li	LiBLi'	freq.	energy	B–Li	freq.	
B3LYP/A	47.27985	2.161	2.270	91.4	109, 184, 211, 417, 462, 616	47.27868	2.155	16i, 198, 403, 582	0.7
B3LYP/B	47.28873	2.146	2.243	91.2	118, 179, 212, 422, 469, 617	47.28725	2.133	23i, 191, 408, 593	0.9
B3LYP/C	47.28902	2.148	2.243	90.2	121, 180, 213, 422, 468, 616	47.28747	2.134	27i, 193, 409, 593	0.9
B3LYP/D	47.28997	2.144	2.236	91.8	117, 180, 212, 422, 471, 615	47.28859	2.130	20i, 191, 410, 594	0.9
HF/A	46.86811	2.183	2.312	97.0	36, 201, 187, 383, 480, 634	46.86836	2.182	69, 211, 411, 587	−0.2
HF/B	46.87871	2.169	2.285	96.8	50, 194, 187, 386, 484, 631	46.87878	2.172	65, 203, 412, 595	0.0
HF/C	46.87908	2.170	2.284	96.8	48, 195, 187, 387, 484, 631	46.87920	2.164	68, 210, 413, 595	−0.1
MP2(full)/A	46.99266	2.178	2.262	94.4	128, 194, 217, 425, 498, 579	46.99094	2.172	30i, 188, 388, 573	1.1
MP2(full)/B	47.05852	2.169	2.236	93.9	124, 180, 213, 427, 514, 594	47.05691	2.160	36i, 176, 403, 585	1.0
MP2(full)/C	47.05969	2.169	2.235	93.9	124, 181, 213, 427, 513, 595	47.05799	2.160	49i, 144, 403, 584	1.1
QCISD/A	47.00746	2.218	2.378	84.1	123, 188, 216, 425, 498, 585	47.00172	2.172	69i, 181, 399, 570	3.6
QCISD/B	47.02444	2.202	2.339	84.2	159, 161, 242, 382, 424, 594	47.01894	2.151	72i, 175, 407, 581	3.5
QCISD/C	47.02539	2.202	2.339	84.2	160, 161, 243, 382, 424, 595	47.01902	2.151	76i, 152, 409, 582	4.0
CASSCF(6,6)/A	46.93623	2.251	2.370	84.9	121, 167, 234, 386, 401, 560	46.93503	2.199	50, 187, 386, 557	0.8

[a] Total energies in −au, relative energies (ΔE) between the two isomers in kcal/mol, bond lengths in Å, angles in degrees, and frequencies in cm^{-1}. [b] A: 6-31G(d), B: 6-311G(d), C: 6-311+G(d), and D: 6-311+G($2df$).

TABLE 4: Structural Parameters and Total and Relative Energies for Li_2 and Li_3 Isomers[a]

level	B	Li	Li_2 ($^1\Sigma_g$)		Li_3 ($^2B_2$)				Li_3 ($^2A_1$)				ΔE
			energy	Li–Li	energy	$\langle s^2 \rangle$	Li–Li'	Li–Li	energy	$\langle s^2 \rangle$	Li–Li'	Li–Li	
B3LYP/A	24.65435	7.49098	15.01426	2.723	22.52356	0.784	2.785	3.377	22.52290	0.776	3.094	2.666	0.4
(U)HF/A	24.52203	7.43137	14.86693	2.807	22.31331	1.216	2.868	3.310	22.30987	0.981	3.305	2.719	2.2
(U)HF/B	24.53010	7.43202	14.87035	2.784	22.31841	1.225	2.837	3.253	22.31455	0.983	3.253	2.683	2.4
(U)HF/C	24.53034	7.43203	14.87035	2.784	22.31845	1.226	2.837	3.253	22.31459	0.984	3.253	2.683	2.4
MP2(full)/A	24.56246	7.43186	14.88685	2.773	22.33044	1.183	2.820	3.447	22.33084	0.963	3.152	2.730	−0.3
MP2(full)/B	24.58580	7.44490	14.91512	2.737	22.37277	1.196	2.775	3.368	22.37312	0.967	3.098	2.687	−0.2
MP2(full)/C	24.58631	7.44494	14.91526	2.737	22.37295	1.198	2.780	3.363	22.37331	0.967	3.098	2.687	−0.2
CASSCF/A			14.87792	2.733	22.32036	0.750	2.843	3.313	22.31729	0.750	3.295	2.699	1.9

[a] Total energies in −au, relative energies (ΔE) between the Li_3 isomers in kcal/mol, and bond lengths in Å. [b] A: 6-31G(d), B: 6-311G(d), C: 6-311+G(d).

TABLE 5: Total and Relative Energies for BLi, BLi_2, and BLi_3 Isomers[a]

level[b]	BLi ($^3\Pi_g$)	BLi ($^1\Sigma^-$)	ΔE	BLi_2 ($^2B_2$)	BLi_2 ($^2B_1$)	ΔE	BLi_3 (C_{2v})	BLi_3 (D_{3h})	ΔE
CASSCF/6-311+G($2df$)//I	32.03663	32.04216	−3.5	39.47439	39.45716	10.8	46.94861	46.94719	0.9
MCQDPT2/6-31G(d)//I	32.04336	32.03601	4.6	39.51922	39.49959	12.3	47.00000	46.99281	4.5
MCQDPT2/6-311+G($2df$)//I	32.06879	32.05905	6.1	39.54723	39.53038	10.6	47.03142	47.02602	3.4
QCISD(T)/6-311+G($2df$)//II	32.07210	32.06190	6.4	39.55125	39.53416	10.7	47.04795	47.04470	2.0
QCISD(T)/6-311+G($3df$)//II	32.07283	32.06268	6.4	39.55206	39.53484	10.8	47.04871	47.04522	2.2
G2	32.07718	32.07270	2.8	39.55958	39.54268	10.6	47.06076	47.05720	2.2
G2(MP2)	32.07709	32.07346	2.3	39.55970	39.54265	10.7	47.06109	47.05712	2.5

[a] Total energies in −au and relative energies (ΔE) between each set of isomers in kcal/mol. [b] I = CASSCF(4,8) for BLi, CASSCF(5,5) for BLi_2, and CASSCF(6,6) for BLi_3, all using the 6-31G(d) basis set. II = MP2(full)/6-311+G(d).

obtained at G2(MP2). All other methods, including B3LYP/6-31G(d), give similar binding energies (Table 7). Expectantly, these energies are in very good agreement with earlier theoretical estimates.[8,10,13]

BLi$_2$. The $^2B_2$ state with C_{2v} symmetry is the ground state of BLi_2. Its energy difference with the $^2B_1$ state is ~11 kcal/mol. The highest levels of theory (QCI, G2, and MCQDPT2) estimate this $\Delta E(^2B_2 - ^2B_1)$ to be between 10.6 and 10.8 kcal/mol (Table 5). Larger energy differences of up to 1.7 kcal/mol are found with the smaller 6-31G(d) basis set. B3LYP/6-31G* performs reasonably well, with an energy difference of 12.3 kcal/mol.

The computed atomization energy of BLi_2 ($^2B_2$) is estimated at 55.6 kcal/mol at QCI. Both G2 and MCQDPT2 give larger values of 58.4 and 59.0 kcal/mol, respectively. After excluding the empirical correction from the G2 energy, the resulting

A - 9

1612 *J. Phys. Chem. A, Vol. 102, No. 9, 1998*   Nguyen and Lammertsm

TABLE 6: Total and Relative Energies for B, Li, Li₂, and Li₃ Isomers [a]

level [b]	B	Li	Li₂ ($^1\Sigma_g$)	Li₃ ($^2B_2$)	Li₃ ($^2A_1$)	ΔE
CASSCF/6-311+G(2df)//I	24.54626	7.43208	14.87964	22.32743	22.32371	2.3
MCQDPT2/6-31G(d)//I	24.56883	7.43137	14.88779	22.33792	22.33536	1.6
MCQDPT2/6-311+G(2df)//I	24.58667	7.43208	14.89319	22.34735	22.34458	1.7
QCISD(T)/6-311+G(2df)//II	24.59673	7.43203	14.90171	22.35490	22.35454	0.2
QCISD(T)/6-311+G(3df)//II	24.59706	7.43203	14.90154	22.35473	22.35437	0.2
G2	24.60204	7.43222	14.90576	22.35776	22.35737	0.2
G2(MP2)	24.60270	7.43222	14.90640	22.35790	22.35766	0.2

[a] Total energies in -au and relative energies (ΔE) between the two Li₃ isomers in kcal/mol. [b] I = CASSCF(2,8) for Li₂ and CASSCF(5,5) for L both using the 6-31G(d) basis set. II = MP2(full)/6-311+G(d).

TABLE 7: Atomization Energies (AE) and Reaction Enthalpies for BLi, BLi₂, and BLi₃ Isomers and for Li₂ and Li₃ [a]

level [b]	BLi ($^3\Pi_g$) AE [c]	BLi₂ ($^2B_2$) AE	(2)	(3)	BLi₃ (C_{2v}) AE	(5)	(6)	(7)	(8)	Li₂ AE	Li₃ ($^2B_2$) AE	(9)
B3LYP/A	27.5	55.8	28.3	36.4	92.8	37.0	46.0	62.0	73.5	19.4	30.8	11.5
MP2(full)/A	22.1	46.7	24.7	32.7	81.6	34.8	45.5	60.7	67.6	14.0	20.9	6.5
MP2(full)/B	24.4	48.6	24.2	33.2	83.7	35.1	43.9	60.8	68.3	15.4	22.9	7.5
MP2(full)/C	24.9	48.8	23.9	33.4	84.0	35.3	43.7	61.1	68.6	15.4	22.9	7.5
MCQDPT2/6-31G(d)//I	20.6	53.5	33.6	38.3	83.3	29.8	48.2	56.9	68.1	15.2	26.4	11.2
MCQDPT2/6-311+G(2df)//I	24.8	59.0	34.0	41.3	90.5	31.5	47.8	59.5	72.8	17.7	31.0	13.3
QCISD(T)/6-311+G(2df)//II	26.4	55.3	28.9	32.1	94.5	39.2	44.9	58.5	71.3	23.2	36.0	12.8
QCISD(T)/6-311+G(3df)//II	26.6	55.6	28.9	32.5	94.8	39.1	45.0	58.9	71.7	23.1	35.9	12.8
G2	26.9	58.4	31.5	32.5	101.7	43.3	48.8	63.4	75.8	25.9	38.3	12.4
G2(MP2)	26.5	58.1	31.6	31.8	101.5	43.4	48.7	63.1	75.2	26.3	38.4	12.1

[a] Energies in kcal/mol. For reactions 1−8 and 9, see text. [b] A: 6-31G(d), B: 6-311G(d), and C: 6-311+G(d). I = CASSCF(4,8) for BI CASSCF(5,5) for BLi₂, CASSCF(6,6) for BLi₃, CASSCF(2,8) for Li₂, and CASSCF(5,5) for Li₃, all using the 6-31G(d) basis set. II = MP2(ful 6-311+G(d). [c] Atomization energies.

TABLE 8: Bond Critical Point Data for BLi, BLi₂, and BLi₃ [a]

level [b]	BLi ($^3\Pi_g$) ρ(BLi)	$\nabla^2\rho$(BLi)	BLi₂ ($^2B_2$) ρ(BLi)	$\nabla^2\rho$(BLi)	BLi₃ (C_{2v}) ρ(BLi)	$\nabla^2\rho$(BLi)	ρ(BLi')	$\nabla^2\rho$(BLi')
B3LYP/A	2.81	11.33	2.14	7.46	2.93	11.51	2.25	8.31
(U)HF/A	3.00	11.77	2.07	7.54	2.96	11.28	2.15	7.17
(U)HF/B	3.20	12.02	2.23	7.90	3.11	12.02	2.27	8.06
(U)HF/C	3.18	11.99	2.23	7.91	3.10	12.06	2.27	8.10
MP2(full)/A	2.90	11.60	2.07	7.48	2.69	10.79	2.29	8.91
MP2(full)/B	3.12	11.69	2.24	7.87	2.83	11.21	2.45	9.68
MP2(full)/C	3.10	11.61	2.24	7.89	2.84	11.22	2.46	9.71
QCISD/A	2.76	11.07			2.63	10.31	1.78	6.31
CASSCF/A	2.68	10.42	1.96	7.09	2.49	9.47	1.82	6.89

[a] Electron densities and their Laplacians are in 10^{-2} au. [b] A: 6-31G(d), B: 6-311G(d), C: 6-311+G(d), and D: 6-311+G(2df).

atomization energy of 55.5 kcal/mol is essentially identical to the QCI energy. The NOONs of the active ($^2B_2$) orbitals of the CASSCF(5,5)/6-31G(d) optimized wave function are 1.954 (a_1), 1.582 (a_1), 1.00 (b_2), 0.411 (a_1), and 0.054 (b_1). Similar values are obtained for the $^2B_1$ state. These NOONs are indicative of some configurational mixing and may contribute to the difference in atomization energies obtained between the QCI and MCQDPT2 methods. Again, we find the performance of B3LYP/6-31G(d) to be very satisfactory, with an atomization energy of 55.8 kcal/mol. Interestingly, this and the high level values for BLi₂ ($^2B_2$) are about twice the atomization energy of BLi ($^3\Pi_g$).

Elimination of one Li atom from BLi₂ ($^2B_2$), as in reaction 2, is endothermic by 28.9 kcal/mol at QCI and 5.1 kcal/mol more at MCQDPT2. The G2 dissociation energy of 31.5 kcal/mol is essentially the same as the QCI value after excluding the empirical correction. These B−Li bond dissociation energies are larger than that estimated for BLi ($^3\Pi_g$). Loss of the Li₂ dimer (reaction 3) requires 32.5 kcal/mol as predicted by both QCI and G2, whereas MCQDPT2 estimates this process to be 8.8 kcal/mol more endothermic. At QCI this Li₂ dissociation reaction is nearly isoenergetic, with loss of a single Li atom from BLi₂.

BLi₃. The ground-state structure of BLi₃, with C_{2v} symmet has an energy difference with the second-order transiti structure (D_{3h}) of only 2.2 kcal/mol at both QCI and G2 and 3.4 kcal/mol at MCQDPT2 (Tables 3 and 5). These valu except for the one at G2, are reduced upon inclusion of zer point-energy corrections. Thus, the upper limit for scrambli of the Li atoms in BLi₃ is in the 2−3 kcal/mol range.

The atomization energy of BLi₃ is predicted to be 94.8 kc mol at QCI (Table 7). The much larger value of 101.7 kc mol obtained with G2 is due to the empirical correctic MCQDPT2 gives a 4.3 kcal/mol lower atomization energy, a the B3LYP/6-31G(d) value of 92.8 kcal/mol is within 2 kc mol of the QCI estimate.

Elimination of a single Li atom (reaction 5) is the le endothermic dissociation channel for BLi₃. It requires 39 kcal/mol at QCI and 4.2 kcal/mol more at G2 due to t empirical correction, whereas the MCQDPT2 estimate is on 31.5 kcal/mol. At the QCI level, Li elimination from BI requires 6.6 kcal/mol more than from BLi₂. In contrast, B3LY 6-31G(d) predicts both reactions 2 and 5 to have simi endothermicities of 37 kcal/mol. Surprisingly, MCQDPT2 gi a 10 kcal/mol larger Li dissociation energy for BLi₂ than BLi₃.

Small Boron–Lithium Clusters

J. Phys. Chem. A, Vol. 102, No. 9, 1998 **1613**
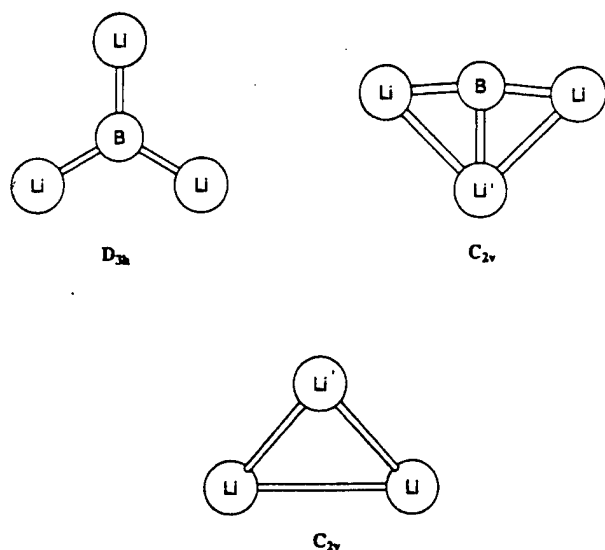
Figure 1. Structures for BLi₃ and Li₃.
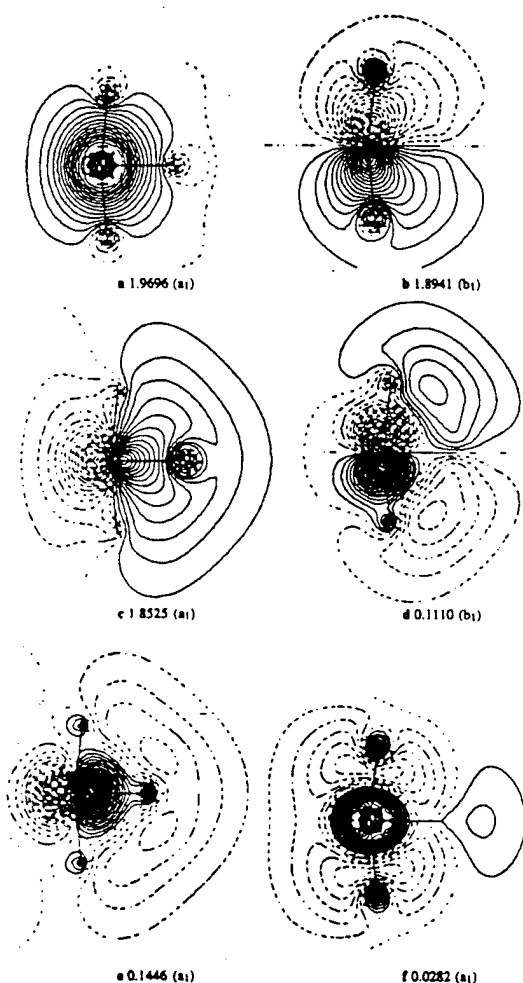
Figure 2. Active orbitals with occupation numbers for the optimized CASSCF(6,6)/6-31G(d) wave function in the σ_v (xz) plane of BLi₃ (C₂ᵥ).

Atomic boron elimination from BLi₃, producing Li₃ in its $^2B_2$ state (reaction 8), requires 71.7 (73.5) kcal/mol at QCI (B3LYP/6-31G(d)). This process is significantly more endothermic than the corresponding 32.5 (36.4) kcal/mol needed for elimination of a boron atom from BLi₂ (reaction 3). Dissociation of Li₂ from BLi₃ to give BLi ($^3\Pi_g$), as in reaction 6, requires
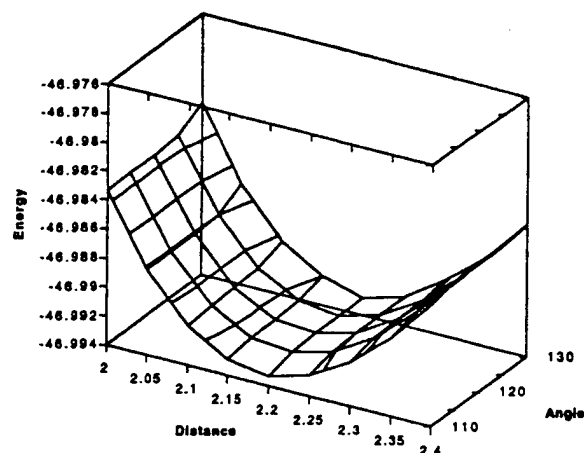
Figure 3. MCQDPT2/6-31G(d) potential energy surface for BLi₃.

45.0 (46.0) kcal/mol at QCI (B3LYP/6-31G(d)). Both reaction 3 and 6 do not appear to be very sensitive to the employed levels of theory. Again, B3LYP performs well.

The atomization energies of both Li₂ and Li₃ are provided in Table 7 for comparison. With the higher level theoretical models, the atomization energy is constant per Li atom, and amounts to ~13 kcal/mol, in accord with literature estimates.[36] Interestingly, we find that the B–Li and Li–Li binding energies are similar at G2 (26 kcal/mol) with QCI giving a slightly stronger B–Li bond by ~3 kcal/mol. The Li-dissociation energy for Li₃ of ~13 kcal/mol (reaction 9) is much smaller than those of 29 and 39 kcal/mol (all QCI) for BLi₂ and BLi₃, respectively, illustrating the strong influence of the boron atom.

Conclusions

We have examined the structures, harmonic vibrational frequencies, bonding patterns, and reaction enthalpies for all possible dissociation channels of BLi ($^3\Pi_g$), BLi₂ ($^2B_2$), and BLi₃ (C₂ᵥ) at several levels of theory with both single reference- and multireference-based correlated methods using a variety of basis sets. Neither of the structures is much influenced by the size of the basis set nor by the method of electron correlation employed. However, dynamic electron correlation is important for characterization of stationary points on the potential energy surface. The D_{3h} symmetry form of BLi₃ is a second-order saddle point with an energy difference of 2.2 kcal/mol with the C_{2v} minimum form. Energy evaluations were done at the QCISD(T)/6-311+G(3df)//MP2(full)/6-311+G(d), MCQDPT2/6-311+G(2df)//CASSCF/6-31G(d), G2 and G2(MP2) levels of theory. The QCI method gives atomization energies of 27, 56, and 95 kcal/mol for BLi ($^3\Pi_g$), BLi₂ ($^2B_2$), and BLi₃ (C₂ᵥ), respectively. After excluding the empirical corrections, the G2 and G2(MP2) energetics are essentially the same as the QCI values. The QCI method estimates the Li-dissociation energies for BLi₂ and BLi₃ at 29 and 39 kcal/mol, respectively. The same method gives an energy difference of 6.4 kcal/mol for the $^3\Pi_g$ and $^1\Sigma^+$ states of BLi and estimates that the $^2B_2$ state of BLi₂ is 10.8 kcal/mol more stable than the $^2B_1$ state. Density functional theory with the hybrid B3LYP functionals using the 6-31G(d) basis set performs extremely well. It provides structures, frequencies, and energetics similar in accuracy to the most sophisticated ab initio methods. This result suggests that the B3LYP functionals with the modest 6-31G(d) basis set may be an attractive alternative for studying larger boron–lithium clusters.

1614 *J. Phys. Chem. A, Vol. 102, No. 9, 1998*

$A-7$

Nguyen and Lammertsm.

References and Notes

(1) Davis, S. C.; Klabunde, K. J. *Chem. Rev.* **1982**, *82*, 153.

(2) Koutecký, J.; Fantucci, P. *Chem. Rev.* **1986**, *86*, 539.

(3) Bonacic-Koutecky, V.; Fantucci, P.; Koutecký, J. *Chem. Rev.* **1991**, *91*, 1035.

(4) Meden, A.; Mavri, J.; Bele, M.; Pejovnik, S. *J. Phys. Chem.* **1995**, *99*, 4252.

(5) Kaufman, J. J.; Sachs, L. M. *J. Chem. Phys.* **1970**, *52*, 645.

(6) Cade, P. E.; Huo, W. M. *At. Data Nucl. Data Tables* **1975**, *15*, 1.

(7) Zhu, Z. H.; Murrell, J. N. *Chem. Phys. Lett.* **1982**, *88*, 262.

(8) Knowles, D. B.; Murrell, J. N. *J. Mol. Struct. (Theochem.)* **1986**, *135*, 169.

(9) Saxon, R. P. Theoretical Studies of Boron Compounds; *Proceedings of the High Energy Density Matter*, 1992; Woods Hole, MA.

(10) Sheehy, J. A. Spectroscopy of Lithium Boride, A candidate HEDM Species; *Proceedings of the High Energy Density Matter*, 1995; Woods Hole, MA.

(11) Ivanic, J.; Marsden, C. J. *J. Am. Chem. Soc.* **1993**, *115*, 7503. Marsden, C. J. *J. Chem. Soc., Chem. Commun.* **1989**, 1356. Ivanic, J.; Marsden, C. J.; Hassett, D. M. *J. Chem. Soc., Chem. Commun.* **1993**, 822.

(12) Nemukhin, A. V.; Almlöf, J. *Chem. Phys. Lett.* **1980**, *76*, 601.

(13) Boldyrev, A. I.; Simons, J.; Schleyer, P. v. R. *J. Chem. Phys.* **1993**, *1993*, 8793.

(14) Bader, R. F. W.; Nguyen-Dang, T. T. *Adv. Quant. Chem.* **1981**, *14*, 63.

(15) Bader, R. F. W.; Nguyen-Dang, T. T.; Tal, Y. *Rep. Prog. Phys.* **1981**, *44*, 893.

(16) Bader, R. F. W. *Chem. Rev.* **1991**, *91*, 893.

(17) Kohn, W.; Sham, L. J. *Phys. Rev. A* **1965**, *140*, 1133.

(18) Rothaan, C. C. J. *Rev. Mod. Phys.* **1951**, *23*, 69.

(19) Pople, J. A.; Nesbet, R. K. *J. Chem. Phys.* **1959**, *22*, 571.

(20) Pople, J. A.; Binkley, J. S.; Seeger, R. *Int. J. Quantum Chem. Symp.* **1976**, *10*, 1.

(21) Pople, J. A.; Krishnan, R.; Schlegel, B.; Binkley, J. S. *Int. J. Quantum Chem. Symp.* **1979**, *13*, 325.

(22) Hehre, W. J.; Ditchfield, R.; Pople, J. A. *J. Chem. Phys.* **1972**, *5c* 2257.

(23) Krishnan, R.; Binkley, J. S.; Seeger, R.; Pople, J. A. *J. Chem. Phy:* **1980**, *72*, 650.

(24) Clark, T. C., J.; Spitznagel, G. W., Schleyer, P. v. R. *J. Compu. Chem.* **1983**, *4*, 294.

(25) Becke, A. D. *J. Chem. Phys.* **1993**, *98*, 5648.

(26) Becke, A. D. *Phys. Rev. A* **1988**, *38*, 3098.

(27) Lee, C.; Yang, W.; Parr, R. G. *Phys. Rev. B* **1988**, *37*, 785.

(28) Roos, B. O.; Taylor, P. R.; Siegbahn, P. E. M. *Chem. Phys.* **198(** *48*, 157.

(29) Curtiss, L. A.; Raghavachari, K.; Trucks, G. W.; Pople, J. A. *Chem. Phys.* **1991**, *94*, 7221.

(30) Curtiss, L. A.; Raghavachari, K.; Pople, J. A. *J. Chem. Phys.* **199:** *98*, 1293.

(31) Raghavachari, K.; Trucks, G. W.; Pople, J. A.; Replogle, E. S. *Chem. Phys. Lett.* **1989**, *158*, 207.

(32) Nakano, H. *J. Chem. Phys.* **1993**, *99*, 7983.

(33) Frisch, M. J.; Trucks, G. W.; Schlegel, H. B.; Gill, P. M. W Johnson, B. G.; Robb, M. A.; Cheeseman, J. R.; Keith, T.; Petersson, (A.; Montgomery, J. A.; Raghavachari, K.; Al-Laham, M. A.; Zakrzewsk V. G.; Ortiz, J. B. F.; Cioslowski, J.; Stefanov, B. B.; Nanayakkara, A Challacombe, M.; Peng, C. Y.; Ayala, P. Y.; Chen, W.; Wong, M. W Andres, J. L.; Replogle, E. S.; Gomperts, R.; Martin, R. L.; Fox, D. J Binkley, J. S.; Defrees, D. J.; Baker, J.; Stewart, J. P.; Head-Gordon, M Gonzalez, C.; Pople, J. A. GAUSSIAN94, Revision B.1; Gaussian, Inc Pittsburgh, PA, 1994.

(34) Schmidt, M. W.; Baldridge, K. K.; Boatz, J. A.; Elbert, S. T Gordon, M. S.; Jensen, J. H.; Koseki, S.; Matsunaga, N.; Nguyen, K. A Su, S.; Windus, T. L.; Dupuis, M.; Montgomery, J. A. *J. Comput. Cher* **1993**, *14*, 1347.

(35) As noted by a referee, this behavior may, in fact, be fortuitot because both states ($^2B_2$ and $^2B_1$) have similar s^2 expectation values.

(36) Boustani, I.; Pewestorf, W.; Fantucci, P.; Bonacic-Koutecký, V Koutecký, J. *Phys. Rev. B* **1987**, *35*, 9437.

A-8

710   *J. Phys. Chem. A* **1999**, *103*, 710−715

Stability of Hyperlithiated Borides

Kiet A. Nguyen,[†,‡] G. Naga Srinivas,[†] Tracy P. Hamilton,[†] and Koop Lammertsma*,[†,§]

*Department of Chemistry, University of Alabama at Birmingham, Birmingham, Alabama 35294, and
Faculty Sciences, Department of Chemistry, Vrije Universiteit, De Boelelaan 1083,
1081 HV Amsterdam, The Netherlands*

Received: October 23, 1998

Structures and energetics of BLi$_n$ ($n = 4-8$) clusters are predicted using the SCF, MP2, and B3LYP methods with the 6-31G(d) basis set, including energy evaluations at G2MP2. Cohesive energies, defined as the enthalpies of the BLi$_n \rightarrow$ B + Li$_n$ reactions, and Li and Li$_2$ elimination reaction enthalpies are also estimated at B3LYP. This level of theory predicts the boron cohesive energy to increase up to the BLi$_6$ cluster after which it levels off. All BLi$_n$ systems are thermodynamically stable with respect to Li and Li$_2$ dissociations; BLi$_4$ has the largest reaction enthalpies. The energetics of the hyperlithiated borides obtained with B3LYP/6-31G(d) are in reasonable agreement with those at G2MP2 but less satisfactory than those of the smaller BLi$_n$ ($n = 1-3$) systems. Computations on BLi$_4$ with multiconfigurational quasidegenerate perturbation theory indicate that the B3LYP/6-31G(d) energies may be more reliable for the larger BLi$_n$ systems.

I. Introduction

Lithium atoms are known to form hypervalent compounds with group 13−17 elements of the periodic table. Structures and energetics for many of these hyperlithiated compounds have been reported in theoretical studies.[1−4] Some have been studied experimentally such as, for example, OLi$_4$ and OLi$_5$, which were detected by Wu.[5] The hyperlithiated carbide CLi$_6$ was observed in 1992 by Kudo[6] a decade after Schleyer et al.[3] predicted its possible existence. Recent theoretical data of Ivanic and Marsden suggest the even larger polylithiated carbon clusters CLi$_8$, CLi$_{10}$, and CLi$_{12}$ to be of reasonable stability.[7]

In contrast to the well-studied hyperlithiated carbides, theoretical studies of similarly sized and larger boron−lithium systems have been limited to the work of Meden et al.[8] They computed structures and energetics at the SCF/6-31G(d) level to evaluate the formation of a Li$_3$B compound in the dissolution of crystalline boron in the lithium melt. Partly on the basis of computed cohesive energies, they argued that boron does not dissolve completely in molten lithium. Although these SCF structures are informative, "electron-deficient" systems are known to require correlated methods for acceptable estimates of structural parameters and energies. In a recent systematic study, we demonstrated the importance of the effects of electron correlation in accurately characterizing stationary points on the potential energy surface (PES) of small BLi$_n$ ($n = 1-3$) systems.[9]

To shed more light on hyperlithiated borides and to assist in their gas-phase detection, we now report ab initio calculations on BLi$_n$ ($n = 4-8$) to examine their structures and thermal stabilities. In particular, we gauge the BLi$_n \rightarrow$ B + Li$_n$ reaction, which measures the stabilization (i.e., cohesive energy) that a boron atom provides to the BLi$_n$ clusters. To explore the thermodynamic driving force for the Li and Li$_2$ elimination

channels, reaction enthalpies for BLi$_n \rightarrow$ BLi$_{n-1}$ + Li and BLi$_n \rightarrow$ BLi$_{n-2}$ + Li$_2$ are reported for ground-state processes.

II. Computational Methods

All electronic structure calculations were carried out using the GAUSSIAN 94 suite of programs.[10] The structures of all BLi$_n$ isomers were calculated at the Hartree−Fock (HF) self-consistent field (SCF) level,[11,12] Møller−Plesset second-order perturbation theory (MP2),[13,14] and Kohn−Sham theory[15] using the 6-31G(d)[16] basis set. For the density functional theory (DFT) calculations we used Becke's three-parameter hybrid exchange functional combined with the Lee−Yang−Parr correlation functional,[17−19] hereafter referred to as B3LYP. The structures were verified to be either minima or transition structures by evaluating the second derivatives of the energy (Hessian matrix).

Enthalpies of formation are estimated at G2MP2. This method[20] uses MP2/6-31G(d) geometries and obtains its energies from the QCISD(T) method,[21] using the 6-311G(d,p) basis set,[22] with basis set additivity corrections at the MP2 level of theory. The combination of basis set and correlation corrections, and two empirical corrections yields

$$E(\text{G2MP2}) = E(\text{QCISD(T)/6-311G(d,p)}) +$$
$$E(\text{MP2/6-311+G(3df,2p)}) - E(\text{MP2/6-311G(d,p)}) +$$
$$E(\text{HLC}) + E(\text{ZPE})$$

where the empirical "higher level correction" is given by $E(\text{HLC}) = (-0.19n\alpha - 4.81n\beta) \times 10^{-3}$ au. $E(\text{ZPE})$ is obtained by scaling the SCF/6-31G(d) harmonic frequencies by 0.8929. For 125 experimental energies, the G2MP2 method is reported to give a mean absolute deviation of 1.58 kcal/mol.[20,23] Kohn−Sham DFT with B3LYP functionals also delivers impressive thermochemical accuracy with a mean absolute deviation of 2.4 kcal/mol for a similar test set that includes 110 experimental energies.[17] Although numerous examples show B3LYP results to compare favorably with high levels of theory and with experiments, such comparisons for boron−lithium systems are limited to only the computed small BLi$_n$ ($n = 1-3$) clusters owing to the absence of experimental data. For these clusters

Hyperlithiated Borides

J. Phys. Chem. A, Vol. 103, No. 6, 1999 **711**

A-9

the DFT geometries and energetics are in excellent agreement with high levels of theory.[9]

Owing to the proximity of the potential energy surfaces of excited states for some of the open-shell systems considered here, HF and HF-based correlated calculations may exhibit multiple solutions that are associated with the same symmetry and electronic configuration. For example, at MP2/6-31G(d), two $^2A_{2u}$ states are found for the D_{4h} form of BLi$_4$ with one exhibiting more spin contamination than the other. In this and in other cases data are reported for the lowest energy and the least spin-contaminated state.

Given the uncertainty in the accuracy of the energies for highly spin-contaminated molecules, we used the GAMESS[24] program to perform complete active space SCF calculations with seven electrons in seven active orbitals (CASSCF(7,7)) for the BLi$_4$ isomers (i.e.,geometry optimizations and frequencies analyses) followed by multiconfigurational quasidegenerate second-order perturbation theory (MCQDPT2)[25] for higher accuracy in the energies. However, throughout B3LYP will be used for all final energy evaluations of the BLi$_n$ systems.

III. Results and Discussion

Structures of BLi$_n$ (n = 4−8) with B3LYP geometrical parameters are displayed in Figure 1 with MP2 values in brackets and those at SCF in parentheses. The geometrical data of these structures, computed with the three methods, compare reasonably well. The average BLi bond length for all systems is 2.170 ± 0.043 Å at MP2, while slightly shorter at B3LYP (2.137 ± 0.051 Å) and comparably longer at SCF (2.217 ± 0.061 Å). More noticeable deviations in some of the structures are due to the flatness of the potential energy surface compounded by the effect of electron correlation. Not surprisingly, CASSCF(7,7) tends to predict longer bonds for BLi$_4$ (shown in italics in Figure 1).

Total and relative energies are tabulated in Tables 1 and 2 for all BLi$_n$ and Li$_n$ (n = 4−8) systems. Table 3 lists the BLi$_n$ boron cohesive energies, defined as the enthalpy for the BLi$_n$ → B + Li$_n$ reaction. Tables 4 and 5 give respectively the Li and Li$_2$ elimination energetics for BLi$_n$, and the corresponding ones for Li$_n$ are listed for comparison in Tables 6 and 7. Thermodynamic data for BLi, BLi$_2$, and BLi$_3$ are included in Tables 3−5, also for comparison. The enthalpies given in these tables include zero-point energy corrections except for Table 1, which lists absolute energies.

As expected, only for a few BLi$_n$ systems do the SCF and MP2 energetics show reasonable agreement with those at G2MP2, which is the highest level of theory we employ. Deviations from the G2MP2 energies for the Li-elimination reactions (Table 4) are as large as 40 and 27 kcal/mol for SCF and MP2, respectively. The differences between B3LYP and G2MP2 are less pronounced but remain significant (up to 15 kcal/mol), in contrast to those found for the smaller BLi$_n$ (n = 1−3) systems. Whereas the overall trends in energetics predicted by both B3LYP and MP2 are consistent with those at G2MP2, this, however, is not the case for SCF. The SCF performance is particularly poor for the B−Li$_n$ cohesive energies listed in Table 3.

In the following subsections, we discuss for each BLi$_n$ cluster their structural features and energetics with emphasis on the most stable forms. Unless noted otherwise, B3LYP data are used.

A. BLi$_4$. Five BLi$_4$ structures were identified with C_{2v}, D_{2d}, C_{4v}, D_{4h}, and T_d symmetry (Figure 1). Of these only the C_{2v} and D_{2d} structures are minima at all levels of theory. At the

TABLE 1: Total (au) and Relative (kcal/mol) Energies for BLi$_n$ Systems[a]

str/sym/level	energy	$\langle S^2\rangle$	rel energy	NIF (cm^{-1})
(a) BLi$_4$				
D_{2d} ($^2B_2$)				
B3LYP	−54.838 87	0.961	0	0
SCF	−54.355 20	2.264	0	0
MP2	−54.476 06	2.173	0	0
G2MP2[b]	−54.583 58		0	
CASSCF(7,7)	−54.406 16		0	0
MCQDPT2	−54.501 73		0	
C_{2v} ($^2B_2$)				
B3LYP	−54.836 00	0.767	1.8	0
SCF	−54.376 38	1.772	−13.3	0
MP2	−54.478 72	1.737	−1.6	0
G2MP2[b]	−54.558 40		15.8	
CASSCF(7,7)	−54.408 35		−1.3	0
MCQDPT2	−54.504 85		−2.0	
D_{4h} ($^2A_{2u}$)				
B3LYP	−54.838 45	0.767	0.2	1 (48i)
SCF	−54.339 52	0.776	9.4	2 (265i, 71i)
MP2	−54.496 99	0.776	−14.5	2 (312i, 20i)
G2MP2	−54.563 56		12.6	
CASSCF(7,7)	−54.404 18		1.2	0
MCQDPT2	−54.500 38		0.8	
C_{4v} ($^2A_1$)				
B3LYP	−54.838 45	0.767	0.2	1 (47i)
SCF	−54.340 74	0.767	8.7	1 (44i)
MP2	−54.497 30	0.767	−13.2	1 (44i)
G2MP2	−54.563 46		12.6	
CASSCF(7,7)	−54.404 86		0.8	0
MCQDPT2	−54.500 64		0.7	
T_d				
B3LYP	−54.827 12	0.764	6.5	2 (1924i, 1923i)
(b) BLi$_5$				
C_{4v}				
B3LYP	−62.401 05		0	0
SCF	−61.809 90		0	0
MP2	−62.015 46		0	0
G2MP2	−62.080 67		0	
D_{3h}				
B3LYP	−62.397 93		1.4	2 (54i, 54i)
SCF	−61.805 56		2.5	2 (40i, 40i)
MP2	−62.013 72		0.6	2 (13i, 13i)
G2MP2	−62.078 00		1.7	
C_{2v}				
B3LYP	−62.397 95		1.5	1 (90i)
SCF	−61.805 56		2.6	1 (67i)
MP2	−62.013 72		0.7	1 (26i)
G2MP2	−62.077 91		1.7	
(c) BLi$_6$				
O_h ($^2A_{1g}$)				
B3LYP	−69.962 79	0.769		0
SCF	−69.316 42	1.936		0
MP2	−69.489 71	1.865		0
G2MP2	−69.581 83			
(d) BLi$_7$				
D_{5h}				
B3LYP	−77.492 94		0.0	0
SCF	−76.740 33		0.0	0
MP2	−76.997 90		0.0	0
G2MP2	−77.067 38		0.0	
C_{3v} (staggered)				
B3LYP	−77.486 94		3.8	0
SCF	−76.740 01		0.2	0
MP2	−76.985 80		7.7	0
G2MP2	−77.061 58		3.6	0
C_{3v} (eclipsed)				
B3LYP	−77.473 00		12.4	1 (116i)
SCF	−76.724 81		9.5	1 (123i)
MP2	−76.967 06		19.1	1 (132i)
G2MP2	−77.048 02		12.1	
(e) BLi$_8$				
C_{3v}				
B3LYP	−85.004 21[b]	0.792	0.0	0
SCF	−84.204 83[b]	1.645	0.0	2 (111i, 111i)
MP2	−84.413 36[b]	1.507	0.0	?
G2MP2				
D_{4h} ($^2A_{2u}$)				
SCF	−84.159 39	1.988	26.6	

[a] Using the 6-31G(d) basis set. Relative energies include zero-point energy corrections. NIF = number of imaginary frequencies. [b] Symmetry-broken solutions for the D_{2d} ($^2B_2$) form of BLi$_4$ at MP2/6-311+G(3df,2p).

A-10

712   J. Phys. Chem. A, Vol. 103, No. 6, 1999   Nguyen et al.
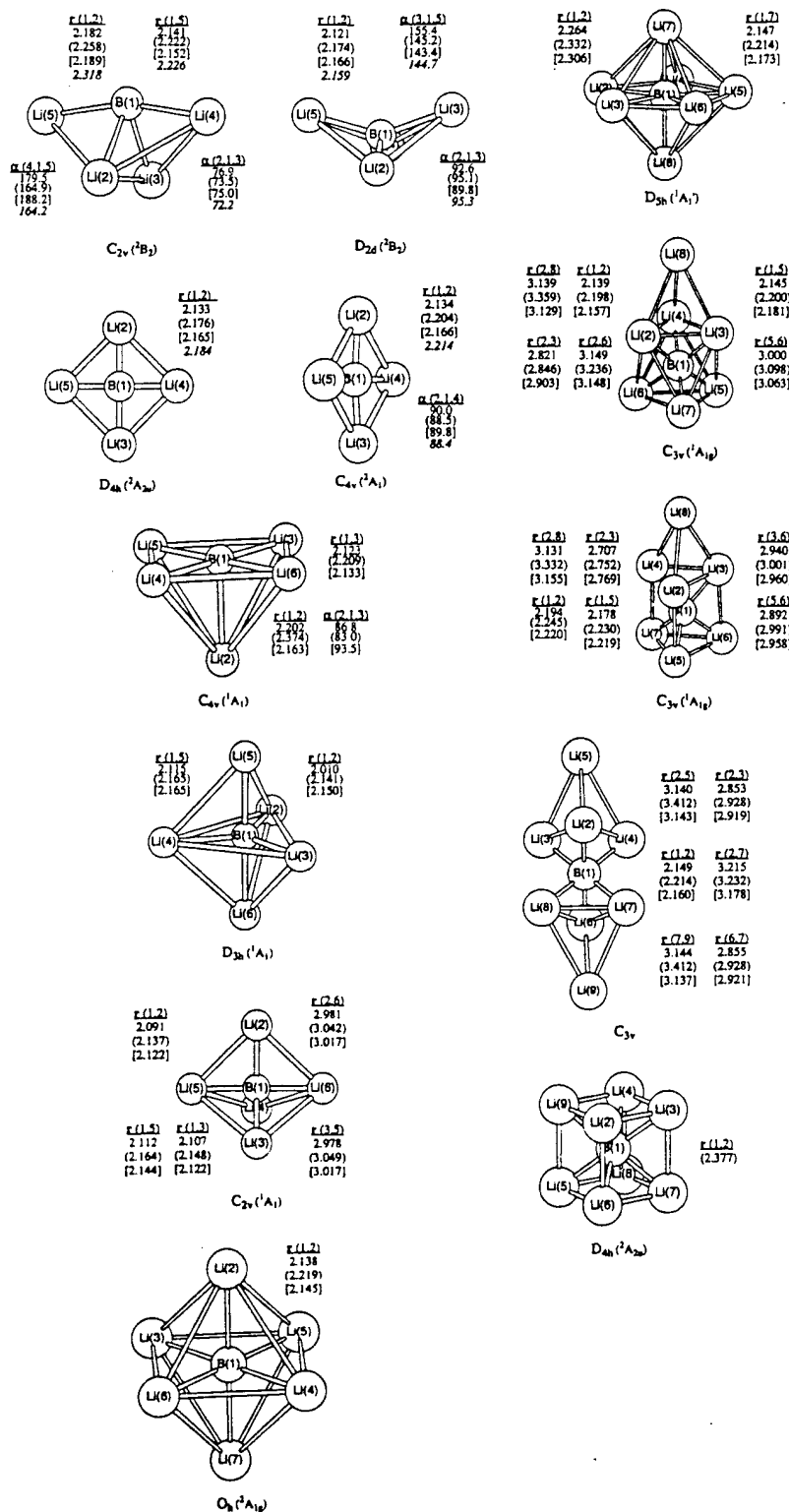
Figure 1. BLi$_n$ ($n = 4-8$) structures with geometrical parameters at B3LYP, MP2 (in brackets), and SCF (in parentheses) with the 6-31G(d) basis set. The CASSCF(7,7) distances and angles for BLi$_4$ are in italics.

MP2 level the D_{2d} structure has a B–Li bond length of 2.166 Å and a large Li–B–Li angle of 143°. The C_{2v} structure, which can be viewed as a bi-Li-capped BLi$_2$ ring, is the only one with Li$_3$ triangular interactions (a common motif in lithium clusters). None of the C_{4v}, D_{4h}, and T_d forms, which are the only BLi$_4$ structures reported by Meden et al.,[8] are minima at SCF or at B3LYP. The C_{4v} isomer is a transition structure at all levels with normal modes leading to the D_{2d} structure. Note that the C_{4v} form is actually planar at B3LYP, thus having D_{4h} symmetry. This D_{4h} structure has two imaginary frequencies at

SCF and MP2 with normal modes leading to the C_{4v} and D_{2d} structures. The T_d form is a "hill-top" structure at B3LYP, at which level it has a symmetry-broken solution. Its two degenerate frequencies have normal modes leading to the D_{2d} structure.

B3LYP predicts the C_{2v} and D_{2d} forms to be nearly isoenergetic with a 1.8 kcal/mol preference for the D_{2d} isomers, while both CASSCF(7,7) and MCQDPT2 give a similar small energy difference in favor of the C_{2v} isomer as does MP2. Interestingly, G2MP2 estimates the C_{2v} to be less stable by a sizable 15.8 kcal/mol. B3LYP, CASSCF(7,7), and MCQDPT2 also predict

A-11

Hyperlithiated Borides

J. Phys. Chem. A, Vol. 103, No. 6, 1999 **713**

TABLE 2: Total (au) and Atomization (kcal/mol) Energies for Li$_n$ Systems^a

level	Li$_4$ (D_{2h})	Li$_5$ (C_{2v})	Li$_6$ (D_{3h})	Li$_7$ (D_{5h})	Li$_8$ (T_d)
			Total Energy		
B3LYP	−30.053 97	−37.574 20	−45.103 27	−52.644 43	−60.174 92
SCF	−29.753 03	−37.218 14	−44.649 76	−52.103 88	−59.556 73
MP2	−29.801 45	−37.251 33	−44.726 09	−52.218 24	−59.688 84
G2MP2	−29.842 68	−37.302 29	−44.784 03	−52.272 83	−59.754 92
			Atomization Energy^b		
B3LYP	54.4	72.4	95.5	130.3	149.6
SCF	15.5	36.3	35.5	49.0	61.3
MP2	44.2	55.3	81.5	110.8	141.3
G2MP2	71.4	88.6	119.7	155.2	186.5

^{a} Using the 6-31G(d) basis set. ^{b} With zero-point energy corrections included.

TABLE 3: Enthalpies (kcal/mol) of Reactions for BLi$_n$ → Li$_n$ + B^a

level	SCF^a	MP2^a	G2MP2	B3LYP^a
BLi$_2$ (C_{2v}, $^2B_2$)	33.5	32.7	31.8	36.4
BLi$_3$ (C_{2v})	18.9	60.7	63.1	62.0
BLi$_4$ (D_{2d})	47.8	67.1	86.7	79.9
BLi$_5$ (C_{4v})	40.6	123.4	110.2	105.0
BLi$_6$ (O_h)	87.7	121.9	122.4	128.0
BLi$_7$ (D_{5h})	68.2	132.7	120.4	118.9
BLi$_8$ (C_{3v})	76.7	101.7^b		107.1

^{a} Using the 6-31G(d) basis set and inclusion of zero-point energy (ZPE) corrections. ^{b} Without ZPE correction.

TABLE 4: Enthalpies (kcal/mol) of Reactions for BLi$_n$ → BLi$_{n-1}$ + Li

level	SCF^a	MP2^a	G2MP2	B3LYP^a
BLi ($^3\Pi_t$)	15.3	22.1	26.5	27.5
BLi$_2$ ($^2B_2$)	20.8	24.7	31.6	28.3
BLi$_3$ (C_{2v})	−6.2	34.8	43.4	37.0
BLi$_4$ (D_{2d})	33.4	29.8	56.6	41.5
BLi$_5$ (C_{4v})	13.5	67.3	40.7	43.1
BLi$_6$ (O_h)	46.4	24.7	43.3	46.2
BLi$_7$ (D_{5h})	−6.0	48.0	33.5	21.0
BLi$_8$ (C_{3v})	20.8	−10.3^b		12.2

^{a} Using the 6-31G(d) basis set and inclusion of zero-point energy (ZPE) corrections. ^{b} Without ZPE correction.

TABLE 5: Enthalpies (kcal/mol) of Reactions for BLi$_n$ → BLi$_{n-2}$ + Li$_2$

level	SCF^a	MP2^a	G2MP2	B3LYP^a
BLi$_2$ ($^2B_2$)	33.5	32.7	31.8	36.4
BLi$_3$ (C_{2v})	11.9	45.5	48.7	46.0
BLi$_4$ (D_{2d})	25.0	50.6	73.7	59.1
BLi$_5$ (C_{4v})	44.8	83.0	71.0	65.2
BLi$_6$ (O_h)	57.7	78.0	57.6	69.8
BLi$_7$ (D_{5h})	38.2	58.7	50.4	47.8
BLi$_8$ (C_{3v})	12.7	23.1^b		13.9

^{a} Using the 6-31G(d) basis set and inclusion of zero-point energy (ZPE) corrections. ^{b} Without ZPE correction.

TABLE 6: Enthalpies (kcal/mol) of Reactions for Li$_n$ → Li$_{n-1}$ + Li^a

level	SCF^a	MP2^a	G2MP2	B3LYP^a
Li$_2$	2.1	14.0	26.3	19.4
Li$_3$ ($^2B_2$)	8.9	6.9	12.1	11.5
Li$_4$ (D_{2h})	4.4	23.4	33.0	23.5
Li$_5$ (C_{4v})	20.8	11.1	17.2	18.0
Li$_6$ (O_h)	−0.8	26.2	31.1	23.2
Li$_7$ (D_{5h})	13.5	41.0	35.5	30.0
Li$_8$ (T_d)	12.3	30.5	31.3	24.1

^{a} Using the 6-31G(d) basis set.

TABLE 7: Enthalpies (kcal/mol) of Reactions for Li$_n$ → Li$_{n-2}$ + Li$_2$

level	SCF^a	MP2^a	G2MP2	B3LYP^a
Li$_4$ (D_{2h})	11.2	16.2	18.7	15.7
Li$_5$ (C_{4v})	23.1	20.4	23.8	22.1
Li$_6$ (O_h)	17.9	23.2	21.9	21.7
Li$_7$ (D_{5h})	10.6	41.5	40.2	33.8
Li$_8$ (T_d)	23.6	45.8	40.5	34.8

^{a} Using the 6-31G(d) basis set.

hardly any energy difference with the C_{4h} and D_{4h} structures, indicating that BLi$_4$ has a very soft potential energy surface. Interestingly, at G2MP2 its D_{2d} form is 12.6 kcal/mol more stable than the C_{4v} isomer, while MP2 gives instead a reversed energetic preference of 13.2 kcal/mol. However, the energies obtained with these methods are influenced by high degrees of spin contamination, which is not the case at B3LYP. These observations suggests that the B3LYP method is well suited for analysis of the BLi$_4$ system. For convenience in comparing BLi$_4$ with the other BLi$_n$ systems we consider the B3LYP D_{2d} structure as the global minimum.

The B3LYP cohesive energy of BLi$_4$ (D_{2d}) is 17.9 kcal/mol larger than that of BLi$_3$ and amounts to a sizable 79.9 or 20.0 kcal/mol per BLi interaction. Similar results are computed at

G2MP2. BLi$_4$ has large endothermicities in the series of BLi$_n$ clusters (vide infra) for both Li (41.5 kcal/mol) and Li$_2$ (59.1 kcal/mol) eliminations.

B. BLi$_5$. The C_{2v}, D_{3h}, and C_{4v} symmetry forms of hyperlithiated BLi$_5$ were studied (Figure 1). Meden et al.[8] reported earlier on the D_{3h} and C_{4v} forms at the SCF level. The C_{4v} structure is a minimum, while the 1.4 kcal/mol less stable D_{3h} form is a "hill-top" structure with two degenerate imaginary frequencies. Following one of its imaginary normal modes leads to the C_{2v} transition structure, which has an imaginary frequency of only 26i cm^{-1} at MP2 (67i cm^{-1} at SCF and 90i cm^{-1} at B3LYP). Tracing the B3LYP minimum energy path for this transition structure was unsatisfactory, since it led to a C_s form (not shown), which is only slightly distorted from C_{2v} symmetry and which also has an imaginary frequency (88i cm^{-1}). We were unable to trace the other minimum energy paths because of the flatness of the PES for BLi$_5$ of which the C_s, C_{2v}, and D_{3h} structures are separated by only 0.1 kcal/mol. For the BLi$_5$ (C_{4v}) minimum the axial B−Li distance of 2.163 Å is virtually identical to that of BLi$_4$ (D_{2d}); the equatorial B−Li distance (2.133 Å) is only slightly shorter. Note that coordination of lithium in BLi$_5$ prefers an open pyramidal arrangement while the most stable Li$_5$ form is planar.

Each of the five lithium atoms in BLi$_5$ is tightly coordinated to the boron atom; i.e., boron is hypercoordinated. The strength of these combined BLi interactions is reflected in the boron cohesive energy of 105.0 kcal/mol (or averaging 21.0 kcal/mol per BLi interaction), which is even 25 kcal/mol more than for BLi$_4$. Elimination of a single Li atom from the even-electron BLi$_5$ requires a significant 43.1 kcal/mol. It should be noted

A-12

714 *J. Phys. Chem. A, Vol. 103, No. 6, 1999*

Nguyen et al.

that these reaction enthalpies are rather sensitive to the theoretical method employed. For example, the enthalpies alternate at the G2MP2 level of theory, and even more severely at both SCF and MP2, which is not surprising in light of the noted spin contamination obtained with these methods for BLi$_4$. Elimination of Li$_2$ from BLi$_5$ requires 65.2 kcal/mol, which is 6.1 kcal/mol more than for the corresponding process for BLi$_4$. For comparison, only 18.0 kcal/mol is required to dissociate a lithium atom from Li$_5$. Likewise, Li$_2$ elimination from Li$_5$ is 47.2 kcal/mol less endothermic than for BLi$_5$.

C. BLi$_6$. The O_h symmetry form is the only structure found for BLi$_6$. It is a minimum at all three levels of theory. Its B–Li bond distance of 2.145 Å (MP2) is somewhat shorter than those of the most stable BLi$_4$ (D_{2d}) and BLi$_5$ (C_{4v}) systems. The effect of electron correlation on the reduction of the B–Li distance by 0.074 Å is significant but smaller than the corresponding 0.21 Å found for the axial B–Li of BLi$_5$ (C_{4v}). BLi$_6$ has the largest cohesive energy (128.0 kcal/mol) of the BLi$_n$ clusters. Li elimination (46.2 kcal/mol) is 31 kcal/mol more exothermic than for BLi$_5$, and Li$_2$ elimination (69.8 kcal/mol) requires 4.6 kcal/mol more than the corresponding process for BLi$_5$. For comparison, Li and Li$_2$ elimination from Li$_6$ (D_{3h}) requires "only" 23.2 and 21.7 kcal/mol, respectively. The BLi$_6$ cluster is predicted to be the most stable BLi$_n$ cluster with respect to loss of Li and Li$_2$.

Positioning a boron atom inside a lithium cage, as in BLi$_6$, may be regarded as a first crude approximation of the energy of solvation for gaseous boron in the lithium melt.[8] The BLi$_6$ cohesive energy of 128.0 kcal/mol is then an estimate of the effect of the first solvation shell. The actual free energy of solvation is likely to be larger due to the entropy of mixing. Thus, on the basis of the 134.0 kcal/mol experimental cohesive energy of the boron crystal (but smaller values have also been reported),[26] the bulk lithium effect only needs to be ca. 6 kcal/mol to make B solvation in lithium a favorable process.

D. BLi$_7$. Three structures were identified for hyperlithiated BLi$_7$, one with D_{5h} symmetry and two with C_{3v} symmetry. The D_{5h} form is the most stable one. It represents a Li insertion in the Li$_4$ periphery of BLi$_6$, which accordingly lengthens the "equatorial" B–Li bond distance by 0.151 Å and the two "axial" B–Li bonds by only 0.027 Å. Capping one of the Li$_3$ faces of BLi$_6$ (O_h) with a Li atom leads to a C_{3v} form of BLi$_7$, which is 3.8 kcal/mol less stable than its D_{5h} isomer. This C_{3v} structure has a staggered conformation of the Li$_3$ and "tetrahedral" Li$_4$ units that are at opposite sites of the B atom. The barrier for rotation of the Li$_3$ plane around the principal axis leading to the C_{3v} eclipsed conformation (a transition structure) requires a significant 8.6 kcal/mol. Note that the C_{3v} structures have hexacoordinated borons.

With a coordination of seven, the boron–lithium cohesive energy has leveled off. This energy of 118.9 kcal/mol formally represents 17.0 kcal/mol per B–Li interaction versus 21.3 kcal/mol for the BLi$_6$ cluster. Accordingly, both Li and Li$_2$ eliminations also become significantly more facile compared to BLi$_6$ with respective reductions in reaction enthalpies of 24.8 and 22.0 kcal/mol. Note that it actually requires 9.0 kcal/mol less to dissociate a Li atom from BLi$_7$ than from Li$_7$. This highlights the special stability of BLi$_6$. However, the endothermicity of 47.8 kcal/mol for Li$_2$ elimination from BLi$_7$ is 14 kcal/mol larger than the corresponding endothermicity for Li$_7$.

E. BLi$_8$. Two structures with C_{3v} and D_{4h} point groups were identified. The most stable C_{3v} form can be viewed as Li-capping of the remaining Li$_3$ face of "staggered" BLi$_7$ (C_{3v}), which renders a structure in which two "tetrahedral" Li$_4$ units are bound

by one boron atom. The boron is than formally hexalithiated. This C_{3v} structure is a minimum at both MP2 and B3LYP (albeit with a broken-symmetry solution) but has two imaginary frequencies at the SCF level. The symmetry of this odd-electron species deviates slightly from a D_{3d} form, as found for CLi$_8$,[7] because of the Jahn–Teller distortion. Comparison with the related BLi$_7$ (C_{3v}, eclipsed) shows that the additional Li cap in BLi$_8$ (C_{3v}) has little influence on the structural parameters, as might be expected.

The octalithiated boride structure (D_{4h}), in which the boron atom is located at the center of a Li$_8$ cube, is 26.6 kcal/mol less stable than the C_{3v} form at the SCF level. This structure has three imaginary frequencies and was not considered further also because of convergence problems at the correlated levels. We note that Meden at al.[8] reported an energy difference at SCF/6-31G(d) of 47.8 kcal/mol between the D_{4h} and C_{3v} structures.

Owing to limitations in resources, we obtained reaction enthalpies for BLi$_8$ (C_{3v}) only at B3LYP, which we discuss here, and at MP2 (excluding zero-point energy corrections). The cohesive energy of 107.1 kcal/mol has decreased compared to BLi$_7$ with 11.8 kcal/mol and compared to BLi$_6$ with 20.9 kcal/mol. The Li and Li$_2$ eliminations are also much less demanding (just as for BLi$_7$) and require at B3LYP only 12.2 and 13.9 kcal/mol, respectively. In contrast, the corresponding Li and Li$_2$ elimination from Li$_8$ require a significant 24.1 and 34.8 kcal/mol (same level), respectively. These are further indications that the hypercoordinated boron has become saturated with lithium atoms.

Conclusion

We examined structures and stabilities of the hyperlithiated borides BLi$_n$ ($n = 4$–8) at the SCF and correlated levels of theory. Inclusion of the effects of electron correlation is important in the characterization of stationary points, consistent with a previous study of the smaller borides BLi$_n$ ($n = 1$–3). Fully hyperlithiated borides, up to BLi$_7$, are predicted to be stable. B3LYP cohesive energies of 79.9, 105.0, 128.0, and 118.9 kcal/mol were obtained for BLi$_4$, BLi$_5$, and BLi$_6$, and BLi$_7$, respectively. The most prominent hyperlithiated boride is BLi$_6$. The maximum Li coordination for boron is seven. Octalithiated boride with a boron atom surrounded by a cage of eight lithium atoms is not a minimum on the PES. Whereas the B3LYP and G2MP2 methods are in excellent agreement for the smaller lithium borides, differences of up to 15 kcal/mol are found for the larger systems. On the basis of cohesive energies and Li and Li$_2$ elimination reactions, B3LYP predicts BLi$_6$ to be the most stable cluster. G2MP2 on the other hand shows BLi$_4$ to have the highest endothermicities for loss of Li and Li$_2$. However, MCQDPT2 calculations for the BLi$_4$ system indicate that B3LYP gives more reliable results.

References and Notes

(1) Ivanic, J.; Marsden, C. J.; Hassett, D. M. *J. Chem. Soc., Chem. Commun.* **1993**, 822.
(2) Sannigrahi, A. B.; Kar, T.; Guha, N. B.; Hobza, P.; Schleyer, P. v. R. *Chem. Rev.* **1990**, *90*, 1061.
(3) Schleyer, P. v. R.; Würthwein, E.-U.; Kaufman, E.; Clark, T.; Pople, J. A. *J. Am. Chem. Soc.* **1983**, *105*, 5930.
(4) Cheng, H.-P.; Barnett, R. N.; Landman, U. *Phys. Rev. B* **1993**, *48*, 1820.
(5) Wu, C. H. *Chem. Phys. Lett.* **1987**, *139*, 357.
(6) Kudo, H. *Nature* **1992**, *355*, 432.

Hyperlithiated Borides

J. Phys. Chem. A, Vol. 103, No. 6, 1999 **715**

A-13

(7) Ivanic, J.; Marsden, C. J. *J. Am. Chem. Soc.* **1993**, *115*, 7503.

(8) Meden, A.; Mavri, J.; Bele, M.; Pejovnik, S. *J. Phys. Chem.* **1995**, *99*, 4252.

(9) Nguyen, K. A.; Lammertsma, K. *J. Phys. Chem. A* **1997**, *102*, 1608.

(10) Frisch, M. J.; Trucks, G. W.; Schlegel, H. B.; Gill, P. M. W.; Johnson, B. G.; Robb, M. A.; Cheeseman, J. R.; Keith, T.; Petersson, G. A.; Montgomery, J. A.; Raghavachari, K.; Al-Laham, M. A.; Zakrzewski, V. G.; Ortiz, J. V.; Cioslowski, J.; Stefanov, B. B.; Nanayakkara, A.; Challacombe, M.; Peng, C. Y.; Ayala, P. Y.; Chen, W.; Wong, M. W.; Andres, J. L.; Replogle, E. S.; Gomperts, R.; Martin, R. L.; Fox, D. J.; Binkley, J. S.; Defrees, D. J.; Baker, J.; Stewart, J. P.; Head-Gordon, M.; Gonzalez, C.; Pople, J. A. *GAUSSIAN94*, revision B.1; Gaussian, Inc.: Pittsburgh, 1994.

(11) Rothaan, C. C. J. *Rev. Mod. Phys.* **1951**, *23*, 69.

(12) Pople, J. A.; Nesbet, R. K. *J. Chem. Phys.* **1959**, *22*, 571.

(13) Pople, J. A.; Binkley, J. S.; Seeger, R. *Int. J. Quantum Chem. Symp.* **1976**, *10*, 1.

(14) Pople, J. A.; Krishnan, R.; Schlegel, B.; Binkley, J. S. *Int. J. Quantum Chem. Symp.* **1979**, *13*, 325.

(15) Kohn, W.; Sham, L. J. *Phys. Rev. A* **1965**, *140*, 1133.

(16) Hehre, W. J.; Ditchfield, R.; Pople, J. A. *J. Chem. Phys.* **1972**, *56*, 2257.

(17) Becke, A. D. *J. Chem. Phys.* **1993**, *98*, 5648.

(18) Becke, A. D. *Phys. Rev. A* **1988**, *38*, 3098.

(19) Lee, C.; Yang, W.; Parr, R. G. *Phys. Rev. B* **1988**, *37*, 785.

(20) Curtiss, L. A. R. K.; Pople, J. A. *J. Chem. Phys.* **1993**, *98*, 1293.

(21) Raghavachari, K.; Trucks, G. W.; Pople, J. A.; Replogle, E. S. *Chem. Phys. Lett.* **1989**, *158*, 207.

(22) Krishnan, R.; Binkley, J. S.; Seeger, R.; Pople, J. A. *J. Chem. Phys.* **1980**, *72*, 650.

(23) Curtiss, L. A.; Raghavachari, K.; Trucks, G. W.; Pople, J. A. *J. Chem. Phys.* **1991**, *94*, 7221.

(24) Schmidt, M. W.; Baldridge, K. K.; Boatz, J. A.; Elbert, S. T.; Gordon, M. S.; Jensen, J. J.; Koseki, S.; Matsunaga, M.; Nguyen, K. A.; Su, S.; Windus, T. L.; Dupuis, M.; Montgomery, J. A. *J. Comput. Chem.* **1993**, *14*, 1347.

(25) Nakano, H. *J. Chem. Phys.* **1993**, *99*, 7983.

(26) Kittel, C. *Introduction to Solid State Physics*, 6th ed.; Wiley: New York, 1986.

Theoretical Studies of B_2Li_n ($n = 1-4$)

Gantasala Naga Srinivas,[†] Tracy P. Hamilton,[†] Jerry A. Boatz,[‡] and Koop Lammertsma*,[†,§]

Department of Chemistry, University of Alabama at Birmingham, Birmingham, Alabama 35294,
Air Force Research Laboratory, AFRL/PRSP, 10 East Saturn Blvd, Edwards AFB, CA-93524, and
Department of Chemistry, Vrije Universiteit, De Boelelaan 1083, 1081 HV Amsterdam, The Netherlands

Structures and energies of the binary B_2Li_n ($n = 1-4$) clusters are predicted with the HF, MP2, and B3LYP methods using the 6-31G(d) basis set, including energy evaluations at G2MP2 and CBS-Q and the larger 6-311+G(2d) basis set for B3LYP. All systems except B_2Li_4 are also computed with the CASSCF method because of spin contamination for several of the open-shell systems. These were followed by energy evaluations with multiconfiguration perturbation theory. The global B_2Li minimum has a C_{2v} triangular form of which the $^2B_1$ state is 13 kcal/mol more stable than the $^2A_1$ state. A bent double Li-bridged structure (C_{2v}) is the global B_2Li_2 minimum with a 2.0 kcal/mol inversion barrier. The global minimum for B_2Li_3 is a triple Li-bridged propellane-like structure (D_{3h}), and for B_2Li_4 it is the quadruple Li-bridged structure (D_{4h}). All these structure have a high degree of ionicity, but in B_2Li_4 stabilization through LiLi interactions also become important. Structural patterns for the isomers of these clusters are examined. Cohesive energies ($B_2Li_n \rightarrow B_2 + Li_n$) and Li and Li_2 elimination energies are analyzed in terms of cluster stabilities.

Introduction

Small boron−lithium clusters are of interest as high-energy additives to cryogenic hydrogen.[1−6] An understanding of the bonding and energetics of these species is therefore important for the design of such fuel additives. Questions about what these clusters look like and how stable they are need to be answered. It is already well-known from the literature that polylithium compounds prefer nonclassical structures that are very different from their common hydrogen analogues.[7−10] For example, $SiLi_4$ prefers a C_{2v} over a T_d geometry.[11] Hyperlithiated compounds with unconventional structures are known, e.g., OLi_4, OLi_6; SLi_6; CLi_x, $x = 6, 8, 10, 12$; FLi_3, FLi_5; $ClLi_3$, $ClLi_5$; PLi_5[12−17] Lithium carbides and lithiated hydrocarbons are of interest in intercalated lithium−graphite (as solid-state ionic conductors) and for their importance as organolithium reagents in organic synthesis.[18−22] Even the simplest carbon−lithium clusters offer structural surprises. For example, the doubly bridged D_{2h} structure is the most stable C_2Li_2 isomer,[20] while the global C_2Li_4 minimum is a $Li^+C_2^{2-}Li_3^+$ triple ion "salt".[22] These two examples are illustrative of the differences in bonding between hydrocarbons and their lithium analogues. Despite the use of lithium boride alloys as anode material, very little is known of boron−lithium clusters. This is sharply contrasted by the abundance of information on boranes, which have been scrutinized for their multicenter bonding.[23] This paper explores how substituting hydrogens for lithium atoms will affect this bonding. Previously, we showed for BLi_n ($n = 1-8$) that each boron−lithium cluster has a large cohesive energy and that boron has a maximum coordination number of six lithiums.[24,25] In the present study we report on the binary B_2Li_n ($n = 1-4$) clusters containing two boron atoms.

[†] University of Alabama at Birmingham.
[‡] Air Force Research Laboratory.
[§] Vrije Universiteit.

Computational Methods

The geometries of the B_2Li_n ($n = 1-4$) clusters were optimized at Hartree−Fock (HF) self-consistent field, at Møller−Plesset second-order perturbation (MP2) theory, and at density functional theory (DFT) using Becke's three-parameter hybrid exchange functional combined with the Lee−Yang−Parr correlation functionals (B3LYP), all using the 6-31G(d) basis set.[10,26,27] These are shown in Figure 1 together with geometrical parameters. The nature of the stationary points was determined by evaluating the second derivatives of the energy (Hessian matrix).[28] More accurate energies were obtained with the G2MP2 and CBS-Q methods.[29,30] The G2MP2, based on MP2/6-31G(d) geometries and energies obtained with the quadratic configuration interaction QCISD(T) method with additional basis set and higher order level corrections, reportedly gives enthalpies of formation to within 2.5 kcal/mol, while the (correlated) complete basis set (CBS) extrapolation method CBS-Q, which also uses MP2/6-31G* geometries, is an alternative also known for its high accuracy. Because of high-spin contamination for some of the B_2Li, B_2Li_2, and B_2Li_3 structures, and since the spin-projected MP2 energies (PMP2) gave little improvement over the unprojected MP2 energies, additional optimizations were carried out with the complete active space (CASSCF) method (see Figure 1) followed by multiconfigurational quasidegenerate second-order perturbation theory (MC-QDPT2) for higher accuracy in the energies.[31] For B_2Li we used an active space consisting of seven electrons distributed over 12 orbitals, denoted as (7,12). For B_2Li_2 it is denoted as (8,10), and for B_2Li_3 it is denoted as (9,9); UHF natural orbitals (occupation numbers between 1.9992 and 0.0002) are used to define the CAS for the B_2Li_3 system, since CASSCF(9,11) encountered convergence problems with MO's.[32] The effect of a larger basis set (6-311+G(2d)) on the energies was also investigated for the more economical B3LYP method using geometries optimized at B3LYP/6-31G(d). Total and relative energies of the B_2Li_n ($n = 1-4$) isomers are given in Tables

9932 *J. Phys. Chem. A, Vol. 103, No. 48, 1999*

Srinivas et al.

A-15
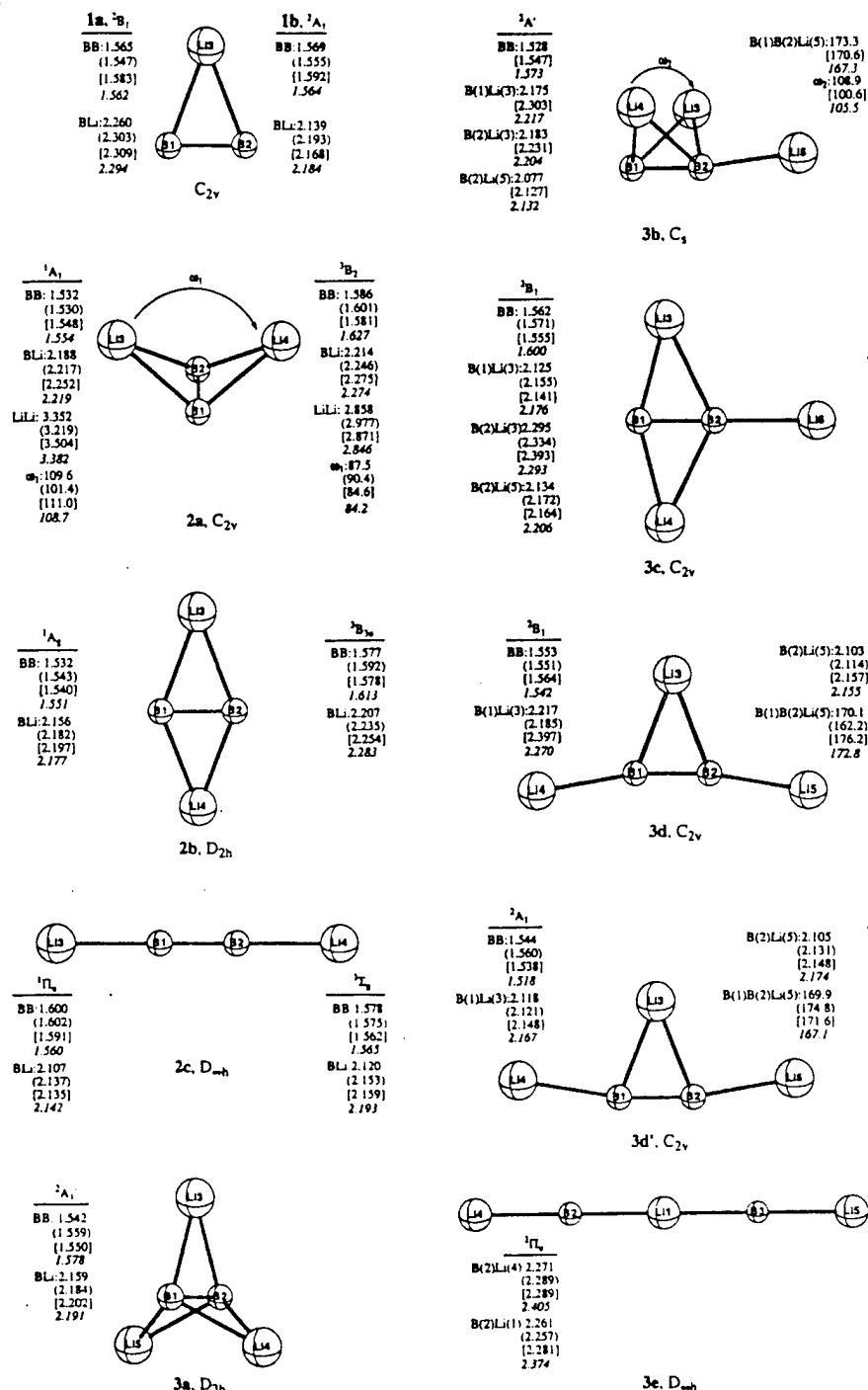
Figure 1. B_2Li_n ($n = 1-4$) structures with geometrical parameters at B3LYP, MP2 (in parentheses), HF (in brackets), and CASSCF (in italics) with the 6-31G(d) basis set.

1–4. All the calculations were carried out with the GAUSSIAN94 and GAMESS program packages.[33,34]

Results and Discussion

Before discussing each B_2Li_n cluster separately, we make some general observations with respect to their geometries. A diversity of structures has been identified with little or no conventional bonding patterns. However, it is evident that in all these structures the two boron atoms are strongly bonded to each other. In fact, the BB bond lengths vary little among these structures, nor are they very sensitive to the different theoretical levels. Thus, the average BB distance is 1.555 ± 0.055 Å at B3LYP. Slightly longer bonds result at both the MP2 (1.562 ± 0.054 Å) and HF (1.558 ± 0.043 Å) levels of theory.

All lithium diborides prefer structures with a maximum of bridging lithiums. Isomers become increasingly less stable with a growing number of terminal lithiums. These terminal BLi bonds have an average BLi distance of 2.135 ± 0.136 Å at B3LYP. Again, slightly longer bonds result at MP2 (2.169 ± 0.120 Å) and HF (2.170 ± 0.119 Å). The bridging BLi bonds are weaker and slightly longer with an average distance of 2.212 ± 0.444 Å at B3LYP. As above, larger distances are found at MP2 (2.241 ± 0.382 Å) and HF (2.272 ± 0.487 Å).

Because no experimental data are yet available for the B_2Li_n clusters, it is important to determine minimum energy structures with some degree of accuracy. Our previous extensive high-level ab initio studies on BLi_n ($n = 1-8$) have shown the need for a careful evaluation of the theoretical methods. For example,

Figure 20.

TABLE 1: Total (au) and Relative Energies (kcal/mol) for the B_2Li System[a]

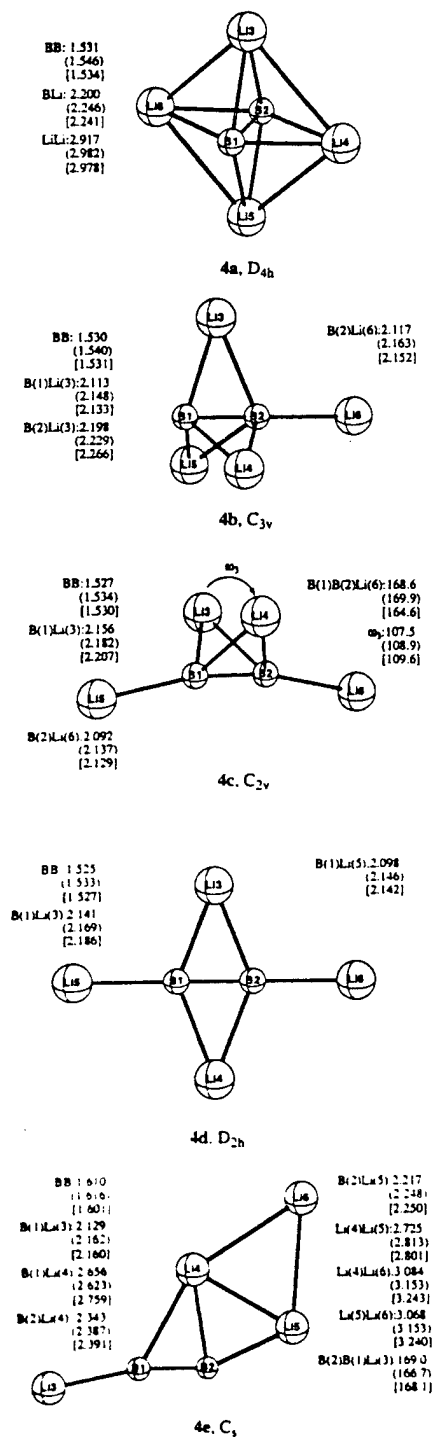| str/sym/level	total energy	$\langle S^2 \rangle$	relative energy	NIF (cm^{-1})
		1a C_{2v} ($^2B_1$)		
HF	−56.569 28	0.759	0.0	0
MP2	−56.722 42	0.759	0.0	0
B3LYP	−56.991 09	0.753	0.0	0
B3LYP(L)	−57.006 92		0.0	
G2MP2	−56.838 18		0.0	
CBS-Q	−56.834 63		0.0	
CASSCF(7,12)	−56.728 24		0.0	
MCQDPT2	−56.773 16		0.0	
		1b C_{2v} ($^2A_1$)		
HF	−56.547 40	0.863	13.7	0
MP2	−56.701 56	0.857	13.1	0
B3LYP	−56.970 37	0.750	13.0	0
B3LYP(L)	−56.987 72		12.0	
G2MP2	−56.817 81		12.8	
CBS-Q	−56.815 37		12.1	
CASSCF(7,12)	−56.706 79		13.5	
MCQDPT2	−56.753 12		12.6	

[a] Using the 6-31G(d) basis set, except for B3LYP(L), which denotes the use of 6-311+G(2d). NIF indicates the number of imaginary frequencies.

whereas B3LYP/6-31G* performs admirably for the smaller BLi_n clusters ($n = 1-3$) the agreement with MCQDPT2 and G2MP2 for the larger ones ($n = 4-8$) is somewhat less satisfactory. Because these evaluations relied also on boron cohesive energies as well as on Li and Li_2 elimination energies, we perform similar analyses for the clusters of the present study. These data, corrected for zero-point energies, are summarized in Table 5 with the boron cohesive energy defined as the enthalpy for the $B_2Li_n \rightarrow B_2 + Li_n$ reaction.

From the relative and cohesive energies (Tables 1−5) it is evident that the agreement between the theoretical methods varies substantially. As expected, the SCF performance is rather poor and will therefore not be discussed. Except for B_2Li_4, the relative and cohesive energies at MP2/6-31G* compare reason-

ably well with those at G2MP2, CBS-Q, and MCQDPT2. The difference between B3LYP and these methods is similar. Because it is the most economical one, we will focus on this method to some degree throughout the following sections in which we discuss the geometries and energetics of the various B_2Li_n clusters. Only B3LYP/6-31G* geometrical parameters are used in the discussion unless specifically noted otherwise. We refrain from discussing features of the BLi_n and Li_n fragments that have already been reported upon.[24,25]

B_2Li. The triangular form is the preferred structure for B_2Li of which the $^2B_1$ state (**1a**) is the global minimum being ca. 13.0 kcal/mol more stable than the $^2A_1$ state (**1b**) at all levels of theory employed. The BB distance of 1.565−1.569 Å is similar for both structures, which is shorter than the 1.618 Å for B_2 ($^3\Sigma_g^-$)[35] but longer than the other lithiated diborides of this study (vide infra). These bond lengths are rather insensitive to the theoretical method employed except for SCF, which generally gives too long bonds. In contrast, the BLi distances differ for the two structures and they vary with the theoretical method. Structure **1b** is the tighter of the two with 0.121 Å shorter BLi distances than the 2.260 Å of **1a**. With CASSCF-(7,12), used because of a small degree of spin contamination at HF and MP2, **1a** and **1b** have respectively 0.034 and 0.045 Å longer BLi bond lengths.

Inspection of the molecular orbitals reveals only a small lithium contribution. Essentially, the lithium atom donates its single valence electron to one of the half-filled π_u orbitals of B_2 ($^3\Sigma_g^-$) leading to the two electronic states $^2B_1$ and $^2A_1$. This charge transfer increases the BB bond order and consequently reduces its bond length relative to B_2 ($^3\Sigma_g^-$), which is also reflected in the increased BB vibrational stretching frequency (i.e., 1118 cm^{-1} for B_2Li (**1a**) and 1014 cm^{-1} for B_2 at B3LYP). The natural population analysis (NPA) of **1a** also indicates significant transfer of charge from Li to B_2, which is reflected in the Li charges of +0.73e.[36] Not surprisingly, this transfer of charge is even more pronounced in the tighter structure **1b**, i.e., +0.85e for Li. It is evident that the BLi interactions in these structures are very polar.

The stability of B_2Li, and thus the tightness of the BLi interaction, is also evident from its cohesive energy of 63 kcal/mol at G2MP2 (62 kcal/mol at CBS-Q). We note that the

A-17

9934 *J. Phys. Chem. A, Vol. 103, No. 48, 1999*   Srinivas et al.

TABLE 2: Total (au) and Relative Energies (kcal/mol) for the B₂Li₂ System[a]

str/sym/level	total energy	$\langle S^2 \rangle$	relative energy	NIF (cm⁻¹)
2a C_{2v} (¹A₁)				
HF	−64.060 43		0.0	0
MP2	−64.257 28		0.0	0
B3LYP	−64.579 28		0.0	0
B3LYP(L)	−64.596 78		0.0	
G2MP2	−64.375 03		0.0	
CBS-Q	−64.368 68		0.0	
CASSCF(8,10)	−64.211 98		0.0	
MCQDPT2	−64.297 59		0.0	
2a C_{2v} (³B₂)				
HF	−64.081 14	2.251	−13.0	1(149i)
MP2	−64.235 45	2.200	13.7	1(71i)
B3LYP	−64.564 78	2.026	9.1	1(410i)
B3LYP(L)	−64.583 68		8.2	
G2MP2	−64.341 10		21.3	
CBS-Q	−64.339 76		18.1	
CASSCF(8,10)	−64.178 26		21.2	
MCQDPT2	−64.270 51		17.0	
2b D_{2h} (¹A_g)				
HF	−64.046 76		8.6	0
MP2	−64.273 86		−10.4	0
B3LYP	−64.575 07		2.6	1(101i)
B3LYP(L)	−64.593 01		2.4	
G2MP2	−64.371 85		2.0	
CBS-Q	−64.366 01		1.7	
CASSCF(8,10)	−64.207 57		2.8	
MCQDPT2	−64.294 26		2.1	
2b D_{2h} (³B₃u)				
HF	−64.091 79	2.034	−19.8	0
MP2	−64.262 00	2.033	−2.9	0
B3LYP	−64.583 99	2.008	−3.4	0
B3LYP(L)	−64.602 05		−3.3	
G2MP2	−64.358 53		10.4	
CBS-Q	−64.356 56		7.6	
CASSCF(8,10)	−64.189 95		13.8	
MCQDPT2	−64.284 74		8.1	
2c $D_{\infty h}$ (¹Π_u)				
HF	−64.057 24		2.0	0
MP2	−64.207 92		30.9	0
B3LYP	−64.544 99		21.5	0
B3LYP(L)	−64.563 13		21.1	
G2MP2	−64.319 52		34.8	
CBS-Q	−64.314 57		34.0	
CASSCF(8,10)	−64.116 02		60.2	
MCQDPT2	−64.230 55		42.1	
2c $D_{\infty h}$ (³Σ_g)				
HF	−64.099 79	2.031	−24.7	0
MP2	−64.237 82	2.029	12.2	0
B3LYP	−64.572 08	2.010	4.5	0
B3LYP(L)	−64.589 05		4.8	
G2MP2	−64.336 08		24.4	
CBS-Q	−64.334 36		21.5	
CASSCF(8,10)	−64.147 49		40.5	
MCQDPT2	−64.253 18		27.9	

[a] See footnote of Table 1.

cohesion energy of 56.3 kcal/mol at B3LYP is slightly less, while the much smaller energies at MP2 and HF for this dissociation of Li indicate the inadequacy of these methods for this system.

B₂Li₂. Three stationary points were characterized on each of the singlet and triplet surfaces. The global minimum at the higher levels of theory is the singlet ¹A₁ structure **2a**, whereas MP2 and B3LYP prefer instead the ¹A_g and ³B₃u states of planar **2b**, respectively. Structure **2a** has a puckering angle of ca. 110°. Inversion via planar **2b** requires only 2.6 kcal/mol (at B3LYP), indicating the butterfly structure to be highly flexible. G2MP2

TABLE 3: Total (au) and Relative Energies (kcal/mol) for the B₂Li₃ System[a]

str/sym/level	total energy	$\langle S^2 \rangle$	relative energy	NIF (cm⁻¹)
3a D_{3h} (²A₁′)				
HF	−71.574 61	0.776	0.0	1(720i)
MP2	−71.791 81	0.776	0.0	0
B3LYP	−72.168 44	0.755	0.0	0
B3LYP(L)	−72.187 95		0.0	
G2MP2	−71.893 90		0.0	
CBS-Q	−71.889 41		0.0	
CASSCF(9,9)	−71.670 69		0.0	
MCQDPT2	−71.811 90		0.0	
3b C_s (²A′)				
HF	−71.569 80	1.523	3.0	0
MP2	collapsed to **3a**			
B3LYP	−72.147 23	0.768	13.3	0
B3LYP(L)	−72.166 11		13.7	
CASSCF(9,9)	−71.652 46		11.4	
MCQDPT2	−71.786 53		15.9	
3c C_{2v} (²B₁)				
HF	−71.556 40	0.793	11.4	1(267i)
MP2	−71.748 27	0.793	27.3	1(539i)
B3LYP	−72.136 68	0.757	19.9	0
B3LYP(L)	−72.155 42		20.4	
G2MP2	−71.854 11		25.0	
CBS-Q	−71.850 19		24.6	
CASSCF(9,9)	−71.637 01		21.1	
MCQDPT2	−71.770 47		25.9	
3d C_{2v} (²B₁)				
HF	−71.559 49	1.337	9.5	1(118i)
MP2	−71.743 10	0.820	30.6	0
B3LYP	−72.135 96	0.755	20.4	0
B3LYP(L)	−72.153 65		21.5	
G2MP2	−71.851 57		22.8	
CBS-Q	−71.847 67		22.4	
CASSCF(9,9)	−71.615 71		34.5	
MCQDPT2	−71.759 24		33.0	
3d′ C_{2v} (²A₁)				
HF	−71.542 49	0.948	20.2	0
MP2	−71.728 94	0.884	39.5	0
B3LYP	−72.121 69	0.769	29.3	0
B3LYP(L)	−72.141 87		28.9	
CASSCF(9,9)	−71.600 68		43.9	
MCQDPT2	−71.753 34		36.7	
3e $D_{\infty h}$ (²Π_u)				
HF	−71.401 03	0.767	108.9	1(43i)
MP2	−71.546 18	0.767	154.1	0
B3LYP	−71.969 20	0.755	125.0	0
B3LYP(L)	−71.981 09		129.8	
G2MP2	−71.671 62		139.5	
CBS-Q	−71.664 19		141.3	
CASSCF(9,9)	−71.438 83		145.5	
MCQDPT2	−71.538 29		171.7	

[a] See footnote of Table 1.

gives a similar inversion barrier (2.0 kcal/mol) as do CBS-Q, CASSCF, and MCQDPT2, but MP2 favors **2b** instead by as much as 10.4 kcal/mol. On becoming planar, the 1.532 Å BB bond length does not alter, even though the BLi distances decrease with 0.03 Å as a result of stronger ionic interactions. The NPA charges on Li(+) and B(−) are larger for **2b** (0.85e) than for **2a** (0.75e). Apparently, the second Li atom donates its valence electron to the singly occupied π orbital of B₂Li. This increases the charges and the BB bond order (which is reflected in 0.07 Å shorter BLi distances and a 0.03 Å shorter BB bond length, respectively), culminating in a tighter packed structure of high ionic character. This increased ionicity of **2a**, compared to B₂Li, is supported by the noted NPA charges. Its cohesive energy (B₂Li₂ → B₂ + Li₂) amounts to a large 102 kcal/mol at G2MP2 and CBS-Q (and 6 kcal/mol less at B3LYP). Its 66

TABLE 4: Total (au) and Relative Energies (kcal/mol) for the B$_2$Li$_4$ System[a]

str/sym/level	total energy	relative energy	NIF (cm^{-1})
4a D_{4h}			
HF	−79.041 30	0.0	0
MP2	−79.296 22	0.0	0
B3LYP	−79.727 47	0.0	0
B3LYP(L)	−79.749 95	0.0	
G2MP2	−79.402 81	0.0	
CBS-Q	−79.394 15	0.0	
4b C_{3v}			
HF	−79.042 87	−1.0	0
MP2	−79.290 98	3.3	0
B3LYP	−79.724 34	2.0	0
B3LYP(L)	−79.744 89	3.2	
G2MP2	−79.398 23	2.9	
CBS-Q	−79.390 86	2.1	
4c C_{2v}			
HF	−79.035 37	3.7	0
MP2	−79.277 91	11.5	0
B3LYP	−79.714 78	8.0	0
B3LYP(L)	−79.734 35	9.8	
G2MP2	−79.385 52	10.8	
CBS-Q	−79.377 68	10.3	
4d D_{2h}			
HF	−79.031 44	6.2	1(66i)
MP2	−79.274 43	13.7	1(49i)
B3LYP	−79.711 59	10.0	1(62i)
B3LYP(L)	−79.731 69	11.5	
G2MP2	−79.382 35	12.8	
CBS-Q	−79.375 18	11.9	
4e C_s			
HF	−78.981 49	37.5	0
MP2	−79.156 91	87.4	0
B3LYP	−79.617 57	69.0	0
B3LYP(L)	−79.634 26	72.6	
G2MP2	−79.285 19	73.8	
CBS-Q	−79.276 43	73.9	

[a] See footnote of Table 1.

kcal/mol endothermicity (G2MP2, 60 kcal/mol at B3LYP) for Li elimination is even slightly more (by 3 kcal/mol) than that for B$_2$Li ($^2B_1$).

On the triplet surface, **2a** ($^3B_2$ state) has a tetrahedral form with a puckering angle of less than 90° and a LiLi distance of only 2.858 Å (B3LYP). This transition structure is 17 kcal/mol less stable than the $^1A_1$ singlet at MCQDPT2. On the other hand, the $^3B_{3u}$ state of rhombic **2b** is a local minimum and only 8.4 kcal/mol (G2MP2, 5.0 kcal/mol at CBS-Q) less stable than the singlet ^1A_g state. We note that the energy differences for these triplet structures are only consistent at the higher levels of theory.

The linear $^1\Pi_u$ state isomer **2c** is a minimum energy structure with a longer BB distance than in **2a** ($^1A_1$) and **2b** (^1A_g). This suggests that in **2c** the Li atom does not donate its valence electron to the Π_u orbitals of B$_2$ as effectively as in **2a** and **2b**, where the Li atoms are bridging rather than terminal. This notion is also supported by the NPA charges in Table S1 in Supporting Information. Structure **2c** is significantly less stable than the butterfly form **2a**. The energy difference depends strongly on the theoretical method employed and ranges, for example, from 21.5 to 34.8 to 42.1 kcal/mol at B3LYP, G2MP2, and MC-QDPT2, respectively. Because of the need for a multiconfigurational approach in these "electron-deficient" linear systems, we consider the energy obtained with multiconfigurational quasidegenerate perturbation theory to be the most accurate. The energy difference of the corresponding $^3\Sigma_g$ state isomer of **2c** (also a minimum) with **2a** varies less with the more sophisticated theories (i.e., 24.4 and 27.9 kcal/mol for G2MP2 and MCQDPT2) but is surprisingly small at B3LYP (4.5 kcal/mol) and large at CASSCF(7,10) (40.5 kcal/mol). The triplet structure is more stable than the singlet form with an energy difference of 14.2 kcal/mol at MCQDPT2.

B$_2$Li$_3$. Six minima were identified on the B3LYP hypersurface of doublet B$_2$Li$_3$, of which five are also stationary points at MP2. These structures extend the features already seen for the smaller homologues. The global minimum is the B$_2$ triple Li-bridged propellane structure **3a**. This structure is very similar to the butterfly B$_2$Li$_2$ structure **2a** but capped with another Li atom. Its BB bond length of 1.542 Å (B3LYP) is between those of singlet and triplet **2a**, respectively, but its 2.159 Å BLi distance is slightly shorter. The NPA charge on the lithiums is +0.77e each, just as for **2a**. Evidently, all three Li atoms donate their valence electrons to the B$_2$ ($^3\Sigma_g^-$) unit to occupy its σ_g and two π_u orbitals; the BB distance in B$_2^{3-}$ ($^2\Sigma_g$) is 1.630 Å (B3LYP). The Li dissociation energy for **3a** of 55 kcal/mol at G2MP2 and CBS-Q, though, is 10 kcal/mol less than that for **2a**, which suggests that the exothermicity is reduced on binding a third Li atom to B$_2$. Because of the LiLi bonding in Li$_n$, this reduced bonding of the third Li atom is not reflected in the B$_2$ cohesive energies, which are 145, 102, and 63 kcal/mol at G2MP2 for B$_2$Li$_3$, B$_2$Li$_2$, and B$_2$Li, respectively, or ca. 42 kcal/mol per *added* Li atom; the CBS-Q data are similar. Interestingly, B3LYP gives Li dissociation energies of ca. 60 kcal/mol for both **3a** and **2a** and a cohesive energy for **3a** identical to that from G2MP2 (145 kcal/mol). Binding energies at both the HF and MP2 levels of theory are less satisfactory.

Structure **3b** can be viewed as resulting from a Li side-on addition to the butterfly structure **2a**, while **3c** represents its planar form. This planarization requires 6.6 kcal/mol at B3LYP

TABLE 5: B$_2$ Cohesive Energies and Li and Li$_2$ Dissociation Energies (in kcal/mol)

reaction	HF[a]	MP2[a]	B3LYP[a]	B3LYP(L)[b]	G2MP2	CBS-Q
B$_2$ Cohesion						
B$_2$Li → B$_2$ + Li	38.2	44.8	56.3	58.5	63.0	62.1
B$_2$Li$_2$ → B$_2$ + Li$_2$	72.0	94.4	96.0	98.4	102.3	102.2
B$_2$Li$_3$ → B$_2$ + Li$_3$	114.3	152.2	145.5	148.1	144.6	142.7
B$_2$Li$_4$ → B$_2$ + Li$_4$	130.2	173.1	163.0	166.7	159.7	160.6
Li Dissociation						
B$_2$Li$_2$ → B$_2$Li + Li	36.1	63.4	59.5	60.3	65.7	64.0
B$_2$Li$_3$ → B$_2$Li$_2$ + Li	51.2	64.4	60.6	61.6	54.4	55.7
B$_2$Li$_4$ → B$_2$Li$_3$ + Li	20.5	44.2	41.4	43.1	48.1	45.6
Li$_2$ Dissociation						
B$_2$Li$_3$ → B$_2$Li + Li$_2$	85.1	113.9	100.3	101.5	93.7	95.8
B$_2$Li$_4$ → B$_2$Li$_2$ + Li$_2$	69.5	94.7	82.2	84.3	76.2	77.4

[a] Using the 6-31G(d) basis set and inclusion of zero-point energy (ZPE) corrections. The MP2 values that involve B$_2$Li$_3$ use HF-ZPE corrections.
[b] Using the 6-311+G(2d) basis set and B3LYP/6-31G(d) ZPE corrections.

9936 *J. Phys. Chem. A, Vol. 103, No. 48, 1999*

Srinivas et al.

H - 17

and 10 kcal/mol at MCQDPT2. Interestingly, B3LYP characterizes both structures as minima, while **3b** could not be obtained at MP2. Double-Li-bridged **3b** is less stable than the triple-bridged form by 13.3 kcal/mol at B3LYP (15.9 kcal/mol at MCQDPT2).

The two single-Li-bridged structures **3d** ($^2B_1$ state) and **3d'** ($^2A_1$ state) differ mainly in the tilting angle of their terminal lithium atoms but also have slightly different BB bond lengths and BLi bridging distances. The energy difference between the two isomers amounts to 3.7 kcal/mol at MCQDPT2 (8.9 kcal/mol at B3LYP) of which **3d** is 33 kcal/mol (20 kcal/mol at B3LYP) less stable than the global minimum. From the presence of significant spin contamination we infer that multiconfigurational quasidegenerate perturbation theory gives the more accurate energies.

Structure **3e** represents a Li insertion into the BB bond, separating the boron atoms, and is clearly a high-energy isomer but nonetheless is a minimum at the MP2 and B3LYP levels. It is merely included in this study to illustrate that Li can fulfill a coordinating role in the formation of B_xLi_y clusters from Li and B atoms.

B_2Li_4. The bonding patterns found in the smaller binary B_2-Li_n clusters are also present and even extended in B_2Li_4. Four minima and a transition structure were identified. Surprisingly, the global minimum is structure **4a**, which has its 1.531 Å B–B bond bridged by four Li atoms. Each boron is pentacoordinated and has an inverted geometry. Because **4a** and propellane **3a** have similar BB bond lengths, it appears that the fourth lithium does not influence the BB bond strength. The NPA charge on the lithiums of $+0.59e$ each is $+0.18e$ less than in **3a**, while the charge on the B_2 fragment remains at ca. $-2.35e$. Thus, the interaction between the lithiums in **4a** is strongly enhanced, which also agrees with the LiLi distances of 2.971 Å. Similar short distances were found for higher coordinated BLi_n ($n = 4-8$) structures. The cohesive energy of ca. 160 kcal/mol (G2MP2, CBS-Q) translates into 40 kcal/mol per lithium, or 8 kcal/mol less than the per lithium energy for **3a**, which infers a different bonding stabilization in the four-Li-bridged structure. Also the Li and Li_2 dissociation energies of the B_2Li_4 global minimum are smaller than for **3a**.

Structure **4b** resembles **3a** but has an extra Li added side-on. This terminal BLi bond distorts the propellane structure only slightly and reduces the charge of the bridging lithiums to $+0.63e$. Its energy difference with **4a** is only 2.9 kcal/mol at G2MP2 with similar values at the other correlated levels. Evidently, the energy surface for binding the fourth lithium is rather soft, and B_2Li_4 should therefore be a rather flexible system.

Isomer **4c** with the added terminal BLi bond extends the butterfly structures of **3b** and **2a**. Their structural properties are similar except that the terminal BLi bonds in **4c** are tilted downward. Inversion via **4d** (a transition structure) requires only 1.6–2.0 kcal/mol, depending on the theoretical method employed, again illustrating the flexible nature of B_2Li_4. The energy difference of **4c** compared to the global minimum is 10.8 at G2MP2 and slightly less with the other methods.

Even though **4e** seems at first sight an unusual structure, it represents a B_2^{2-} dianion complexed with Li^+ and Li_3^+ cations at opposite sides. The terminal Li has indeed, as expected, an NPA charge of $+0.74e$, but the side-complexed triangular Li_3^+ is strongly polarized with, in fact, a negative charge of $-0.40e$ on the distal Li. Interestingly, the carbon analogue of this structure is among the two most stable C_2Li_4 isomers[22] and has also been formulated as a $Li^+C_2^{2-}Li_3^-$ acetylene triple ion "salt".

Diboride **4e** is, however, by far the least stable of the B_2Li_4 isomers.

Conclusions

This computational study of the structural and energetic details of small binary B/Li clusters reveals several characteristics, some of which are unexpected. The structural diversity of these clusters is large and differs from those of both Li/C clusters and diboranes. The most salient features are the following. (1) All B_2Li_n ($n = 1-4$) structures contain a B_2 unit with a short BB bond. (2) Bridging of this B_2 unit by lithiums is preferred for all B_2Li_n ($n = 1-4$) systems including the four Li-bridged B_2Li_4 structure. (3) All display a high degree of ionicity except for the B_2Li_4 structure in which case stabilization also occurs through LiLi interactions. (4) As a result, all structures are rather flexible. (5) B3LYP/6-31G(d) performs rather well in calculating geometries and their relative energies. Use of the extended 6-311+G(2d) basis set has little influence on the relative energies and on neither the B_2 cohesive energies nor the Li and Li_2 dissociation energies. (6) These dissociation energies and even more importantly the relative energies of the isomeric structures are less than satisfactory with HF and MP2/6-31G(d). (7) G2MP2, CBS-Q, and MCQDPT2 perform equally well for most systems. (8) The B_2 cohesive energy tapers off when the fourth lithium is added.

Supporting Information Available: Tables of NPA charges and harmonic vibrational frequencies. This material is available free of charge via the Internet at http://pubs.acs.org.

References and Notes

(1) Kaufman. J. J.; Sachs. L. M. *J. Chem. Phys.* **1970**, *52*, 645.

(2) Cade. P. E.; Huo. W. M. *At. Data Nucl. Data Tables* **1975**, *15*, 1.

(3) Zhu. Z. H.; Murrell. J. N. *Chem. Phys. Lett.* **1982**, *88*, 262.

(4) Knowles. D. B.; Murrell. J. N. *J. Mol. Struct.: THEOCHEM* **1986**, *135*, 169.

(5) Saxon, R. P. Theoretical Studies of Boron Compounds. *Proceedings of the High Energy Density Matter*, Woods Hole, MA, 1992.

(6) Sheehy, J. A. Spectroscopy of Lithium Boride, A candidate HEDM Species. *Proceedings of the High Energy Density Matter*, Woods Hole, MA, 1995.

(7) Schleyer, P. v. R. *Pure Appl. Chem.* **1983**, *55*, 355; **1984**, *56*, 151.

(8) Maercker, A.; Thies, M. *Top. Curr. Chem.* **1987**, *138*, 1.

(9) Ritchie, J. P.; Bachrach. S. M. *J. Am. Chem. Soc.* **1987**, *109*, 5909.

(10) Hehre, W.; Radom, L.; Schleyer, P. v. R.; Pople, J. A. *Ab Initio Molecular Orbital Theory*; Wiley: New York, 1986.

(11) Schleyer, P. v. R.; Reed, A. E. *J. Am. Chem. Soc.* **1988**, *110*, 4453.

(12) Gillespie, R. J.; Hargittai, I. *The VSEPR Model of Molecular Geometry*; Allyn and Bacon: Boston, 1991.

(13) Schleyer, P. v. R.; Wurthwein, E.-U.; Pople, J. A. *J. Am. Chem. Soc.* **1982**, *104*, 5839.

(14) Ivanic, J.; Marsden, C. J.; Hassett, D. M. *J. Chem. Soc., Chem. Commun.* **1993**, 822.

(15) Schleyer, P. v. R.; Wurthwein, E.-U.; Kaufmann, E.; Clark, T.; Pople, J. A. *J. Am. Chem. Soc.* **1983**, *105*, 5930.

(16) Ivanic, J.; Marsden, C. J. *J. Am. Chem. Soc.* **1993**, *115*, 7503.

(17) Marsden, C. J. *J. Chem. Soc., Chem. Commun.* **1989**, 1356.

(18) Fan, Q.; Pfeiffer, G. V. *Chem. Phys. Lett.* **1989**, *162*, 479.

(19) Ivanic, J.; Marsden, C. J. *Organometallics* **1994**, *13*, 5141.

(20) Schleyer, P. v. R. *J. Phys. Chem.* **1990**, *94*, 5560.

(21) Kos, A.; Poppinger, D.; Schleyer, P. v. R.; Thiel, W. *Tetrahedron Lett.* **1980**, *21*, 2151.

(22) Dorigo. A. E.; van Eikema Hommes. N. J. R.; Krog-Jesperson, K.; Schleyer, P. v. R. *Angew. Chem., Int. Ed. Engl.* **1992**, *31*, 1602.

B_2Li_n ($n = 1-4$)

J. Phys. Chem. A, Vol. 103, No. 48, 1999 **9937**

(23) Cotton, F. A.; Wilkinson, G. *Advanced Inorganic Chemistry*; Interscience: New York, 1972.

(24) Nguyen, K. A.; Lammertsma, K. *J. Phys. Chem. A* **1998**, *102*, 1608.

(25) Nguyen, K. A.; Srinivas, G. N.; Hamilton, T. P.; Lammertsma, K. *J. Phys. Chem. A* **1999**, *103*, 710. Meden, A.; Mavri, J.; Bele, M.; Pejovnik, S. *J. Phys. Chem.* **1995**, *99*, 4252.

(26) Hehre, W. J.; Ditchfield, R.; Pople, J. A. *J. Chem. Phys.* **1972**, *56*, 2257. Møller, C.; Plesset, M. S. *Phys. Rev.* **1934**, *46*, 618.

(27) Becke, A. D. *J. Chem. Phys.* **1993**, *98*, 5648. Becke, A. D. *Phys. Rev. A* **1988**, *38*, 3098. Lee, C.; Yang, W.; Parr, R. G. *Phys. Rev. B* **1988**, *37*, 785. Vosko, S. H.; Wilk, L.; Nusair, M. *Can. J. Phys.* **1980**, *58*, 1200.

(28) Pople, J. A.; Raghavachari, K.; Schlegel, H. B.; Binkley, J. S. *Int. J. Quantum Chem. Symp.* **1979**, *13*, 255.

(29) Curtiss, L. A.; Raghavachari, K.; Pople, J. A. *J. Chem. Phys.* **1993**, *98*, 1293. Curtiss, L. A.; Raghavachari, K.; Trucks, G. W.; Pople, J. A. *J. Chem. Phys.* **1991**, *94*, 7221.

(30) Ochterski, J. W.; Petersson, G. A.; Montgomery, J. A., Jr. *J. Chem. Phys.* **1996**, *104*, 2598. Ochterski, J. W.; Petersson, G. A.; Wiberg, K. B. *J. Am. Chem. Soc.* **1995**, *117*, 11299.

(31) Nakano, H. *J. Chem. Phys.* **1993**, *99*, 7983.

(32) Pulay, P.; Hamilton, T. P. *J. Chem. Phys.* **1988**, *88*, 4926.

(33) Frisch, M. J.; Trucks, G. W.; Schlegel, H. B.; Gill, P. M. W.; Johnson, B. G.; Robb, M. A.; Cheeseman, J. R.; Keith, T.; Petersson, G. A.; Montgomery, J. A.; Raghavachari, K.; Al-Laham, M. A.; Zakrzewski, V. G.; Ortiz, J. V.; Foresman, J. B.; Cioslowski, J.; Stefanov, B. B.; Nanayakkara, A.; Challacombe, M.; Peng, C. Y.; Ayala, P. Y.; Chen, W.; Wong, M. W.; Andres, J. L.; Replogle, E. S.; Gomperts, R.; Martin, R. L.; Fox, D. J.; Binkley, J. S.; Defrees, D. J.; Baker, J.; Stewart, J. P.; Head-Gordon, M.; Gonzalez, C.; Pople, J. A. *GAUSSIAN 94*, revision E.2; Gaussian, Inc.: Pittsburgh, PA, 1995.

(34) Schmidt, M. W.; Baldridge, K. K.; Boatz, J. A.; Elbert, S. T.; Gordon, M. S.; Jensen, J. J.; Koseki, S.; Matsunaga, M.; Nguyen, K. A.; Su, S.; Windus, T. L.; Dupuis, M.; Montgomery, J. A. *J. Comput. Chem.* **1993**, *14*, 1347.

(35) Boldyrev, A. I.; Gonzales, N.; Simons, J. *J. Phys. Chem.* **1994**, *98*, 9931.

(36) Reed, A. E.; Curtiss, L. A.; Weinhold, F. *Chem. Rev.* **1988**, *88*, 899.

Will an η^3-Si$_3$H$_3$ Ligand Form Sandwich Compounds with Main Group Elements?

Gantasala N. Srinivas,[†] Tracy P. Hamilton,[†] Eluvathingal D. Jemmis,*,[‡]
Michael L. McKee,[‖] and Koop Lammertsma*,[†,⊥]

*Contribution from the Department of Chemistry, University of Alabama at Birmingham,
Birmingham, Alabama 35294, School of Chemistry, University of Hyderabad, Hyderabad 500 046, India,
Department of Chemistry, Auburn University, 179 Chemistry Building, Auburn, Alabama 36849, and
Faculty of Chemistry, Vrije Universiteit, De Boelelaan 1083, 1081 HV Amsterdam, The Netherlands*

Abstract: η^3-Si$_3$H$_3$ sandwich compounds **5** and **6**, with classical and H-bridged ligands, respectively, having the main group elements boron and carbon as central atoms are minima at B3LYP/6-311++G(2d,2p). The stability of these systems is assisted by transfer of charge from the ligands to the central atom and is reversed from that of cyclopentadienyl sandwiches. The C and B containing pyramidal complexes **7**, containing both a η^3-Si$_3$H$_3$ and a μ^2-Si$_3$H$_3$ ligand, are more stable than **5** by 20.7 and 8.5 kcal/mol, respectively. The spiro compounds **8**, in which the C and B atoms are sandwiched by two allylic μ^2-Si$_3$H$_3$ ligands, are still more stable by 29.6 and 21.9 kcal/mol, respectively. All three types (face-face, face-side, side-side) of sandwich structures are considered viable targets for synthetic pursuit. The Be complexes deviate from the C and B analogues because Be is much more electropositive. In the preferred cluster structure **9** the Be atom sits in a Si$_6$H$_6$ basket.

Introduction

Sandwich compounds have become important structural elements in chemistry. The discovery of ferrocene in 1951[1] led to the development of sandwiched transition metals and actinides and even main group metals such as Cp$_2$Li$^-$, Cp$_2$Na$^-$, and Cp$_2$Mg.[2,3] All have electropositive metals sandwiched by η^5-cyclopentadienyl anion (Cp) rings. Extension to larger rings led to the involvement of f-orbitals such as in bis-cyclooctatetraenyluranium, while similar attempts at smaller η^3-ligands have been limited to mixed systems such as CpNi(C$_3$Ph$_3$).[2,4]

It has been suggested that sandwiches with cyclopropenyl cation ligands and a central atom from the first-row elements are feasible.[5] Formally, each η^3-ring provides 3π electrons with two coming from the central atom (charge adjusted) leading to eight interstitial valence electrons to fill the bonding orbitals. The cationic ligands require the central atom to be less electropositive, giving a reversed polarity from that of the Cp$_2$M sandwiches. It is then not surprising that an early theoretical study showed the cyclopropenyl (C$_3$H$_3$$^+$) sandwiches of Be and

B to be unstable.[5] We now explore the heavier congener, the trisilacyclopropenium cation Si$_3$H$_3$$^+$, as a sandwich ligand for the main group elements Be, B, and C.

Si$_3$H$_3$$^+$ has been detected in the gas phase.[6] Its ring structure **1** (D_{3h}) is 23.7 kcal/mol more stable at B3LYP/6-311++G-(2d,2p) than the triply H-bridged isomer **2** (C_{3v})[7] and has shown potential as a η^3-ligand in pyramidal structures **3** (C_{3v}) and **4** (C_{3v}).[8] We are unaware of reports on sandwiches with two such ligands. Cyclic Si$_3$H$_3$$^+$ is a weakly delocalized 2π system and may function as a η^3-ligand (face-on) and as a μ^2-ligand (side-on) resulting in the face-face (**I**, π-complex), face-side (**II**, σ,π-complex), and side-side (**III**, σ-complex) structural arrangements. Of these, **I** relates to the Cp$_2$M systems, **III** relates to the spiro structures, and **II** is an extension of pyramidal structure **3**. We will show remarkable examples of these three forms for

1   **2**

3   **4**
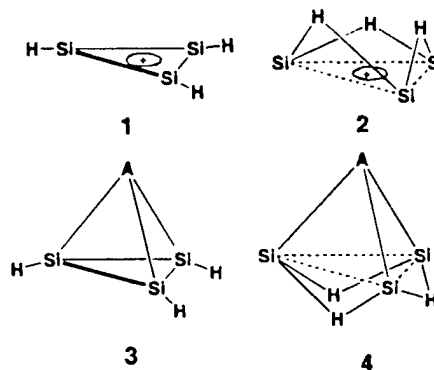
A = BH⁻, CH, N, NH⁺, NO, SiH, P, PH⁺ and PO

the main group elements boron and carbon, i.e., (Si$_3$H$_3$)$_2$B$^+$ and

† University of Alabama at Birmingham.
‡ University of Hyderabad.
‖ Auburn University.
⊥ Vrije Universiteit. E-mail: lammert@chem.vu.nl.
(1) (a) Kealy, T. J.; Pauson, P. L. *Nature* **1951**, *168*, 1039. (b) Cotton, F. A.; Wilkinson, G.; Murillo, C. A.; Bochmann, M. *Advanced Inorganic Chemistry*, 6th ed.; Wiley-Interscience: New York, 1999.
(2) Elschenbroich, Ch.; Salzer, A. *Organometallics: A Concise Introduction*, 2nd revised ed.; VCH: New York, 1992.
(3) (a) Harder, S.; Prosenc, M. H.; Rief, U. *Organometallics* **1996**, *15*, 118. (b) Kwon, O.; Kwon, Y. *THEOCHEM* **1997**, *401*, 133. (c) Harder, S.; Prosenc, M. H. *Angew. Chem., Int. Ed. Engl.* **1994**, *33*, 1744. (d) Stalke, D. *Angew. Chem., Int. Ed. Engl.* **1994**, *33*, 2168. (e) Bünder, W.; Weiss, E. *J. Organomet. Chem.* **1975**, *92*, 1. (f) Haaland, A.; Lusztyk, J.; Brunvoll, J.; Starowieyski, K. B. *J. Organomet. Chem.* **1975**, *85*, 279.
(4) (a) Streitwieser, A., Jr.; Mueller-Westerhoff, U. *J. Am. Chem. Soc.* **1968**, *90*, 7364. (b) Rausch, M. D.; Tuggle, R. M.; Weaver, D. L. *J. Am. Chem. Soc.* **1970**, *92*, 4981.
(5) Collins, J. B.; Schleyer, P. v. R. *Inorg. Chem.* **1977**, *16*, 152.

(6) (a) Mandich, M. L.; Reents, W. D., Jr. *J. Chem. Phys.* **1991**, *95*, 7360. (b) Stewart, G. W.; Henis, J. M. S.; Gaspar, P. P. *J. Chem. Phys.* **1973**, *58*, 890.

B   *J. Am. Chem. Soc.*   *Srinivas et al.*

A-22

$(Si_3H_3)_2C^{2+}$, as well as the limited ability of beryllium to play a similar role. The focus is on ligand 1 because its derivatives are more amenable for synthetic pursuit. For the low-energy structures, permethyl substitution is also studied to explore experimental feasibility.

Computational Methods

Structures 5X—10X (X = Be, B, C) were first optimized and characterized by their Hessian signature at the HF and B3LYP levels using the 6-31G(d) basis set.[9-11] We next optimized sandwiches I, II, and III at B3LYP/6-311++G(2d,2p).[9,12] Correlation effects were computed by energy evaluation at MP2/6-311++G(2d,2p) using the B3LYP/6-311++G(2d,2p) geometries.[13] All the calculations were done using the GAUSSIAN94 suite of programs.[14] The permethyl-substituted systems were optimized at the HF/6-31G(d) level using PQS (Parallel Quantum Solutions)[15] on a 4-node QS4-450 Quantum Station. The nature of the stationary points was determined by evaluating the second derivatives of the energy using GAUSSIAN94. Figure 1 shows the relevant structures with selected geometrical parameters. The total and relative energies are given in Table 1. We use natural charges obtained from the natural bond orbital (NBO) analysis.[16] Emphasis is given to the "classical" sandwich forms, and particularly to those with boron and carbon, to stimulate their experimental pursuit as the propensity for bridging may not go beyond hydrogen.[7,8,17]

Results and Discussions

π-Sandwiches (I). Given the unusual coordination number of carbon and boron with $Si_3H_3^+$ ligands in structures 5C and 5B, it was quite surprising to find that both structures were minima in the D_{3h} point group. Also, structures 6B and 6C (D_{3d}) with the H-bridging "nonclassical" $Si_3H_3^+$ ligand 2 are minima. The π-stabilization in these systems must be very effective in light of boron and carbon's high propensity for covalent bonding. Why do these structures exist as minima?

Molecular orbital analysis of dication 5C shows the valence 2e′ and 2a″ MOs to contain contributions from both the $Si_3H_3^+$

(7) (a) Jemmis. E. D.; Srinivas, G. N.; Leszczynski, J.; Kapp, J.; Korkin, A. A.; Schleyer, P. v. R. *J. Am. Chem. Soc.* **1995**, *117*, 11361. (b) Srinivas, G. N.; Jemmis. E. D.; Korkin, A. A.; Schleyer, P. v. R. *J. Phys. Chem. A.* **1999**, *103*, 11034.

(8) (a) Jemmis. E. D.; Srinivas, G. N. *J. Am. Chem. Soc.* **1996**, *118*, 3738. (b) Srinivas, G. N.; Jemmis. E. D. *J. Am. Chem. Soc.* **1997**, *119*, 12968.

(9) (a) Hehre. W. J.; Radom. L.; Schleyer, P. v. R.; Pople, J. A. *Ab Initio Molecular Orbital Theory*; Wiley: New York, 1986. (b) Hehre, W. J.; Ditchfield, R.; Pople, J. A. *J. Chem. Phys.* **1972**, *56*, 2257.

(10) (a) Becke. A. D. *J. Chem. Phys.* **1993**, *98*, 5648. (b) Lee, C.; Yang, W.; Parr, R. G. *Phys. Rev. B* **1988**, *37*, 785.

(11) Pople, J. A.; Raghavachari, K.; Schlegel, H. B.; Binkley, J. S. *Int. J. Quantum Chem. Symp.* **1979**, *13*, 255.

(12) Clark. T.; Chandrasekhar, J.; Spitznagel, G. W.; Schleyer, P. v. R. *J. Comput. Chem.* **1983**, *4*, 294.

(13) Møller, C.; Plesset, M. S. *Phys. Rev.* **1934**, *46*, 618.

(14) Frisch. M. J.; Trucks, G. W.; Schlegel, H. B.; Gill, P. M. W.; Johnson, B. G.; Robb, M. A.; Cheeseman, J. R.; Keith, T.; Petersson, G. A.; Montgomery, J. A.; Raghavachari, K.; Al-Laham, M. A.; Zakrzewski, V. G.; Ortiz, J. V.; Foresman, J. B.; Cioslowski, J.; Stefanov, B. B.; Nanayakkara, A.; Challacombe, M.; Peng, C. Y.; Ayala, P. Y.; Chen, W.; Wong, M. W.; Andres, J. L.; Replogle, E. S.; Gomperts, R.; Martin, R. L.; Fox, D. J.; Binkley, J. S.; Defrees, D. J.; Baker, J.; Stewart, J. P.; Head-Gordon, M.; Gonzalez, C.; Pople, J. A. GAUSSIAN94, Revision E.2; Gaussian, Inc.: Pittsburgh, PA, 1995.

(15) PQS version 2.0, Parallel Quantum Solutions, Fayetteville, Arkansas, 1998.

(16) (a) Reed, A. E.; Curtiss, L. A.; Weinhold, F. *Chem. Rev.* **1988**, *88*, 899. (b) Weinhold, F.; Carpenter, J. E. *The Structure of Small Molecules and Ions*; Naaman, R., Vager, Z., Eds.; Plenum: New York, 1988; p 227.

(17) (a) Sekiguchi, A.; Tsukamoto, M.; Ichinohe, M. *Science* **1997**, *275*, 60. (b) Schleyer, P. v. R. *Science* **1997**, *275*, 39. (c) Yates, B. F.; Schaefer, H. F., III *Chem. Phys. Lett.* **1989**, *155*, 563. (d) Nagase, S.; Kobayashi, K.; Nagashima, M. *J. Chem. Soc., Chem. Commun.* **1992**, 1302. (e) Wiberg, N.; Finger, C. M. M.; Polborn, K. *Angew. Chem., Int. Ed. Engl.* **1993**, *32*, 1054.
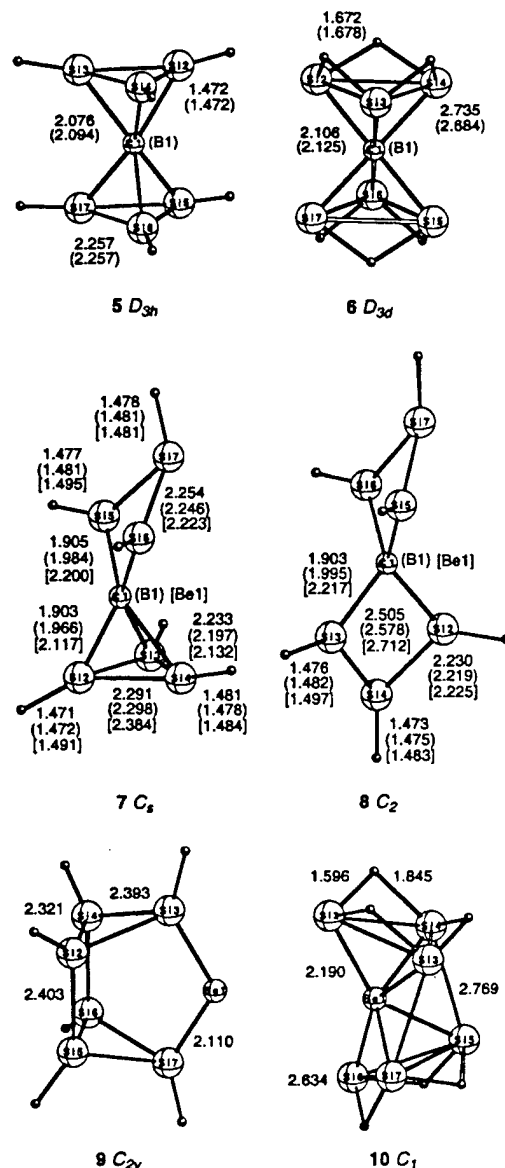
Figure 1. Optimized geometries at B3LYP/6-311++G(2d,2p). For 5—8 the C-sandwiches are shown with those for B complexes in parentheses and Be complexes in brackets.

rings (requiring D_{3h} symmetry) and from the C-center, indicating transfer of charge from the rings to the carbon. The NBO charges (SCF) of −2.16, 0.77, and −0.08 e for C, Si, and H support this interpretation. The charges for B, Si, and H in monocation 5B (D_{3h}) of −2.04, 0.61, and −0.11 e are analogous. This transfer of charge reduces the antibonding interactions between the rings, but only for the elements B (2.04) and C (2.55) because of their higher electronegativity than Si (1.90).[18] Since Be (1.57) is more electropositive a destabilizing transfer of charge from the central atom to the rings would be favored instead. With an NBO charge of +1.03 e for Be in neutral 5Be (D_{3h}) it is not surprising that the Be-sandwich structures are not minima. Likewise, the earlier investigated (η^3-C_3H_3)$_2$Be and (η^3-C_3H_3)$_2$B$^+$ sandwiches[5] are higher order saddle points with corresponding Be and B charges of 1.53 and 0.02 e.

The short C—Si distances of 2.076 Å in 5C (D_{3h}) reflect a strong π-complex, but it is less tight (1.904 Å) than pyramidal 3 (A = CH).[8] The Si—Si bond lengths of 2.257 Å in 5C are

(18) (a) Allerd, A. L. *Inorg. Chem.* **1978**, *17*, 215. (b) Allen, L. C.; Huheey, J. E. *J. Inorg. Nucl. Chem.* **1980**, *42*, 1523.

A-23

Table 1. Total (in au), Zero Point (ZPE, in kcal/mol), and Relative Energies (in kcal/mol)[a]

structure	level	total energy	ZPE	NIF	rel energy	structure	level	total energy	ZPE	NIF
5-C²⁻, D₃ₕ	HF/A	−1774.01409	40.16	0	0.0	7-B⁻, C₅	HF/A	−1761.24106	39.09	0
	B3LYP/A	−1777.82176	36.09	0	0.0		B3LYP/A	−1765.02060	35.68	0
	B3LYP/B	−1777.98909			0.0		B3LYP/B	−1765.18445		
	MP2/B	−1774.90504			0.0		MP2/B	−1762.10633		
6-C²⁻, D₃ᵈ	HF/A	−1773.96897	38.91	0	27.2	8-B⁻, C₂	HF/A	−1761.28670	39.35	0
	B3LYP/A	−1777.83236	36.29	0	−6.5		B3LYP/A	−1765.05637	36.21	0
	B3LYP/B	−1778.01948			−18.9		B3LYP/B	−1765.22032		
	MP2/B	−1774.94176			−24.2		MP2/B	−1762.13449		
7-C²⁻, C₅	HF/A	−1774.04461	40.02	1	−19.3	5-Be, D₃ₕ	HF/A	−1751.38578	37.05	4
	B3LYP/A	−1777.85340	36.40	0	−19.6		B3LYP/A	−1755.15389	33.45	2
	B3LYP/B	−1778.02263			−20.7	7-Be, C₅	HF/A	−1751.41728	36.46	0
	MP2/B	−1774.93206			−17.1		B3LYP/A	−1755.16760	33.62	0
8-C²⁻, C₂	HF/A	−1774.09924	40.62	0	−53.0		B3LYP/B	−1755.32762		
	B3LYP/A	−1777.90063	37.18	0	−48.4		MP2/B	−1752.24745		
	B3LYP/B	−1778.07091			−50.3	8-Be, C₂	HF/A	−1751.45253	36.72	0
	MP2/B	−1774.97556			−43.8		B3LYP/A	−1755.19557	34.02	0
5-B⁻, D₃ₕ	HF/A	−1761.22843	39.40	0	0.0		B3LYP/B	−1755.35525		
	B3LYP/A	−1765.00769	35.37	0	0.0		MP2/B	−1752.26880		
	B3LYP/B	−1765.17038			0.0	9, C₂ᵥ	HF/A	−1751.52868	39.05	0
	MP2/B	−1762.10268			0.0		B3LYP/A	−1755.25142	35.69	0
6-B⁻, D₃ᵈ	HF/A	−1761.19432	38.60	0	20.7		B3LYP/B	−1755.40648		
	B3LYP/A	−1765.02612	35.96	0	−11.0		MP2/B	−1752.32655		
	B3LYP/B	−1765.20388			−20.4	10, C₁	HF/A	−1751.35420	35.98	0
	MP2/B	−1762.14381			−26.5		B3LYP/A	−1755.17066	33.83	0
							B3LYP/B	−1755.34404		

[a] A: 6-31G(d). B: 6-311++G(2d,2p). NIF indicates the number of imaginary frequencies. Relative energies include ZPE corrections, scaled by 0.9135 for HF and by 0.9806 for B3LYP.[29] ZPE's calculated at B3LYP/A and HF/A are used for the B3LYP/B and MP2/B relative energies, respectively.

elongated from those of the free ligand (2.198 Å) and shortened with respect to **3** (A = CH, 2.337 Å),[8] trisilacyclopropane (2.332 Å),[19] and disilane (2.334 Å);[20] the nonbonded SiSi distance of 3.232 Å is much longer than that in hexasilaprismane (2.375 Å).[21] Interestingly, the hydrogens of **5C** are tilted inward, toward the carbon, by as much as 7°. Structure **5B** (D₃ₕ) has B−Si distances of 2.094 Å, marginally longer than the C−Si bond lengths of **5C**, and has its hydrogens tilted outward by 4°. Such tilting of peripheral hydrogens is common in 3D-aromatics,[22] bridged olefins, and alkynes,[23] and indicates strong π-interactions.

Sandwich structures **6B** and **6C** (D₃ᵈ) are both about 19 kcal/mol more stable than their "classical" isomers at B3LYP/6-311++G(2d,2p). This difference in stability is not even half the related preference of pyramidal **4** over **3** (44.0 kcal/mol (A = CH), B3LYP/6-31G(d)). However, we note that the energy difference is rather sensitive to the basis set employed, which is not surprising in light of the multitude of H-bridges. D₃ᵈ structures are preferred due to the arrangement of the Si lone pair (the D₃ₕ forms are transition structures for ligand rotation).

σ,π-Sandwiches (II). Replacing one η^3-Si₃H₃ (**1**) unit for a μ²-ligand results in the kinetically stable structures **7B** and **7C**. These are remarkably similar to pyramidal structure **3** in which the C−H/B−H cap is formally replaced by a cyclic CSi₃H₃²⁺/BSi₃H₃⁺ group, maintaining the six interstitial electrons for 3D aromaticity. However, the mixed inward (−22.8°) and outward (7.0°) tilting of the peripheral hydrogens of **7C** illustrates a

distortion from such ideal behavior. The distortion is caused by puckering (141°) of the 4-ring bridge, which is similar to that of the cyclobutadienyl dication (137°).[9,24] The equal C−Si-(2) and C−Si(5,6) bond lengths of 1.903 Å with longer C−Si-(3,4) bonds of 2.204 Å suggests carbonium ion character for the central carbon and thus C−Si σ-bonds in its bridge.[20] Structure **7B** shows a similar puckering (145°) of its BSi₃H₃⁺ bridge and corresponding boronium ion properties. It is interesting to note that the σ−π sandwich structure is a minimum for Be. The puckering (153°) of the 4-ring bridge is much less compared to that of **7C** and **7B**. Structure **7C** is 20.7 kcal/mol more stable than the **5C** sandwich and for the boron analogue this energy difference is 8.5 kcal/mol.

σ-Sandwiches (III). Replacing both η^3-Si₃H₃ (**1**) units for μ²-ligands gives spiro compounds **8C** and **8B** (C₂), which are 50.3 and 30.5 kcal/mol, respectively, more stable than sandwich structures **5C** and **5B** (the D₂ᵈ structures are second-order saddle points with imaginary frequencies for ring puckering). σ-Bonding is evident from the 1.903 Å C−Si and 1.995 Å B−Si bond lengths, which is in line with the corresponding 2.505 and 2.578 Å Si(2,5)−Si(3,6) distances that suggest opening of the Si₃H₃⁺ rings to "allylic" units. The XSi₃H₃ rings are puckered, 143.1° for **8C** and 148.8° for **8B**, but less than in the σ,π-sandwich (II) structures. Also **8Be** is a minimum with properties similar to **8C** and **8B**. This isomer is 17.0 kcal/mol more stable than **7Be**: its BeSi₃H₃ ring puckering (152°) is similar to that of **7Be**. The energetic preference of these spiro compounds is a reflection of the σ-bonding that the central atoms favor. Cp₂C is also reported to show similar behavior.[25]

Isomer **9Be** is obtained by following the imaginary vectors in **5Be**. This cluster type structure, in which Be is sitting in a Si₆H₆ basket, is more stable than the sandwich type structures (I, II, and III) discussed above. Structure **10Be**, the Be-

(19) (a) Srinivas, G. N.; Kiran, B.; Jemmis, E. D. *J. Mol. Struct. (THEOCHEM)* **1996**, *361*, 205. (b) Nagase, S.; Kobayashi, K.; Nagashima, M. *J. Chem. Soc., Chem. Commun.* **1992**, 1302.

(20) Schleyer, P. v. R.; Kaupp, M.; Hampel, F.; Bremer, M.; Mislow, K. *J. Am. Chem. Soc.* **1992**, *114*, 6791.

(21) (a) Nagase, S.; Nakano, M.; Kudo, T. *J. Chem. Soc., Chem. Commun.* **1987**, 60. (b) Nagase, S. *Acc. Chem. Res.* **1995**, *28*, 469. (c) Zhao, M.; Gimarc, B. M. *Inorg. Chem.* **1996**, *35*, 5378.

(22) (a) Jemmis, E. D.; Schleyer, P. v. R. *J. Am. Chem. Soc.* **1982**, *104*, 4781 and references therein. (b) Jemmis, E. D. *J. Am. Chem. Soc.* **1982**, *104*, 7017.

(23) Lammertsma, K.; Ohwada, T. *J. Am. Chem. Soc.* **1996**, *118*, 7247.

(24) Krogh-Jesperson, K.; Schleyer, P. v. R.; Pople, J. A.; Cremer, D. *J. Am. Chem. Soc.* **1978**, *100*, 4301.

(25) Schoeller, W. W.; Friedrich, O.; Sundermann, A.; Rozhenko, A. *Organometallics* **1999**, *18*, 2099.

D *J. Am. Chem. Soc.* PAGE EST: 3.5

Srinivas et al.

A-24

embedded basket with H-bridges, is 37.4 kcal/mol less stable than the conventional form **9Be**.

Are the discussed sandwich structures viable synthetic targets? The "classical" form may be a reasonable possibility if substituted with adequately large groups. The analogy with tetrasilatetrahedrane Si_4H_4 is instructive. While **3SiH** is 20.6 kcal/mol less stable than its H-bridged **4SiH** isomer at MP2/6-31G(d) and even 49.3 kcal/mol compared to a four-membered ring structure,[8,17c,d] its "super silyl" ($^tBu_3Si$) substituted derivative has nevertheless been synthesized.[17e] To present a more tangible picture, the permethylated structures of **5** and **8** (i.e., **5'** and **8'**) were studied for B and C and found to be minima. at HF/6-31G(d) isomers **8B'** and **8C'** are 37.6 and 57.3 kcal/mol more stable than **5B'** and **5C'**, respectively.[26] These relative energies of these permethyl derivatives are very close to those of the parent molecules at the same level of theory. The recent experimental preparation and X-ray analysis of the trisilacyclopropenium ion Si_3R_4 (R = $SiMe^tBu_2$) is illustrative of the importance of bulky substituents.[27] Therefore, we feel that any of the three sandwich structures are intriguing targets for experimental pursuit, with that of structure **5C** being the greatest challenge. If anything, silyl substituents will only increase the donation of electron density into the Si_3 ring and strengthen the π bonding as in disilenes.[28]

(26) Total energies at HF/6-31G(d) level: **8C'**, −2008.46153 au; **8B'**, −1995.59881 au.

(27) Ichinohe, M.; Matsuno, T.; Sekiguchi, A. *Angew. Chem., Int. Ed. Engl.* **1999**, *38*, 2194.

(28) Grev, R. S. *Advances in Organometallic Chemistry*; Stone, F. G. A., West, R., Eds.; Academic Press Inc.: New York, 1991; Vol. 33, p 125.

(29) Scott, A. P.; Radom, L. *J. Phys. Chem.* **1996**, *100*, 16502.

Conclusions

The η^3-Si_3H_3 sandwich compounds with boron and carbon as central atoms are found to be minima. The stability of these systems is due to charge transfer from the ligands to the central atom, which is a reversed flow compared to the cyclopentadienyl sandwiches. With Be as the central atom, the sandwich structures are found to be unstable due to the higher electropositive nature of Be. However, the pyramidal complex **7Be**, containing both a η^3-Si_3H_3 and a μ^2-Si_3H_3 ligand, is a minimum. The C- and B-containing pyramidal complexes (**7C** and **7B**) are more stable than **5** by 20.7 and 8.5 kcal/mol, respectively. Spiro compounds **8**, in which the central atom is sandwiched by two allylic μ^2-Si_3H_3 ligands, are still more stable by 21.9 and 29.6 kcal/mol for B and C, respectively. Calculations on the permethylated sandwiches **5'** and **8'** reveal these structures to be minima with relative energies similar to those of the parent molecules. The preferred Be complex is a cluster type molecule **9** where the Be atom sits in a Si_6H_6 basket.

Supporting Information Available: Cartesian coordinates of the structures in Figure 1 (PDF). This information is available free of charge via the Internet at http://pubs.acs.org.

JA992302A

A Theoretical Study of B_2Li_6

Gantasala N. Srinivas[a], Zhi Chen[a], Tracy P. Hamilton[a] and K. Lammertsma[a,b]*

[a]Department of Chemistry, University of Alabama at Birmingham, Birmingham, Alabama.

[b]Department of Chemistry, Vrije Universiteit, De Boelelaan 1083, 1081 HV Amsterdam, The Netherlands.

fax: +31-(0)20-444-7488, email: lammert@chem.vu.nl

Abstract

Structures and energeties of the B_2Li_6 system are predicted with the HF, MP2 and B3LYP methods using the 6-31G(d) basis set, including energy evaluations with the G2MP2 and CBS-Q methods and the larger 6-311G(2d) basis set for B3LYP. An extensive search on the singlet surface revealed six local minima. The structure of the B_2Li_6 global minimum consists of a B_2 unit containing two bridging Li ligands and a bridging tetrahedral Li_4 unit. The cohesive ($B_2Li_6 \rightarrow B_2 + Li_6$) and Li_2 elimination energies ($B_2Li_6 \rightarrow B_2Li_4 + Li_2$) indicate significant stability for this binary cluster. Sandwich structure **3d**, containing two triangular Li_3 units and relating to a C_2Li_6 isomer is 6.9 kcal/mol less stable than **3a**. Diborane[6] structure **3g**, which contains a strongly bonded B_2 unit with loosely bound lithiums, is not a minimum.

1

Introduction

Insight into the structures and energetics of boron-lithium clusters is needed to evaluate their potential as high energy additives to cryogenic hydrogen, and also for comprehending Li-B alloys [1,2]. Recently, Meden and coworkers presented a computational study on a large and diverse set of B/Li clusters using the Hartree-Fock level with the 6-31G* basis set.[3] Subsequently, we studied in great detail the small BLi_{1-8} and B_2Li_{1-4} clusters with sophisticated correlation methods and found these to display extraordinary bonding features, to be stable against atomization, and to have large cohesive energies $(B_{1-2}Li_n \rightarrow B_{1-2} + Li_n)$ [4-6].

It is well known that lithiocarbides, in contrast to the common hydrocarbons, exhibit multicenter bonding [5-8] due to both ionic C-Li interactions and the tendency of lithium atoms to cluster. For example, the global minimum for C_2Li_4 contains a C_2^{2-} unit which receives its charge by ionic bonding with a Li atom and a Li_3 unit [6]. Also the lithioborides differ from the boranes, even though the latter are known for their multicenter bonding interactions. For example, the global B_2Li_4 minimum contains a quadruple-Li-bridged B_2 unit [4]. This suggests that structural differences must also be expected between other boron-lithium and carbon-lithium clusters.

The differences between C_2H_6 and B_2H_6 are well known in the literature [9], and there are detailed theoretical investigations available on C_2Li_6 [7,8]. Only two minima (**1** and **2**, Figure 1) were found for C_2Li_6. Structure **1** is the (notably planar!) global minimum and isomer **2** is a transition structure with an imaginary vector leading to **1** at the SCF/DZP level [8]. Here we present our results on B_2Li_6 and show that it differs greatly both from diborane[6], B_2H_6, and from C_2Li_6.

2

Computational Methods

The geometries of B_2Li_6 were optimized at the HF and MP2 levels using the 6-31G* basis set [10-12]. The density functional calculations were performed at the B3LYP level using the same basis set [13,14]. The nature of the stationary points was determined by evaluating the second derivatives of the energy (Hessian matrix) [15]. The G2MP2 and CBS-Q methods were employed to get more accurate energies [16,17]. The effect of a larger basis set, 6-311+G(2d), on the energies was also investigated for the more economical B3LYP method using geometries optimized at B3LYP/6-31G(d). Natural charges were obtained by the Natural Population Analysis (NPA) [18]. All calculations were performed using the GAUSSIAN 94 suite of programs [19].

Results and Discussion

An extensive search of the many possible geometrical configurations led to six stationary points, **3a-3f**, on the singlet energy surface of B_2Li_6. These are displayed in Figure 2 and their energies are given in Table 1. Before discussing them separately, some general observations are made. In these we exclude the high energy isomer **3f** as it has no B-B bond.

The variation in B-B bond lengths (Table 2) among the B_2Li_6 structures is minimal. The average B-B distance of 1.534 ± 0.016 Å at B3LYP is shorter than that of the smaller B_2Li_n clusters (n = 1-4, B-B$_{av}$ = 1.555 ± 0.055 Å) [6]. This difference is attributed to an increased negative charge on the B atoms of the B_2Li_6 structures resulting from the larger number of electropositive lithium atoms. At MP2 still longer bonds are obtained (1.545 ± 0.015 Å) but at HF they are slightly shorter (1.529 ± 0.015 Å). On the other hand, the average bridging B-Li distances (B3LYP: 2.220 ± 0.223 Å, MP2: 2.256 ± 0.190 Å, HF: 2.260 ± 0.147 Å) are longer when compared to the smaller B_2Li_n

(n=1-4) clusters (2.212 ± 0.444 Å, B3LYP) [6]. The average terminal B-Li$_t$ distance at both MP2 (2.206 ± 0.099 Å) and HF (2.182 ± 0.059 Å) is lengthened compared to that at B3LYP (2.150 ± 0.063 Å). Due to the weak interactions, the Li-Li distances show large deviations with an average value of 2.993 ± 0.429 Å at B3LYP which is slightly shorter than those at MP2 (3.068 ± 0.406 Å) and HF (3.147 ± 0.584 Å).

The relative energies show some variation among the different theoretical methods (Table 1). However, those at B3LYP using the larger 6-311+G(2d) basis set compare very well with both the G2MP2 and CBS-Q energies, just as is the case for the smaller BLi$_n$ (n=1-8) and B$_2$Li$_n$ (n=1-4) clusters [4-6]. The deviation of the MP2/6-31G* energies from these data is only modest, except for the high energy **3f**, but the performance of HF is poor. For simplicity, we will use B3LYP/6-31G* geometries and G2MP2 energies throughout the following discussion unless otherwise indicated.

Structures and Energies. The global B$_2$Li$_6$ minimum is the condensed C$_s$ structure **3a**, which contains two Li atoms interacting with the quadruple-bridged B$_2$Li$_4$ (D_{4h}) system. The side-on addition of Li3 to the bridging Li6 and Li7 of B$_2$Li$_4$ creates a Li$_3$ triangle to which a second lithium (Li8) caps to form a Li$_4$ pyramid. There is only a small decrease in the B-B distance (0.005 Å) in going from B$_2$Li$_4$ to **3a**. Molecular orbital analysis of **3a** (and indeed of all the B$_2$Li$_6$ isomers) reveals that the contribution of the lithium valence atomic orbitals to the bonding MOs are minimal. That is, the lithium atoms donate their valence electrons to the B$_2$ unit leading to a formal triple bond and two lone pairs. The NPA charge on the B$_2$ fragment amounts to -2.77e (Table 3), which is a 0.41e increase compared to the B$_2$Li$_4$ (D_{4h}) cluster. Interestingly, the Li$_4$ tetrahedron in **3a** is highly polarized due its interaction with the B$_2$ unit leading to a negative charge (-0.36) on the distal Li

4

atom. The transfer of charge from the two bridging lithium atoms and the Li_4 pyramid is also reflected in the increased B-B vibrational stretching frequency (1207 cm^{-1} for **3a**, 1184 cm^{-1} for B_2Li_4 (D_{4h}), 1014 cm^{-1} for B_2 ($^3\Sigma_g^-$)).

Isomer **3b** (C_s) is also a minimum energy structure only 2.0 kcal/mol less stable than **3a**. Structure **3b**, which has a side-on triangular Li_3 unit connected to doubly Li-bridged B_2Li_3, can be viewed to result from complexing a Li_2 unit in a coplanar side-on fashion to the propellane-like (C_{3v}) isomer of B_2Li_4; this C_{3v} isomer of B_2Li_4 is 2.9 kcal/mol less stable than its D_{4h} form [6]. The NPA charge of -2.81e for the B_2 fragment of **3b** is slightly higher than that of **3a**. The tendency for clustering lithium atoms is also evident in **3b**. Folding one of its Li-bridges to the Li_3 unit gives structure **3c** which carries a tetrahedral Li_4 unit besides a bridging and a terminal Li atom. Its energy difference of 3.3 kcal/mol with global minimum **3a** reflects the difference in bonding between a terminal and a bridging lithium atom. Isomer **3c** is a minimum at B3LYP but a transition structure at MP2 and HF.

Isomer **3d** (C_{2h}) represents a sandwich structure with B_2^{2-} capped by two triangular Li_3^+ units. It is 6.9 kcal/mol less stable than **3a** and differs from the C_2Li_6 minimum structure **2** in that its Li_3 units are rotated by 60°; the B_2Li_6 form analogous to **2** is a second order saddle point. More charge is transferred from the two Li_3 units to B_2 than to C_2, which contains two more valence electrons. We calculate a NPA charge on boron of -1.66e versus a reported charge of -0.92e on each carbon of **2** [5]. Structure **3d** can also be viewed to result from addition of two lithiums to quadruple bridged B_2Li_4 (D_{4h}) in a *anti* fashion. A *syn* addition leads to a still 1.5 kcal/mol less stable hexa-coordinated B_2 structure **3e** (C_2). In this structure the Li-capped B_2 unit (with a B_2 charge of 3.12e) can be considered to lie in a Li_5 basket.

The high energy structure **3f** (C_s), being 95.4 kcal/mol less stable than **3a**, has a single B atom equatorially complexed to the BLi_6 cluster. It is the only structure we were able to find in which the B-B bond of B_2Li_6 is completely dissociated, which also explains the large energy difference with the other isomers. For comparison, the Li insertion into the B_2 bond of B_2Li_3 (D_{3h} ($^2A_1'$) → $D_{\infty h}$ ($^2\Pi_u$)) requires 139.5 kcal/mol [6].

Diborane-like Structures. We investigated several other B_2Li_6 structures, none of which proved to be a minimum energy species. For example, a C_{2h} structure analogous to C_2Li_6 isomer **1** and the global minimum for $Li_2B_2H_4$ [20,21] has several imaginary frequencies and was not further investigated. Interestingly, the diborane[6] equivalent **3g** has three imaginary frequencies! An MO analysis reveals minimal bonding contributions from the Li valence orbitals. The schematic MO diagrams for the D_{2d} structures of B_2Li_6 (**3g**) and B_2H_6, given in Figure 3, show that the lithiums contribute little to bonding. In diborane[6] the 3c-2e bonding is due to the $2a_g$ (and $3a_g$) and $1b_{1u}$ MOs, whereas in **3g** the contribution of the bridging lithiums is small in the $4a_g$ and $2b_{1u}$ MOs. Similar differences are found for the terminal $B-H_t$ and $B-Li_t$ bonds. The contribution of the lithiums in the MOs $3b_{3u}$, $2b_{2u}$ and $5a_g$ is minimal and this culminates in a short BB distance of 1.534 Å. The HOMO ($6a_g$) of **3g** has only lithium and no boron contributions, in contrast to the $1b_{1g}$ MO of B_2H_6, and is illustrative of its undesirable bonding arrangement. Interestingly, the one-electron density analysis [22] of **3g** shows a non-nuclear attractor along the BB bond path, in analogy with related electron deficient (bi)metalloid systems [22-25]. In sharp contrast, B_2H_6 contains no BB bond but has instead a ring critical point in the center of the ring [22,26].

Cohesive and Li_2-Elimination Energies. B_2Li_6 is stable with respect to loss of Li_2 (Table 4) The Li_2-elimination energy of 35.2 kcal/mol is much less than the 76.2 kcal/mol for B_2Li_4 and the

6

93.7 kcal/mol for B_2Li_3 and compares better to those of the pure Li_n clusters [3,4]. The stability of B_2Li_6 is further confirmed by the cohesive energy of 173 kcal/mol between B_2 and the Li_6 cluster (Table 4), which is however a marginal increase of 13 kcal/mol over that of B_2Li_4 [4]. This indicates that the two additional lithium atoms are weakly interacting with the B_2 unit, perhaps reflecting the fact that the charge transfer and coordination of the two borons is near its maximum.

Conclusions

An extensive investigation of the B_2Li_6 singlet potential energy surface revealed six stationary points at the HF, MP2 and B3LYP levels of theory using the 6-31G(d) basis set. None of the C_2Li_6 related isomers nor the B_2H_6 diborane structure are minima on the B_2Li_6 singlet surface. The global minimum at G2MP2, CBS-Q, and B3LYP/6-311+G(2d) is **3a**. This structure contains a B_2 unit with three bridging ligands, two of which are single lithiums and the third a tetrahedral Li_4 unit. Propeller-like structure **3b**, with a Li_3 group as one of its 'blades', is 2.0 kcal/mol less stable. Sandwich structure **3d**, which contains two triangular Li_3 units and thereby relates to the global C_2Li_6 minimum, is 6.9 kcal/mol less stable than **3a**. Diborane[6] structure **3g** contains a tight B_2 unit with loosely bonded lithiums and is not a minimum. The stability of the B_2Li_6 structures is governed by maximizing the Li-Li interactions and distributing the charged Li_n units around the B_2^{2-} frame. The 137 kcal/mol cohesive energy ($B_2Li_6 \rightarrow B_2 + Li_6$) and the 35 kcal/mol Li_2 elimination energy ($B_2Li_6 \rightarrow B_2Li_4 + Li_2$) of **3a** indicate significant stability for this binary cluster.

Supporting Material. Cartesian coordinates of the structures in Figure 1. Ordering information is given on any current masthead page.

References

[1] B. Pihlar, V. Pavlovič, S. Pejovnik, S. Spaić "Electrochemical Characterization of Lithium-Boron Alloys" in Practical Lithium Bateries. Y. Matsuda, C.R. Schlaikjer, Eds. JEC Press Inc., Ohio, 1988.

[2] J.A. Sheehy, "Spectroscopy of Lithium Boride, A candidate HEDM Species." Proceedings of the High Energy Density Matter, Woods Hole, MA,1995.

[3] A. Meden, J. Mavri, M. Bele, S. Pejovnik, J. Phys. Chem. 99 (1995) 4252.

[4] K.A. Nguyen, K. Lammertsma, J. Phys. Chem. A 102 (1998) 1608.

[5] K.A. Nguyen, G.N. Srinivas, T.P. Hamilton, K. Lammertsma, J. Phys. Chem. A 103 (1999) 710.

[6] G.N. Srinivas, T.P. Hamilton, J. A. Boatz, K. Lammertsma, J. Phys. Chem. A 103 (1999) 0000.

[7] A. Streitwieser, S.M. Bachrach, A. Dorigo, P.v.R. Schleyer, "Bonding, Structure and Energies in Organolithium Compounds" (Ch. 1) in *Lithium Chemistry - A theoretical and experimental overview*, A.-M. Sapse, P.v.R. Schleyer, Eds. Wiley, 1995, and references cited.

[8] J. Ivanic, C.J. Marsden, Organometallics 13 (1994) 5141.

[9] F.A. Cotton, G. Wilkinson, C.A. Murillo, M. Bochmann, Advanced Inorganic Chemistry, 6th Ed., Wiley-Interscience, New York, 1999.

[10] W.J. Hehre, L. Radom, P.v.R. Schleyer, J.A. Pople, Ab Initio Molecular Orbital Theory, Wiley, New York, 1986.

[11] W.J. Hehre, R. Ditchfield, J.A. Pople, J. Chem. Phys. 56 (1972) 2257.

[12] C. Møller, M.S. Plesset, Phys. Rev. 46 (1934) 618.

[13] A.D. Becke, J. Chem. Phys. 98 (1993) 5648.

[14] C. Lee, W. Yang, R.G. Parr, Phys. Rev. B 37 (1988) 785.

[15] J.A. Pople, K. Raghavachari, H.B. Schlegel, J.S. Binkley, Int. J. Quantum Chem. Symp. 13 (1979) 255.

[16] L.A. Curtiss, K. Raghavachari, J.A. Pople, J. Chem. Phys. 98 (1993) 1293.

[17] J.W. Ochterski, G.A. Petersson, J.A. Montgomery, Jr., J. Chem. Phys. 104 (1996) 2598.

[18] A.E. Reed, L.A. Curtiss, F. Weinhold, Chem. Rev. 88 (1988) 899.

[19] M. J. Frisch, G. W. Trucks, H. B. Schlegel, P. M. W. Gill, B. G. Johnson, M. A. Robb, J. R. Cheeseman, T. Keith, G. A. Petersson, J. A. Montgomery, K. Raghavachari, M. A. Al-Laham, V. G. Zakrzewski, J. V. Ortiz, J. B. Foresman, J. Cioslowski, B. B. Stefanov, A. Nanayakkara, M. Challacombe, C. Y. Peng, P. Y. Ayala, W. Chen, M. W. Wong, J. L. Andres, E. S. Replogle, R. Gomperts, R. L. Martin, D. J. Fox, J. S. Binkley, D. J. Defrees, J. Baker, J. P. Stewart, M. Head-Gordon, C. Gonzalez, and J. A. Pople, Gaussian, Inc., Pittsburgh PA, 1995.

[20] E. Kaufmann, P.v.R. Schleyer, Inorg. Chem. 27 (1988) 3987.

[21] T. Kar, K. Jug, Chem. Phys. Lett. 214 (1993) 615.

[22]   R.F.W. Bader, "Atoms in Molecules — A Quantum Theory," Oxford University Press, Oxford, 1991.

[23]   J. Cioslowski, J. Phys. Chem. 94 (1990) 5496.

[24]   K. Lammertsma, O.F. Güner, J. Am. Chem. Soc. 112 (1990) 508.

[25]   P.V. Sudhakar, K. Lammertsma, J. Chem. Phys. 99 (1993) 7929.

[26]   M.J. van der Woerd, K. Lammertsma, B.J. Duke, H.F. Schaefer, III, J. Chem. Phys. 95 (1991) 1160.

Legend to the Figures.

Figure 1. C_2Li_6 structures [5].

Figure 2. B_2Li_6 structures that are minima.

Figure 3. Schematic diagram representing the valence occupied MOs for B_2Li_6 (left side) and B_2H_6 (right side). The MOs $6a_g$ and $1b_{1g}$ are the HOMO of B_2Li_6 and B_2H_6 respectively.

TABLE 1: Total energy (au), number of imaginary frequencies (NIM) and relative energy (kcal/mol) of B_2Li_6 isomers.[a]

Structure	Level	Total Energy	NIF(cm^{-1})	Relative Energy
3a C_s	HF	-93.96268	0	0.0
	MP2	-94.23613	0	0.0
	B3LYP	-94.79609	0	0.0
	B3LYP(L)	-94.81952		0.0
	G2MP2	-94.36523		0.0
	CBS-Q	-94.35445		0.0
3b C_s	HF	-93.96727	0	-2.9
	MP2	-94.23437	0	1.1
	B3LYP	-94.79575	0	0.2
	B3LYP(L)	-94.81687		1.7
	G2MP2	-94.36196		2.0
	CBS-Q	-94.35123		2.0
3c C_s	HF	-93.96327	1(33i)	-0.4
	MP2	-94.23094	1(46i)	3.3
	B3LYP	-94.79350	0	1.6
	B3LYP(L)	-94.81513		2.8
	G2MP2	-94.35990		3.3
	CBS-Q	-94.34882		3.5

TABLE 1: (Continued)

Structure	Level	Total Energy	NIF(cm⁻¹)	Relative Energy
3d C_{2h}	HF	-93.94377	1(67i)	11.9
	MP2	-94.22534	0	6.8
	B3LYP	-94.78621	0	6.2
	B3LYP(L)	-94.81131		5.2
	G2MP2	-94.35423		6.9
	CBS-Q	-94.34329		7.0
3e C_2	HF	-93.92962	1(366i)	20.7
	MP2	-94.21761	0	11.6
	B3LYP	-94.77950	0	10.4
	B3LYP(L)	-94.80416		9.6
	G2MP2	-94.35176		8.4
	CBS-Q	-94.33868		9.9
3f C_s	HF	-93.80734	0	97.5
	MP2	-94.06728	0	105.9
	B3LYP	-94.63967	0	98.2
	B3LYP(L)	-94.66373		97.8
	G2MP2	-94.21323		95.4
	CBS-Q	-94.19985		97.0
3g D_{2d}	HF	-93.93413	3	
	MP2	-94.21756	2	
	B3LYP	-94.77645	3	

[a] Using the 6-31G(d) basis set, except for B3LYP(L) which denotes the use of 6-311+G(2d). NIF indicates the number of imaginary frequencies.

TABLE 2: Optimized geometric distances (in angstroms) at B3LYP, MP2 and HF levels.

Structure	Parameter	B3LYP	MP2	HF
3a C_s	B(1)-B(2)	1.526	1.542	1.526
	B(2)-Li(3)	2.173	2.220	2.214
	Li(3)-Li(7)	2.899	2.988	3.025
	Li(6)-Li(7)	2.615	2.678	2.682
	Li(3)-Li(8)	3.102	3.186	3.310
	Li(6)-Li(8)	3.325	3.367	3.528
	B(1)-Li(6)	2.237	2.267	2.278
	B(2)-Li(6).	2.332	2.398	2.393
	B(1)-Li(4)	2.152	2.202	2.187
	B(2)-Li(4)	2.198	2.217	2.258
	Li(4)-Li(7)	3.088	3.143	3.160
	Li(4)-Li(5)	3.001	3.061	3.079
3b Cs	B(1)-B(2)	1.525	1.539	1.523
	B(1)-Li(3)	2.115	2.159	2.158
	B(1)-Li(4)	2.175	2.216	2.234
	B(1)-Li(6)	2.315	2.317	2.380
	B(2)-Li(4)	2.135	2.151	2.171

TABLE 2. (Continued)

Structure	Parameter	B3LYP	MP2	HF
	B(2)-Li(6)	2.236	2.285	2.269
	B(2)-Li(7)	2.201	2.244	2.244
	Li(6)-Li(7)	2.715	2.789	2.787
	Li(6)-Li(8)	3.150	3.196	3.355
	Li(7)-Li(8)	3.046	3.123	3.222
3c C$_s$	B(1)-B(2)	1.525	1.539	1.523
	B(1)-Li(4)	2.289	2.298	2.340
	B(1)-Li(8)	2.116	2.157	2.156
	B(1)-Li(6)	2.164	2.208	2.215
	B(2)-Li(3) ·	2.169	2.213	2.220
	B(2)-Li(4)	2.195	2.241	2.229
	B(2)-Li(6)	2.139	2.161	2.178
	Li(3)-Li(4)	2.897	2.987	2.997
	Li(4)-Li(5)	2.781	2.877	2.911
	Li(3)-Li(7)	3.085	3.176	3.259
	Li(4)-Li(7)	3.422	3.474	3.731

TABLE 2: (continued)

Structure	Parameter	B3LYP	MP2	HF
3d C$_{2h}$	B(1)-B(2)	1.550	1.560	1.544
	B(1)-Li(6)	2.121	2.156	2.148
	B(1)-Li(7)	2.316	2.378	2.407
	B(1)-Li(4)	2.195	2.209	2.245
	Li(7)-Li(8)	2.760	2.856	2.976
	Li(6)-Li(7)	3.119	3.244	3.399
3e C$_2$	B(1)-B(2)	1.542	1.546	1.538
	B(1)-Li(3)	2.147	2.192	2.187
	B(1)-Li(4)	2.443	2.446	2.489
	B(1)-Li(5)	2.301	2.333	2.394
	B(1)-Li(6)	2.117	2.186	2.164
	B(1)-Li(7)	2.213	2.305	2.241
	Li(4)-Li(8)	2.889	2.932	3.009
	Li(4)-Li(5)	2.833	2.903	2.922
	Li(5)-Li(8)	3.149	3.245	3.288
	Li(3)-Li(4)	3.139	3.195	3.217

TABLE 2: (Continued)

Structure	Parameter	B3LYP	MP2	HF
3f C_s	B(1)-Li(2)	2.120	2.173	2.171
	B(1)-Li(3)	2.119	2.173	2.171
	B(1)-Li(4)	2.146	2.198	2.190
	B(1)-Li(6)	2.161	2.215	2.247
	Li(2)-Li(4)	2.994	3.037	3.045
	Li(2)-Li(6)	3.040	3.181	3.171
	Li(3)-Li(4)	2.985	3.049	3.045
	Li(3)-Li(6)	3.078	3.136	3.173
	Li(4)-Li(5)	3.046	3.136	3.175
	Li(4)-Li(6)	3.329	3.416	3.449
	Li(6)-Li(7)	2.391	2.415	2.351
	Li(6)-B(8)	2.649	2.677	2.667

TABLE 4: B_2 cohesive energies and Li_2 dissociation energies (in kcal/mol)

Reaction	HF	MP2	B3LYP	B3LYP(L)[a]	G2MP2	CBS-Q
$B_2Li_6 \rightarrow B_2 + Li_6$	145.5	183.9	174.8	178.5	173.0	175.1
$B_2Li_6 \rightarrow B_2Li_4 + Li_2$	33.2	33.2	33.0	32.6	35.2	36.5

[a] See foot note of Table 1

TABLE 3: Natural Charges in Electrons for B_2Li_6 cluster.

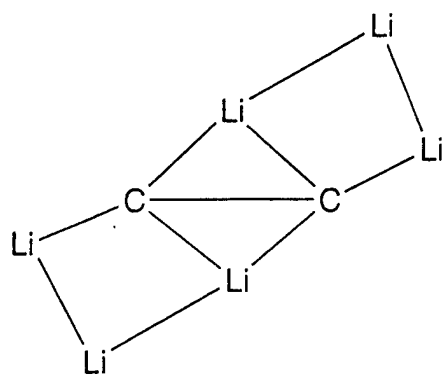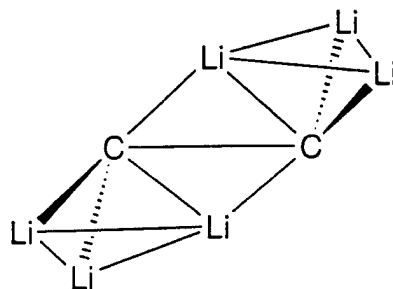| Structure	Atom	Charge	Structure	Atom	Charge
3a	B(1)	-1.20	**3d**	B(1)	-1.66
	B(2)	-1.57		Li(3)	0.57
	Li(3)	0.61		Li(4)	0.54
	Li(4)	0.65	**3e**	B(1)	-1.56
	Li(6)	0.61		Li(3)	0.71
	Li(8)	-0.36		Li(4)	0.52
3b	B(1)	-1.48		Li(5)	0.61
	B(2)	-1.33		Li(7)	0.38
	Li(3)	0.72	**3f**	B(1)	-2.62
	Li(4)	0.69		B(8)	-0.55
	Li(6)	0.57		Li(2)	0.58
	Li(7)	0.56		Li(3)	0.57
	Li(8)	-0.42		Li(4)	0.43
3c	B(1)	-1.52		Li(6)	0.58
	B(2)	-1.38			
	Li(3)	0.62			
	Li(4)	0.64			
	Li(6)	0.71			
	Li(7)	-0.43			
	Li(8)	0.72			

1 C_{2h} **2** C_{2h}

Fig.1 (G.N.Srinivas et al)
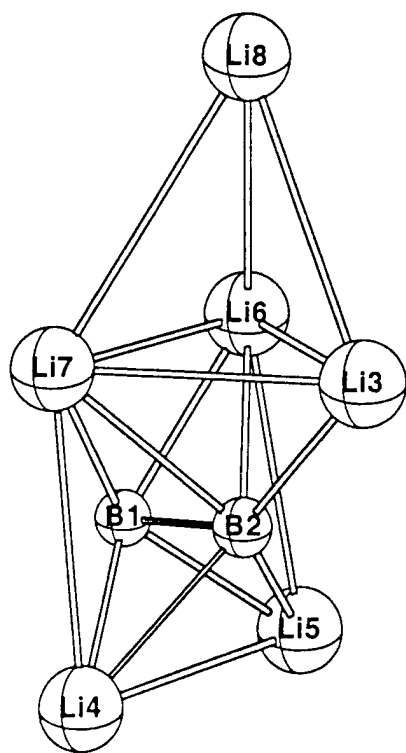
3a C_s
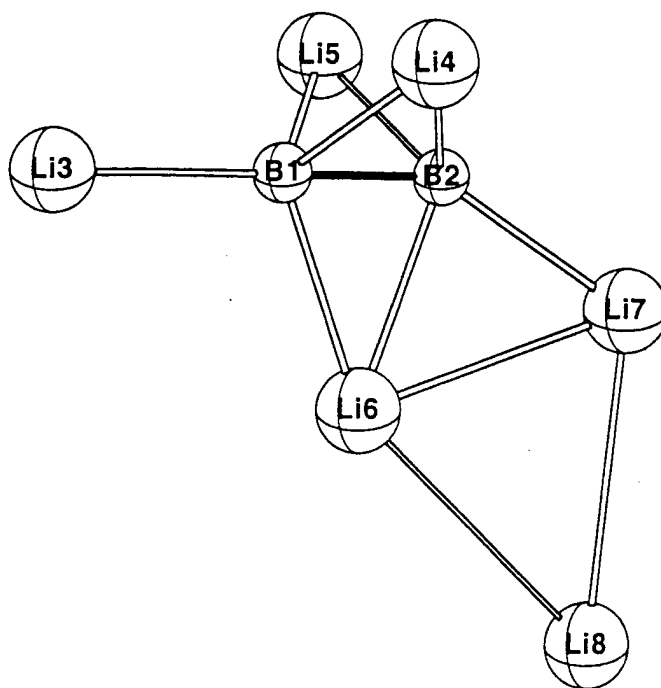
3b C_s
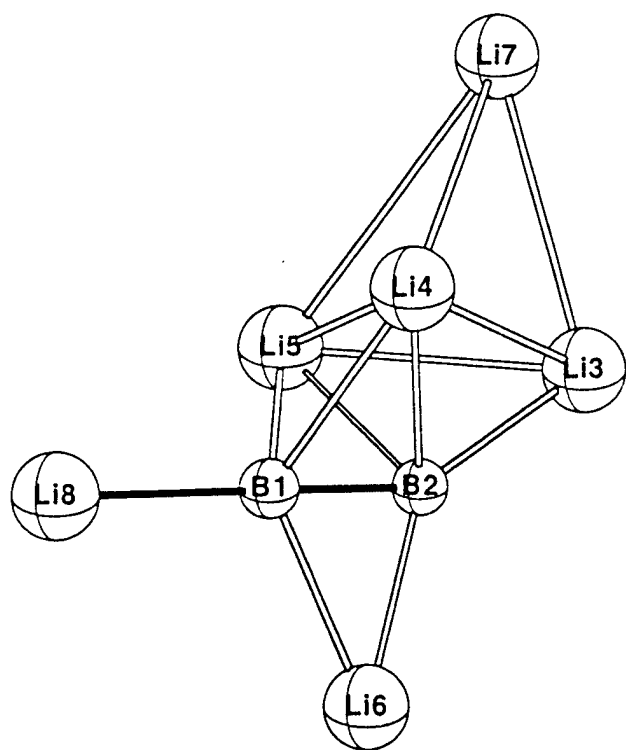
3c C_s
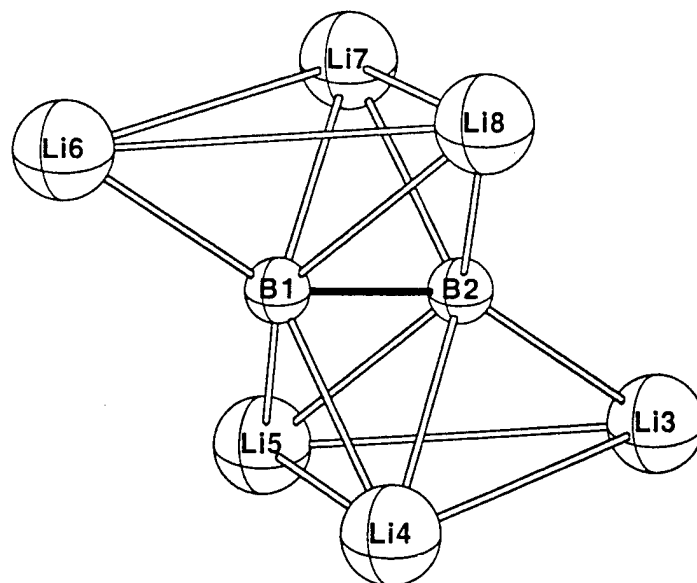
3d C_{2h}

Fig.2 (G.N.Srinivas et al)

3e C_2

3f C_s

Fig.2 (G.N.Srinivas et al)

Fig.3: Schematic diagram representing the valence occupied MOs for B_2Li_6 (left side) and B_2H_6 (right side). The MOs $6a_g$ and $1b_{1g}$ are the HOMO of B_2Li_6 and B_2H_6 respectively.

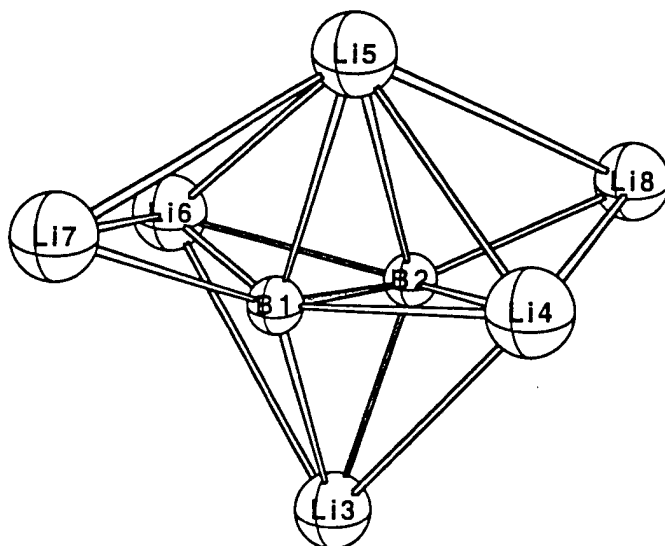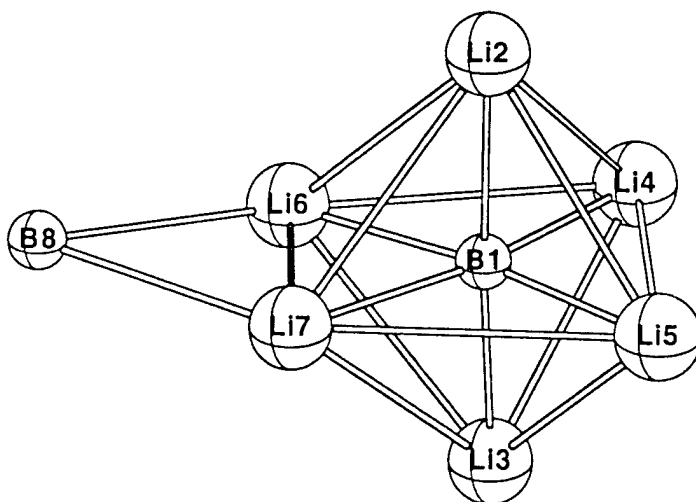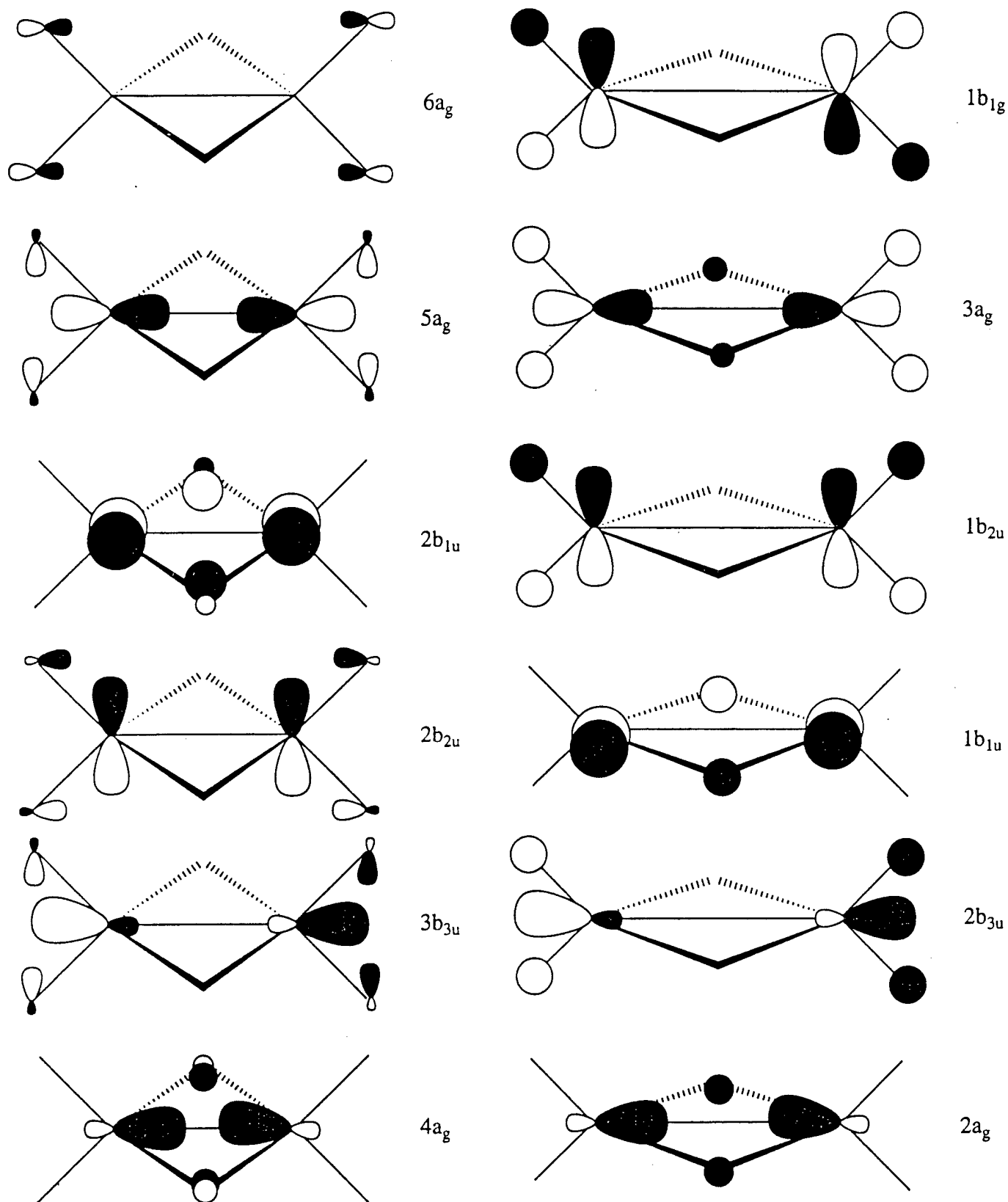# Keto _ Enol, Imine _ Enamine, and Nitro _ *aci*-Nitro Tautomerism and Their Interrelationship in Substituted Nitroethylenes. Keto, Imine, Nitro, and Vinyl Substituent Effects and the Importance of H-bonding.

by Koop Lammertsma[a,b]* and Prasad V. Bharatam[a,c]

[a] Department of Chemistry, University of Alabama at Birmingham, Birmingham, AL 35294
[b] Department of Chemistry, Scheikundig Laboratorium, Vrije Universiteit, De Boelelaan 1083, 1081 HV Amsterdam, The Netherlands.
[c] Department of Chemistry, Guru Nanak Dev University, Amritsar 143 005, India.

Abstract. Tautomeric isomers and conformers of 2-nitrovinyl alcohol, (**1**), 2-nitrovinyl amine, (**2**), and 1-nitropropene, (**3**) are reported at the MP2 and B3LYP levels of theory, using the 6-31G* basis set, with energy evaluation at B3LYP/6-311+G** and G2MP2. The nitroalkenes are the global minima on their respective potential energy surfaces. The barriers for the concerted 1,5-H transfer to the corresponding nitronic acids amount to only 5.0 kcal/mol for **1**, 13.2 kcal/mol for **2**, and a sizeable 37.8 kcal/mol for **3**. Whereas the *aci*-nitro tautomer of 2-nitrovinyl alcohol is easily accessible, β-iminonitronic acid has little kinetic stability. H-bonding is a strong stabilizing factor in these nitroalkenes, estimated at 7.0 and 3.7 kcal/mol for the OH and NH_2 derivatives, respectively, while its stabilization in their nitronic acids amounts to as much as 13 kcal/mol. The H-bonds are evident from the very short O···H and N···H distances and are characterized by bond critical points. The NO_2 substituent effect of about 11.4 kcal/mol at G2MP2 on both the classical keto _ enol and imine _ enamine tautomeric processes stabilizes the nitroethylene derivatives. The keto, imine, and vinyl substituent effects at G2MP2 on the nitro _ *aci*-nitro tautomeric process are also determined as are their π-resonance components. The substituents have a large influence on the ionization energies of the nitroethylene derivatives.

Introduction

In the many studies devoted to tautomerism in conjugated systems, the nitro group has received less attention than for example the keto and imine groups (Scheme 1). In the present study we explore the combined effect of the keto _ enol,[1,] imine _ enamine,[2b] and nitro _ aci-nitro[2] tautomeric processes in conjugated systems. Particular emphasis is placed on the 1,5-H shift in *cis*-2-nitroethenol 1, *cis*-2-nitrovinyl amine 2, and *cis*-1-nitropropene 3 to investigate the accessibility of nitronic acids (Scheme 2).

Nitronic acids[3] are compounds containing a -N(=O)-OH or *aci*-nitro group. They are the thermodynamically unfavorable tautomers of nitroalkanes,[2-4] as illustrated by the 14 kcal/mol energy difference (G2 theory) between the nitromethane tautomers. Still, nitronic acids play an important role as reactive intermediates in many redox, photochemical, and pyrolysis processes,[2-6] and in syntheses such as the Nef and Victor Meyer reactions.[7] Nitronic acids become more stable on aromatic substitution of the α-carbon as in diphenylmethanenitronic acid,[8] and by inter-[8] or intramolecular[9] hydrogen bonding.[9] As a radical cation the *aci*-nitro tautomer is even preferred over that of nitromethane.[10] Due to the high energy barrier for 1,3-hydrogen transfer, nitronic acids are typically formed via acid-base equilibria.[2,8,11]   Both the protonation[12] and deprotonation[13] of nitromethane have been the subject of theoretical studies.

Appropriately substituted aromatic nitro derivatives may also yield nitronic acids as suggested by the incipient formation of anthranil derivatives during pyrolysis of, *e.g.*, *ortho*-nitrotoluene.[14] In such conjugated systems the 1,5-hydrogen transfer formally represents a 6 el. thermally allowed sigmatropic rearrangement. Politzer et al.[15] reported the nitro _ *aci*-nitro tautomerism in *ortho*-nitrophenol indeed to be a low energy process at HF/3-21G, but also found such a process not to be feasible for *ortho*-nitroaniline. In an earlier related study, the nitro _ *aci*-nitro tautomerism for *cis*-1-nitropropene was reported to be a high energy process.[16]

2

In the present study, using different levels of ab initio theory, we explore various tautomeric processes with emphasis on the 1,5-H-shifts in parent olefinic systems that render nitronic acids. To provide accurate energies for this process we report in detail on a spectrum of structural conformers and isomers. The extent of H-bonding associated with the 1,5-H-shifts will be detailed as will be the substituent effect on the classic tautomeric processes.

Computational Methods

Ab initio molecular orbital[17] and density functional (DFT)[18] calculations were performed with the GAUSSIAN94[19] suite of programs using IBM RS6000 workstations. Geometries of 2-nitrovinyl alcohol (**1A,**), 2-nitrovinyl amine (**2A**), and 1-nitropropene (**3A**); their nitronic acid tautomers (**1-3B**); the related keto (**1C**) and enamine (**2C**) tautomers and 3-nitropropene (**3C**); the corresponding anions (**1-3D**); and the transition structures for the 1,5-H shift (**1-3E**) were optimized at the HF, MP2(full),[20] and B3LYP[21] levels of theory using the 6-31G* basis set. All the isomers and conformers of these systems that are used in this study are identified in Scheme 3. Selected structures are displayed with their important geometrical parameters in Figures 1-5. For all species the Hessian index, which is the number of negative eigenvalues of the force constant matrix, was determined at the SCF level. HF/6-31G* zero point vibrational energies (ZPE) are scaled by a factor of 0.8929.[22] Single point calculations were performed at B3LYP/6-311+G** and MP4(SDTQ)/6-31G* using the B3LYP and MP2(full)/6-31G* geometries, respectively, to obtain better estimates of relative energies. G2MP2 theory was used to obtain more accurate absolute energies on selected structures. Tables 1s-3s summarize the absolute energies (Additional Material). Relative energies for all isomers and anions are summarized in Tables 1-3. Bonding properties were investigated at MP2(full)/6-31G* with Bader's topological one-electron density analysis.[23] Bond critical points for **1-3A,B** are detailed in Table 4s (Additional

3

Material). Relief maps for ρ are shown in Figure 6 for **1A,B**. Throughout the discussion B3LYP/6-31G* geometric parameters and B3LYP/6-311+G** energies will be used unless indicated otherwise.

Results and Discussion

The discussion is organized in three sections: (a) structures and energeties of stable molecules and anions, (b) 1,5-H shifts in substituted nitroethylenes, and (c) aspects of conventional keto-enol, imine-enamine, nitro-*aci*-nitro tautomerisms. Similarities and differences between the parent systems **1**, **2**, and **3** are the focal points in these sections.

A. Isomers, Tautomers, and Conformers. We start with the substituted nitroethylenes, followed by their related nitronic acids, 'aliphatic' nitro derivatives, and anions.

1. Substituted nitroethylenes. A prerequisite for inducing 1,5-H-shifts is having access to *Z*-substituted derivatives. These structures **1Aa**, **2Aa**, and **3Aa** are indeed minima, which comes as no surprise in light of the maximum delocalization that results between the unsaturated groups[16] and the stabilizing hydrogen bonding between the olefinic OH and NH_2 substituents and the nitro group.[24,25] The strength of the H-bond can be estimated from the NO_2-rotation barrier and from the differences in stabilities of both the *Z-E* isomers (double bond isomerism) and the *syn-anti* conformers (substituent conformation).[26]

Cis-2-nitrovinyl alcohol (**1A**). We start with the *syn*-conformer **1Aa** (C.), the global minimum for **1**, in which the alcohol group is directed toward the nitro group. The 15.3 kcal/mol needed for rotation around its $C-NO_2$ bond is much more than the 5.6 kcal/mol needed for the unsubstituted nitroethylene.[27] Attributing this enhanced barrier of 9.7 kcal/mol entirely to H-bonding seems appealing, but ignores the conjugative effect of the OH group that is evident from

4

the difference in the NO₂ rotation barriers for **1Ac** (8.9 kcal/mol) and nitroethylene (5.6 kcal/mol). Incorporating this effect gives a H-bond strength of 6.4 kcal/mol.

Alternatively, C–OH bond rotation (**1Aa** → **1Ab**), which does not effect the π-delocalization between the nitro and olefinic groups, suggests a 11.9 kcal/mol H-bond strength, but ignores both the OH *syn-anti* effect and the O···O lone-pair repulsion. The *syn-anti* energy difference, ΔE(**1Ac-1Ad**), is a mere 0.3 kcal/mol (B3LYP) for the *E*-isomer (compared to 1 (ca. 2) kcal/mol at G1[1d] (exp.[1f]) for unsubstituted vinyl alcohol). The O···O lone-pair repulsion in the *Z*-isomer is estimated at 4.1 kcal/mol, *i.e.*, ΔE(**1Ab-1Ad**). Including these contributions gives a H-bond strength of 7.5 kcal/mol, which is also obtained from the energy difference of the *cis* (**1Aa**) and *trans* (**1Ac**) isomers. Averaging the values obtained by these methods gives a H-bond strength of 7.0 kcal/mol at B3LYP. At MP2 and MP4 the averaged H-bonding estimates are 6.9 and 6.5 kcal/mol, respectively.

The strong intra-molecular hydrogen bond in **1Aa** is also reflected in the short O···H distance of 1.713 (1.775) Å at B3LYP (MP2) between the nitro and alcohol groups and the presence of a bond critical point ($\rho(r)$ = 2.63 e.Å^{-3}) along the O···H path. The relief map of $\rho(r)$ (Figure 6a) visualizes this hydrogen bond path.

Cis-2-nitrovinyl amine (**2A**). The longer O···H distance of 1.967 (1.992) Å at B3LYP (MP2) and the less prominent O···H bond critical point (Table 4s) already suggest a weaker hydrogen bond in planar **2Aa**, the global minimum for **2**, than in *cis*-2-nitrovinyl alcohol.

Indeed, only a bond strength of 4.3 kcal/mol is estimated, based on the *cis* (**2Aa**) and *trans* (**2Ab**) energy difference. An even smaller value of 3.0 kcal/mol results from their difference in C–NO₂ bond rotation barriers - that of **2Aa** is 14.7 kcal/mol - giving an averaged H-bond strength of 3.7 kcal/mol with MP2 and MP4 values of 3.6 and 3.1 kcal/mol, respectively. These energies show that the strength of the H-bond between the NH₂ and NO₂ groups is about half of the

OH···ONO interaction, which is also reflected in the bond critical point ($\rho(r) = 0.184$ e.Å^{-3}) of its bond path. This H-bonding causes the NH_2 group to be planar, albeit that the N-pyramidalization angle of **2Ab** is only 2.3°. In contrast, vinyl amine has a N-inversion barrier of 1.4 kcal/mol at G1 (exp. 1.1 kcal/mol).[2b,28] We note that the geometric parameters of **2Ab** compare well with those reported for a X-ray crystal structure determination of *trans*-N,N-dimethyl-2-nitroethenamine.[29]

1-Nitropropene (**3A**). The CH_3-staggered form (**3Aa**) is the preferred conformation for the *Z*-isomer with a CH_3-rotation barrier of 0.9 kcal/mol, implying an absence of H-bonding. The smaller C–NO_2 rotation barrier (3.7 kcal/mol) than in nitroethylene (5.6 kcal/mol) even signals a slight repulsion between the NO_2 and CH_3 groups. A van der Waals interaction between these groups is suggested by the electron density analysis (see Table 4s), which is not surprising given the 2.278 Å O···H distance. In fact, the *E*-isomer (**3Ac**) is more stable by 2.7 kcal/mol.

2. Conjugated nitronic acids. Again, the tautomers are discussed by substituent (O, N, C) with focus on H-bonding and relative stabilities. Only the most relevant isomers and conformers are used from the many that are possible due to the *syn/anti*-arrangement of the nitronic acid group.

β-Ketonitronic acid (**1B**). Structure **1Ba**, having an *anti*-ONOH group and a *s-cis* conformation for the conjugated unsaturated functionalities, is the preferred nitronic acid. It is only 4.1 kcal/mol less stable than nitro isomer **1Aa**. The 1.565 Å short O···H distance in **1Ba** and the critical point data ($\rho(r) = 2.033$ e.Å^{-3}, $H(r) = -3.126$ Hartree.Å^{-3}) of its bond path, visualized in Figure 6b, imply strong H-bonding. Its strength can be estimated by rotation of the nitronic acid's OH group as well as by *s-cis* → *s-trans* rotation of the C=O and C=N groups around the C–C bond.

Changing to a *syn*-ONOH conformation raises the energy by 8.8 kcal/mol (8.0 and 6.9 kcal/mol at MP2 and MP4, respectively). Instead, nitromethane prefers the *syn*-ONOH form by 7.1 (6.8) kcal/mol at B3LYP (G1),[2a] which suggests an upper value of 15.9 kcal/mol for H-bonding in **1Ba**. Correcting for the 3.3 kcal/mol O⋯O lone-pair repulsion, based on the energetic preference of the *s-cis* over the *s-trans* conformation, gives a final H-bond strength of 12.6 kcal/mol. A nearly identical estimate of 12.8 kcal/mol results from the energy difference between **1Ba** and **1Bd**, both with *anti*-ONOH groups. The corresponding MP2 and MP4 values are 14.2 and 12.9 kcal/mol. Evidently, H-bonding in the nitronic acid is much stronger than in *cis*-nitrovinyl alcohol **1Aa**.

β-Iminonitronic acid (**2B**). The imine derivative also prefers a *s-cis* conformation (**2Ba**), in analogy with β-ketonitronic acid **1Ba**, but it has a much larger energy difference (13.0 kcal/mol) with its nitro tautomer (**2Aa**). Still, the short O⋯H distance of 1.548 Å suggests significant H-bonding, which is also evident from the bond critical point data, *i.e.*, $\rho(r) = 2.077$ e.Å^{-3}, $H(r) = -3.374$ Hartree.Å^{-3}. Its strength is estimated at 13.1 kcal/mol, based on the 6.0 kcal/mol energy difference between **2Ba** and **2Bb** and the 7.1 kcal/mol preference for the *syn*-ONOH conformation. The H-bond strength, calculated as the energy difference between the *s-cis* and *s-trans* conformations ($\Delta E = $ **2Ba** -**2Bc**), is similar and amounts to 14.3 kcal/mol, giving an average value of 13.7 kcal/mol. The corresponding MP2 and MP4 values are 13.4 and 11.1 kcal/mol, respectively.

3-Propylenenitronic acid (**3B**). The energy difference between *cis*-1-nitropropene **3Aa** and nitronic acid **3Ba** is 10.1 kcal/mol. The structure has a *syn*-ONOH arrangement because of steric congestion due to the neighboring methylene group. Consequently, structure **3Ba** displays no H-bonding and, in fact, the *s-trans* form **3Bb** is even 2.9 kcal/mol more stable. In passing, we

note that 1,3-butadiene and X=C-C=X, (X = NH, PH) prefer twisted *s-cis* forms with planarization barriers of ca. 2 kcal/mol.[30]

3. Non-conjugative nitro derivatives. Of the remaining tautomers nitroacetaldehyde (**1C**), nitroacetaldimine (**2C**), and 3-nitropropene, (**3C**) we highlight only features specific to these compounds because acetaldehyde, acetaldimine, nitromethane, and propene have already been discussed extensively in the literature. These compounds can only have *anticlinical* and *synperiplanar* conformations (Figure 3) due to the gearing effect around the C–C and C–N single bonds. Of these the *anticlinical* form is preferred by 1.4, 2.1, and 2.0 kcal/mol for **1C**, **2C**, and **3C**, respectively. Its NCCX (X = O,N,C) torsion angle becomes more pronounced on going from **1Ca** (156.6°) to **2Ca** (134.9°) to **3Ca** (123.6°), while the twists of the NO_2 group are similar ($\angle CCNO = 46\text{-}51°$), resulting in a nearly fully eclipsed conformation for the propene derivative. Of the *synperiplanar* arrangements only **3Cb** deviates (14°) from the frame's plane, while all three structures have similar NO_2 rotations, *i.e.*, 89° for **1Cb**, 90° for **2Cb**, and 73° for **3Cb**. None of the geometrical parameters of these structures displays any sign of delocalization between the two functional groups.

These non-conjugated nitro derivatives (*anticlinical* forms) are less stable than the conjugated global minima, but the energy differences are only 3.9 (0.4) kcal/mol for nitroacetaldehyde (**1Ca**) and 3.8 (2.9) kcal/mol for 3-nitropropene (**3Ca**) at B3LYP (G2MP2). Apparently, these systems are stabilized by a significant substituent effect. A larger difference of 12.4 (7.3) kcal/mol is obtained for nitroacetaldimine (**2Ca**), which is also more sensitive to the theoretical method employed.

4. Conjugated anions. Deprotonation of any of the tautomeric structures gives anions in which the charge is delocalized. This delocalization is reflected in the geometries of anions **1D**, **2D**, and **3D** (Figure 4). These favor a *s-trans* (**Db**) over a *s-cis* (**Da**) conformation by 6.0 (5.8),

8.7 (8.2), and 2.1 (1.3) kcal/mol at B3LYP (G2MP2), respectively. This *s-trans* preference of

1Db and **2Db** results from the lone pair repulsion of the carbonyl and imine groups, respectively,

with the NO_2 group. Because significant charge is located on the nitro group of these anions

(Table 5s), they may even be viewed as nitronates.

The G2MP2 ionization energies for the global minima of *cis*-2-nitrovinyl alcohol, *cis*-2-

nitrovinyl amine, and *cis*-1-nitropropene to give the conjugated anions are 326.7, 342.3, and 345.1

kcal/mol, respectively. They are much lower than the 366.2, 378.6, 356.9, and 388.7 kcal/mol for

acetaldehyde, acetaldimine, nitromethane, and propene, respectively (similar G1 and G2 energies

have been reported).[2b] Nitro substitution in these systems, because of its electron withdrawing

nature, clearly increases the acidity, thereby facilitating acid-base directed tautomerism.

B. Sigmatropic 1,5 hydrogen transfer. This pericyclic process concerns tautomerism

between the above discussed conjugated nitro derivatives and nitronic acids. G2MP2 energies

used in this section (in parentheses) are without ZPE corrections to eliminate bias in discussing

low activation energies.

Cis-2-nitrovinyl alcohol (**1Aa**) and β-ketonitronic acid (**1Ba**) differ in energy by only 4.1

(5.7) kcal/mol. Both have strong H-bonds, estimated at 7.0 and 12.7 kcal/mol, respectively,

illustrating their close relationship. It is then not surprising that H-transfer is an extremely facile

process with a **1Aa** → **1Ba** barrier of 5.0 (7.1) kcal/mol and only 0.9 (1.4) kcal/mol for the reverse

process. Expectantly, transition structure **1E** (Figure 5) shows similarities with both minima.

The energy difference of 13.0 (12.7) kcal/mol between *cis*-2-nitrovinyl amine (**2Aa**) and

β-iminonitronic acid (**2Ba**) is much larger, but also in this case both structures have distinct

hydrogen bonds estimated at ca. 3.7 and 13.7 kcal/mol, respectively. H-transfer from the nitronic

acid to the more stable nitro tautomer is, however an extremely facile process, requiring only 0.2

(1.2) kcal/mol, emphasizing the low kinetic stability of the nitronic acid. The geometrical parameters of transition structure **2E** (Figure 5) relate to those of the nitronic acid.

Cis-1-nitropropene (**3Aa**) and 3-propylenenitronic acid (**3Ba**) have also a rather large energy difference of 10.1 (11.6) kcal/mol. However, neither structure displays signs of H-bonding implying that the concerted H-transfer is energetically a much more demanding process than in the other two systems. The required methyl-group rotation in **3Aa** to enable H-transfer and the subsequently needed N-OH bond rotation to give nitronic acid **3Ba** also suggest a high barrier. Indeed, this barrier is estimated at a large 35.1 (40.2) kcal/mol. Transition structure **3E** (Figure 5) shows an out-of-plane motion for the transferring hydrogen. Following its intrinsic reaction coordinate in both directions confirmed **3E** as the transition structure for H-transfer.

Comparison between the sigmatropic 1,5 hydrogen shifts of **1**, **2** and **3** shows the tautomerism to be a facile process for **1**, does not lead to a kinetically stable nitronic acid tautomer in the case of **2**, and is a high energy process for **3**.

C. Conventional tautomerism. Acid-base induced 1,3 hydrogen shifts underlie the common keto _ enol, imine _ enamine and nitro _ *aci*-nitro tautomeric processes in organic chemistry. The data of the present study enable an evaluation of the nitro, keto, imine, and vinyl substituent effects on these tautomerisms. Without substituents the equilibria favor the keto, imine, and nitro isomers as has been established in several theoretical studies.[2] Table 4 summarizes the B3LYP and G2MP2 energy differences for these parent acetaldehyde _ vinyl alcohol, acetaldimine _ vinyl amine, and nitromethane _ *aci*-nitromethane tautomeric pairs. They compare well with reported G1/G2 energy differences for these systems.[2a,b] These earlier studies showed that the ΔE values decrease with improved levels of theory. The illustration of this trend is not repeated here. Table 4 also lists the energy differences for the nitro derivatives of the tautomeric pairs. For brevity, the HF, MP2, and MP4 data are not tabulated as the trends in decreasing ΔE values are

similar to those for the non-substituted pairs. The G2MP2 energies show that the NO_2 substituent effect is 11.5 kcal/mol for the keto/enol tautomeric pair and essentially the same (11.3 kcal/mol) for the imine/enamine pair. While very similar values are obtained at lower levels of theory, the respective NO_2 substituent effects of 14.3 and 14.7 kcal/mol obtained at B3LYP are slightly larger. The energetic preference of 1- over 3-nitropropene amounts to only 2.9 kcal/mol at G2MP2, and 3.8 kcal/mol at B3LYP. We consider the G2MP2 values to be the more accurate ones and assume that B3LYP slightly overestimates the NO_2-stabilization.[31]

The significant NO_2 substituent effect in favor of the enol and imine forms has two contributors, $i.e.$, intra-molecular H-bonding and π-resonance delocalization. The resonance effect in the enol and imine can be obtained by subtracting the H-bond strengths (using average values from section A) from the NO_2 substituent effect. We perform this analysis at B3LYP and MP4 (given in parentheses) as not all data needed for G2MP2 analysis are available.

Subtracting the H-bond strength of 7.0 (6.5) kcal/mol from the 14.3 (12.6) kcal/mol NO_2 substituent effect gives a NO_2 π-resonance effect of 7.3 (6.1) kcal/mol for enol **1Aa**. The magnitude of this resonance effect compares well with the slightly larger 8.9 (7.8) kcal/mol for the NO_2 rotation barrier of **1Ac**. Likewise, subtracting the 3.7 (3.1) kcal/mol H-bond strengths from the 14.7 (11.0) kcal/mol NO_2 substituent effect for the imine/enamine tautomeric pair gives a π-resonance effect of 11.7 (7.9) kcal/mol for enamine **2Aa**. Again a good comparison is obtained with the rotation barrier of 11.0 (9.1) kcal/mol for **2Ab**. Apparently, because H-bonding is stronger in the enol and the π-resonance is more prominent in the imine, the NO_2 substituent effect is coincidentally the same for the enol and imine forms. We realize that neither σ-substituent effects nor steric factors were included in this analysis. The difference between the NO_2 substituent effect of 3.8 (3.0) kcal/mol for propene and the 6.6 (5.9) kcal/mol rotation barrier for **3Ac** may be illustrative of their contributions.

The influence of the keto, imine, and vinyl groups on the nitro _ *aci*-nitro tautomerism can be determined in a manner similar as discussed above for the nitro substituent effect. Table 4 summarizes these substituent effects at B3LYP and G2MP2. Expectantly, the preference for the nitro derivatives reduces substantially by stabilizing the nitronic acid through H-bonding and conjugation. We find similarly large keto and imine substituent effects of 13.9 (9.9) and 13.5 (9.2) kcal/mol, respectively - G2MP2 values are in parentheses. The magnitude of these effects largely results from the strong H-bonding of 12.6 and 12.9 kcal/mol in **1Ba** and **2Ba**, respectively. Consequently, the deduced resonance stabilization for the conjugated systems is small, 1.4 and 0.5 kcal/mol for the keto and imine groups, respectively, smaller than the 3.0 (3.6) kcal/mol vinyl substituent effect.

Finally, we briefly comment on the influence of substituents on the reactivity of nitroalkenes, which are used as dienes in Michael additions for the synthesis of delicate heterocycles.[32] Earlier studies mainly focused on the influence of the α-substituent,[32c] but changing the β-substituent is also expected to modify the reactivity profile of the nitroalkene (or nitronate anion). The NPA[33] group charge distribution for the olefinic units of **1A-3A** (Table 5s, Additional Material) shows that on β-substitution ($CH_3 \rightarrow NH_2 \rightarrow OH$) the positive (group) charge reduces modestly at the α-center with a concurrent strong increase at the β-center. Thus, the Michael (diene) acceptor ability of nitroethylenes is expected to increase with more electronegative β-substituents.

Conclusions

Strong interrelationships are demonstrated for the prototypic keto _ enol, imine _ enamine, and nitro _ *aci*-nitro tautomeric processes in β-substituted 1-nitroalkenes. Hydrogen bonding and substituent effects profoundly impact the tautomeric equilibria. The following specific conclusions are made:

(1) The β-OH, β-NH$_2$, and β-CH$_3$ *cis*-substituted nitroethylenes are global minima. (2) The NO$_2$-substituent effect on the enol and enamine forms of the keto _ enol and imine _ enamine tautomers is about 11.4 kcal/mol for both. The NO$_2$ group reduces the keto _ enol energy difference from 11.1 to –0.4 kcal/mol, favoring the enol form. Likewise it reverses the 4.0 kcal/mol energy difference for the imine _ enamine pair to favor the enamine form by 7.3 kcal/mol. The conjugated 1-nitropropene is 2.9 kcal/mol more stable than the 3-nitro isomer. (3) The HC=O, HC=NH, and HC=CH$_2$ substituent effects stabilize the nitronic acid tautomer of the nitro _ *aci*-nitro pair by 9.9, 9.2, and 3.6 kcal/mol, respectively. (4) Intramolecular H-bonding is a major contributor to these substituent effects. The strength of the H-bond is 7.0 and 3.7 kcal/mol for the OH and NH$_2$ substituted nitroethylenes, respectively, and about 13 kcal/mol for the related nitronic acids of both. The H-bonds are characterized by critical points on correspondingly short O···H and N···H bond paths. (6) The 5.0 kcal/mol barrier for intramolecular H transfer in 2-nitrovinyl alcohol makes the tautomeric process very facile. Tautomerism does not lead to a kinetically stable nitronic acid in the case of 2-nitrovinyl amine, because its barrier of 13.2 kcal/mol for 1,5-H transfer is similar to the energy difference between the tautomers. Tautomerism by intramolecular H-transfer is a much more demanding process in 1-nitropropene with a barrier of 37.8 kcal/mol. (7) The NH$_2$ group shows a slightly stronger conjugative stabilization than the OH group. (8) 2-Nitrovinyl alcohol, 2-nitrovinyl amine, and 1-nitropropene have low ionization energies of 326.7, 342.3, and 345.1 kcal/mol, respectively. (9) Throughout, the B3LYP/6-311+G** relatively energies are slightly larger that the G2MP2 energies.

Supplementary Material Available : Tables 1s-3s, absolute energies of all the structures; Table 4s, bond critical point data of **1Aa**, **2Aa**, **1Ba**, and **2Ba**; Table 5s, NPA group charges (5 pages). This information is available free of charge via the Internet at http://pubs.acs.org.

References.

1. (a) Rappaport, Z. (Ed.) *The Chemistry of Enols,*: Wiley: Chichester, 1990. (b) Capon, B.; Guo, B.; Kwok, F.C.; Siddhanta, A.K.; Zucco, C. *Acc. Chem. Res.* **1988**, *21*, 135 and references cited therein. (c) Smith, B.J.; Nguyen, M.T.; Bouma, W.J.; Radom, L. *J. Am. Chem. Soc.* **1991**, *113*, 6452. (d) Smith, B.J.; Radom, L. *J. Am. Chem. Soc.* **1992**, *114*, 36. (e) Nagaoka, M.; Suenobu, K.; Yamabe, T. *J. Am. Chem. Soc.* **1997**, *119*, 8023. (f) Fraser, R.R.; Banville, J. *J. Chem. Soc., Chem. Commun.* **1979**, 47.

2. (a) Lammertsma, K.; Prasad, B.V. *J. Am. Chem. Soc.* **1993**, *115*, 2348 and references cited therein. (b) Lammertsma, K.; Prasad, B.V. *J. Am. Chem. Soc.* **1994**, *116*, 642. (c) Harris, N.J.; Lammertsma, K. *J. Am. Chem. Soc.* **1996**, *118*, 8045.

3. (a) Nielson, A.T. In *The Chemistry of the Nitro and Nitroso Groups*, Feuer, H., Ed.: Interscience; New York, 1969; Part 1, p349. (b) Noland, W.E. *Chem. Rev.* **1955**, *55*, 137. (c) *The Chemistry of Amine, Nitroso, and Nitro Compounds and Their Derivatives*, Patai, S., Ed.: Wiley: New York, 1982. Morrison, H.A., p165; Chow, Y.L.; Batt, L., p 417. (d) *International Agency of Carcinogenic Risk of Chemicals to Man*, WHO: Lyon, 1982; Vol. 29, p 331.

4. (a) McKee, M.L. *J. Am. Chem. Soc.* **1986**, *108*, 5784. (b) McKee, M.L. *J. Phys. Chem.* **1986**, *90*, 369. (c) Qian, K.; Shukla, A.; Futrell, J. *J. Am. Chem. Soc.* **1991**, *113*, 7121. (d) Ritchie, J.P. *J. Org. Chem.* **1989**, *54*, 3553. (e) Ritchie, J.P. *Tetrahedron* **1988**, *44*, 7465. (f) Tao, Y. *Top. Mol. Organ. Eng.* **1996**, *14*, 421. (g) Khrapkovski, G.M.; Shamov, A.G.; Shamov, G.A.; Shlyapochnikov, V.A. *Mendeleev Commun.* **1997**, 169.

5. *The Chemistry of Amine, Nitroso, and Nitro Compounds and Their Derivatives*, Patai, S., Ed. Wiley: New York, 1982: Schwarz, H., Levsen, K., p85; (b) ibid. Fry, A.J., p. 319. (c) Sartori, G.; Bigi, F. Maggi, R.; Tomasini, F. *Tetrahedron Letts.* **1994**, *35*, 2393. (d) Hey-

Motherwell, R.S., Wilkinson, G.; Sweet, T.K.N.; Hursthouse, M.B. *J. Chem. Soc., Dalton Trans.* **1994**, 2223.

6. (a) Kheir, A.A.; Haw, F. *J. Am. Chem. Soc.* **1994**, *116*, 817. (b) Allouche, A. *J. Phys. Chem.* **1996**, *100*, 1820.

7. (a) Edward, J.T.; Tremaine, P.H. *Can. J. Chem.* **1971**, *49*, 3483. (b) Edward, J.T.; Tremaine, P.H. *Can. J. Chem.* **1971**, *49*, 3489.

8. Bock, H., Dienelt, R.; Schodel, H.; Havlas, Z.; Herdtweck, E.; Herrmann, W.A. *Angew. Chem. Int. Ed. Engl.* **1993**, *32*, 1758.

9. Kang, F.-A.; Yin, C.-L.; She, S.-W. *J. Org. Chem.* **1996**, *61*, 5523.

10. Beijersbergen, J.H.M.; Zande, W.J.v.d.; Kistemaker, P.G.; Los, J.; Drewello, T.; Nibbering, M.M. *J. Phys. Chem.* **1992**, *96*, 9288.

11. (a) Erden, I.; Keeffe, J.R.; Xu, F.-P.; Zheng, J.-B. *J. Am. Chem. Soc.* **1993**, *115*, 9834. (b) Kresge, A.J. *Chemtracts : Org. Chem.* **1994**, *7*, 187. (c) Cao, W.; Erden, I.; Keeffe, J.R. *Angew. Chem. Int. Ed. Engl.* **1995**, *34*, 1091.

12. (a) Bernasconi, C.F.; Zitomer, J.L.; Schuck, D.F. *J. Org. Chem.* **1992**, *57*, 1132. (b) Bernasconi, C.F.; Wenzel, P.J.; Keeffe, J.R.; Gronert, S. *J. Am. Chem. Soc.* **1997**, *119*, 4008.

13. (a) Beksic, D.; Bertran, J.; Lluch, J.M.; Hynes, J.T. *J. Phys. Chem. A* **1998**, *102*, 3977. (b) Politzer, P.; Seminario, J.M.; Zacarias, A.G. *Mol. Phys.* **1996**, *89*, 1511.

14. (a) He, Y.Z.; Cui, J.P.; Mallard, W.G.; Tsang, W. *J. Am. Chem. Soc.* **1988**, *110*, 3754. (b) Chattopadhyay, S.K.; Craig, B.B. *J. Phys. Chem.* **1987**, *91*, 323.(c) Menapace, J.A.; Marlin, J.E. *J. Phys. Chem.* **1990**, *94*, 1906.

15. Politzer, P.; Seminario, M.J.; Bolduc, P.R. *Chem. Phys. Lett.* **1989**, *158*, 463.

16. Cox, J.R.; Hillier, I.H. *Chem. Phys.* **1988**, *124*, 39.

17. For an introduction of the methods employed, see: Hehre, W.J.; Radom, L.; Schleyer, P.v.R.; Pople, J.A. *Ab Initio Molecular Orbital Theory*, Wiley: New York, 1986.

18. Parr, R.G.; Yang, W. *Density Functional Theory of Atoms and Molecules*, Oxford University Press: Oxford, 1989.

19. Gaussian 94, Revision E.2, Frisch, M.J.; Trucks, G.W.; Schlegel, H.B. Gill, P.M.W.; Johnson, B.G.; Robb, M.A.; Cheeseman, J.R.; Keith, T.; Petersson, J.A.; Montgomery, J.A.; Raghavachari, K.; Al-Laham, M.A.; Zakrzewski, V.G.; Ortiz, J.V.; Foresman, J.B.; Cioslowski, J.; Stefanov, B.B.; Nanayakkara, A.; Challacombe, M.; Peng, C.Y.; Ayala, P.Y.; Chen, W.; Wong, M.W.; Andres, J.L.; Replogle, E.S.; Gomperts, R.; Martin, R.L.; Fox, D.J.; Binkley, J.S.; Defrees, D.J.; Baker, J.; Stewart, J.P.; Head-Gordon, M.; Gonzalez, C.; Pople, J.A. Gaussian, Inc., Pittsburgh PA, 1995.

20. (a) Moller, C.; Plesset, M.S. *Phys. Rev.* **1934**, *46*, 618. (b) Pople, J.A.; Binkley, J.S.; Seeger, R. *Int. J. Quantum Chem. symp* **1976**, *10*, 1.(c) Krishnan, R.; Frisch, M.J.; Pople, J.A. *J. Chem. Phys.* **1980**, *72*, 4244.

21. (a) Becke, A.D. *J. Chem. Phys.* **1993**, *98*, 5648. (b) Becke, A.D. *Phys. Rev. A* **1988**, *38*, 3098. (c) Lee, C.; Yang, W.; Parr, R.G. *Phys. Rev. B.* **1988**, *37*, 785.

22. Pople, J.A.; Schlegel, H.B.; Krishnan, R.; DeFrees, D.J.; Binkley, J.S.; Frisch, M.J.; Whiteside, R.A. Int. J. Quantum Chem., Quantum Chem. Symp. 1981, 15,269.

23. (a) Bader, R.F.W. *Chem. Rev.* **1991**, *91*, 893. Bader, R.F.W. in *Atoms in Molecules: A Quantum Theory*, Univ. of Oxford Press, Oxford, 1990.

24. (a) Varnali, T.; Aviyente, V.; Ruiz-Lopez, M.F. *Struct. Chem.*, **1994**, *5*, 357. (b) Karelson, M.; Katritzky, A.R. *Int. J. Quantum Chem.* **1996**, *60*, 41. (c) Varnali, T.; Hargittai, I. *THEOCHEM* **1996**, *383*, 315.

25.   (a) Foresman, J.B.; Keith, T.A.; Wiberg, K.B.; Snoonian, J.; Frisch, M.J. *J. Phys. Chem.* **1996**, *100*, 16098. (b) Parrondo, R.M.; Karafiloglou, P.; Pappalardo, R.R.; Marcos, E.S. *J. Phys. Chem.* **1995**, *99*, 6461.

26.   (a) Luth, K.; Scheiner, S. J. Phys. Chem. 1994, 98, 3582. (b) Rovira, M.C.; Scheiner, S. J. Phys. Chem. 1995, 99, 9854. (c) Scheiner, S. *Hydrogen Bonding : A Theoretical Perspective,* Oxford University Press : New York, 1997.

27.   (a) The C-N rotation barrier was calculated from the B3LYP/6-31G* energy differences between nitroethylene (-283.08790 au) and its rotational transition structure (-283.07729 au). (b) Head-Gordon, M.; Pople, J.A. *Chem. Phys. Lett.,* **1990**, *173*, 585.

28.   (a) Prasad, B.V.; Uppal, P.; Bassi, P.S. *Chem. Phys. Lett.* **1977**, *276*, 31. (b) Prasad, B.V.; Uppal, P.; Grover, G.; Kaur, D. *THEOCHEM,* **1999**, *458*, 227.

29.   Hazel, A.; Mukhopadhyay, A. *Acta. Cryst.* **1980**, *B36*, 747.

30.   (a) Bachrach, S.M.; Liu, M. *J. Am. Chem. Soc.* **1991**, *113*, 7929. (b) Bharatam, P.V.; Kumar, R.S.; Mahajan, M.P. *Perkin Trans. 2,* submitted for publication.

31.   Karpfen, A.; Choi, C.H.; Kertesz, M. *J. Phys. Chem. A.* **1997**, *101*, 7426.

32.   (a) Denmark, S.E.; Thorarensen, A. *Chem. Rev.,* **1996**, *96*, 137. (b) Denmark, S.E.; Hurd, A.R. *J. Org. Chem.* **1998**, *63*, 3045.   (c) Barrett, A.G.M. *Chem. Soc. Rev.* **1991**, *20*, 95.

33.   Reed, A.E.; Weinstock, R.B.; Weinhold, F. *J. Chem. Phys.* **1985**, *83*, 735. (b) Reed, A.E.; Curtiss, L.A.; Weinhold, F. *Chem. Rev.* **1988**, *88*, 899.

Figure Captions

Fig. 1   Selected geometric parameters for **1Aa**, **2Aa**, and **3Aa** at MP2/6-31G* and B3LYP/6-31G* (in parenthesis). Distances are in Ångstrom and angles in degrees.

Fig. 2   Selected geometric parameters for **1Ba**, **2Ba**, and **B3a** at MP2/6-31G* and B3LYP/6-31G* (in parenthesis). Distances are in Ångstrom and angles in degrees.

Fig. 3   Selected geometric parameters for **1Ca**, **2Ca**, and **C3a** at MP2/6-31G* and B3LYP/6-31G* (in parenthesis). shown in two different orientations. Distances are in Ångstrom and angles in degrees.

Fig. 4   Selected geometric parameters for **1Da**, **2Da**, and **3Da** at MP2/6-31G* and B3LYP/6-31G* (in parenthesis). Distances are in Ångstrom and angles in degrees.

Fig. 5   Selected geometric parameters for **1E**, **2E**, and **3E** at MP2/6-31G* and B3LYP/6-31G* (in parenthesis). Distances are in Ångstrom and angles in degrees.

Fig. 6   Relief maps of $\rho(r)$ at MP2(full)/6-31G* for (a) **1Aa** and (b) **1Ba.**

Table 1. Relative Energies (in kcal/mol) of Nitrovinylalcohol, **1**, its Conformers, Tautomers and Anions.

Structure	HF/6-31G*	MP2/6-31G*	MP4/6-31G*	B3LYP/ 6-31G*	B3LYP/ 6-311+G**	G2MP2
1Aa	0.0	0.0	0.0	0.0	0.0	0.0
1Ab	11.6	12.3	11.9	13.7	11.9	--
1Ac	5.6	7.4	7.1	8.6	7.5	--
1Ad	6.5	8.5	8.1	9.5	7.8	--
1Ba	8.9	4.7	5.4	3.5	4.1	5.1
1Bb	13.7	12.7	12.3	12.9	12.9	--
1Bc	10.1	10.0	9.3	10.3	9.6	--
1Bd	22.5	18.9	18.3	18.2	16.9	--
1Ca	-4.0	-3.4	-4.6	2.1	3.9	0.4
1Cb	-2.2	-2.6	-3.6	3.7	5.3	--
1Da	347.1	346.0	348.0	347.1	336.2	332.5
1Db	340.2	340.4	342.3	341.5	330.2	326.7
1E	14.0	7.3	9.0	4.8	5.0	4.0
1Aa (ts)	15.4	14.3	13.7	18.9	15.3	--
1Ac (ts)[a]	10.7	8.0	7.8	10.3	8.9	--

a relative to 1Ac

Table 2. Relative Energies (in kcal/mol) of Nitrovinylamine, **2**, its Conformers, Tautomers, and Anions.

Structure	HF/6-31G*	MP2/6-31G*	MP4/6-31G*	B3LYP/ 6-31G*	B3LYP/ 6-311+G**	G2MP2
2Aa	0.0	0.0	0.0	0.0	0.0	0.0
2Ab	2.7	4.2	3.7	4.5	4.3	--
2Ac	2.7	4.4	4.1	4.5	4.3	--
2Ba	19.9	14.0	14.5	13.4	13.0	12.7
2Bb	19.7	18.5	16.6	19.2	19.0	--
2Bc	32.9	29.3	27.4	28.8	27.3	--
2Ca	4.7	4.5	2.5	10.3	12.4	7.3
2Cb	7.4	6.2	4.4	12.8	14.5	--
2Da	370.5	367.6	368.8	368.4	357.2	350.5
2Db	360.8	359.2	360.3	360.0	348.5	342.3
2E	25.1	15.3	16.7	13.6	13.2	11.2
2Aa (ts)	14.3	12.6	11.6	16.4	14.7	--
2Ab (ts)[a]	12.6	9.7	9.1	12.9	11.7	--

[a] relative to 2Ab

22

Table 3. Relative Energies (in kcal/mol) of 1-Nitropropene, **3**, its Conformers, Tautomers and Anions.

Structure	HF/6-31G*	MP2/6-31G*	MP4/6-31G*	B3LYP/ 6-31G*	B3LYP/ 6-311+G**	G2MP2
3Ac	0.0	0.0	0.0	0.0	0.0	0.0
3Aa	3.1	2.2	2.2	2.5	2.7	2.3
3Ab	3.4	2.9	2.9	2.6	2.6	--
3Ba	21.5	21.4	20.9	17.3	12.8	13.9
3Bb	18.1	18.8	18.3	14.7	9.9	--
3Ca	3.4	3.1	3.0	5.2	3.8	2.9
3Cb	5.7	4.7	4.7	7.3	5.8	--
3Da	371.0	367.5	370.5	365.1	349.6	346.4
3Db	367.9	366.0	368.8	362.8	347.5	345.1
3E	61.1	44.4	47.7	39.8	37.8	39.6
3Ac (ts)	8.1	6.1	5.9	7.7	6.6	--
3Aa (ts) [a]	5.0	3.5	3.5	5.1	3.7	--

[a] relative to **3Aa**.

24

Table 4. B3LYP/6-311+G** (G2MP2) Energy Differences between Tautomers and the Influence of

the NO_2, CHO, CHNH, Vinyl Substituent Effects.[a]

	-H		-NO$_2$		-C(H)=O		-C(H)=NH		-C(H)=CH$_2$	
ΔE										
Keto _ Enol	10.4	(11.1)	-3.9	(-0.4)						
Imine _ Enamine	2.3	(4.0)	-12.4	(-7.3)						
Nitro _ *Aci*-nitro	14.1	(14.6)			0.2	(4.7)	0.6	(5.4)	9.0	(11.0)
Substituent effect										
Keto _ Enol			14.3	(11.5)						
Imine _ Enamine			14.7	(11.3)						
Nitro _ *Aci*-nitro					13.9	(9.9)	13.5	(9.2)	5.1	(3.6)

[a] Energies are in kcal/mol.

25

Keto _ Enol, Imine _ Enamine, and Nitro _ *aci*-Nitro Tautomerism and Their Interrelationship in Substituted Nitroethylenes. Keto, Imine, Nitro, and Vinyl Substituent Effects and the Importance of H-bonding.

by

Koop Lammertsma[a,b]* and Prasad V. Bharatam[a,c]

[a] Department of Chemistry, University of Alabama at Birmingham, Birmingham, AL 35294

[b] Department of Chemistry, Scheikundig Laboratorium, Vrije Universiteit, De Boelelaan 1083, 1081 HV Amsterdam, The Netherlands.

[c] Department of Chemistry, Guru Nanak Dev University, Amritsar 143 005, India

Supporting Material.

Table 1s. Absolute Energies of Nitrovinylalcohol, 1, its Conformers, Tautomers, Transiton Structures and Anions.

Table 2s. Absolute Energies of Nitrovinylamine, 2, its Conformers, Tautomers, Transtion Structures and Anions.

Table 3s. Absolute Energies of 1-Nitropropene, 3, its Conformers, Tautomers, Transition Structures and Anions.

Table 4s. Summary of the MP2(full)/6-31G* Bond Critical Point Data for the Hydrogen Bonds of Nitroethylenes 1Aa and 2Aa and Their *aci*Nitro Tautomers, 1Ba and 2Ba.

Table 5s. NPA group charges of R-C^1(H)=C^2(H)-NO$_2$ at MP2(full)/6-31G*.

Table 1s. Absolute Energies (in -hartrees) of Nitrovinylalcohol, 1, its Conformers, Tautomers, Transiton Structures

and Anions.[a]

Structure		HF/6-31G*	MP2/6-31G*	MP4/6-31G*[b]	B3LYP/6-31G*	B3LYP/6-311+G**[c]	G2MP2	ZPE[d]
1Aa	C,	356.37129 (0)	357.36069	357.39829	358.32154	358.44111	357.83458	37.6
1Ab	C,	356.35286 (0)	357.34116	357.37938	358.29974	358.42211	--	37.1
1Ac	C,	356.36242 (0)	357.34887	357.38704	358.30777	358.42917	--	37.1
1Ad	C,	356.36090 (0)	357.34721	357.38535	358.30635	358.42864	--	37.0
1Ba	C,	356.35703 (0)	357.35329	357.38967	358.31603	358.43458	357.82638	37.0
1Bb	C,	356.34941 (0)	357.34040	357.37866	358.30104	358.42054	--	36.6
1Bc	C,	356.35520 (0)	357.34473	357.38352	358.30507	358.42576	--	36.5
1Bd	C,	356.33550 (1)	357.33056	357.36903	358.29253	358.41410	--	35.9
1Ca	C₁	356.37765 (0)	357.36617	357.40566	358.31824	358.43482	357.83390	36.5
1Cb	C₁	356.37488 (0)	357.36492	357.40411	358.31561	358.43260	--	36.7
1Da	C,	355.81821 (0)	356.80925	356.84379	357.76834	357.90529	357.30469	28.3
1Db	C,	355.82913 (0)	356.81826	356.85287	357.77741	357.91486	357.31398	28.9
1E	C,	356.34804 (1)	357.34911	357.38392	358.31385	358.43320	357.82827	34.5
1Aa (ts)	C₁	356.34669 (1)	357.33789	357.37643	358.29258	358.41670	--	36.7
1Ac (ts)	C₁	356.34531 (1)	357.33609	357.37469	358.29129	358.41494	--	36.6

[a] Values in parentheses are the number of imaginary frequencies.

[b] Using MP2/6-31G* geometries.

[c] Using B3LYP/6-31G* geometries.

[d] Zero Point Vibrational Energies at HF/6-31G*, scaled by 0.8929.

Table 2s. Absolute Energies (in -hartrees) of Nitrovinylamine, **2**, its Conformers, Tautomers, Transtion Structures and Anions. [a]

Structure		HF/6-31G*	MP2/6-31G*	MP4/6-31G*[b]	B3LYP/6-31G*	B3LYP/6-311+G**[c]	G2MP2	ZPE[d]
2Aa	C$_s$	336.54755 (0)	337.52181	337.56267	338.46034	338.57464	337.97065	44.5
2Ab	C$_1$	336.54323 (0)	337.51516	337.55674	338.45316	338.56775	--	44.1
2Ac	C$_s$	336.54319 (1)	337.51482	337.55606	338.45314	338.56784	--	43.8
2Ba	C$_s$	336.51574 (0)	337.49950	337.53963	338.43904	338.55396	337.95040	44.5
2Bb	C$_s$	336.51610 (0)	337.49230	337.53621	338.42979	338.54434	--	44.4
2Bc	C$_s$	336.49502 (1)	337.47515	337.51896	338.41449	338.53120	--	43.6
2Ca	C$_1$	336.54003 (0)	337.51459	337.55875	338.44398	338.55487	337.95896	44.5
2Cb	C$_1$	336.53573 (0)	337.51190	337.55567	338.43998	338.55148	--	44.4
2Da	C$_s$	335.95711 (0)	336.93604	336.97493	337.87329	338.00548	337.41216	36.2
2Db	C$_s$	335.97255 (0)	336.94944	336.98845	337.88666	338.01924	337.42509	36.3
2E	C$_s$	336.50763 (1)	337.49748	337.53609	338.43860	338.55360	337.95273	41.8
2Aa (ts)	C$_1$	336.52477 (1)	337.50170	337.54411	338.43426	338.55120	--	44.0
2Ab (ts)	C$_1$	336.52319 (1)	337.49965	337.54221	338.43268	338.54904	--	43.9

[a] Values in parentheses are the number of imaginary frequencies.

[b] Using MP2/6-31G* geometries.

[c] Using B3LYP/6-31G* geometries.

[d] Zero Point Vibrational Energies at HF/6-31G*, scaled by 0.8929.

Table 3s. Absolute Energies (in -hartrees) of 1-Nitropropene, **3**, its Conformers, Tautomers, Transition Structures and Anions.[a]

Structure		HF/6-31G*	MP2/6-31G*	MP4/6-31G*[b]	B3LYP/6-31G*	B3LYP/6-311+G**	G2MP2	ZPE[c]
3Ac	C_s	320.54667 (0)	321.48899	321.53577	322.41067	322.51157	321.91539	50.6
3Aa	C_s	320.54169 (0)	321.48544	321.53231	322.40669	322.50720	321.91168	50.7
3Ab	C_s	320.54120 (1)	321.48438	321.53118	322.40661	322.50740	--	50.6
3Ba	C_1	320.51239 (0)	321.45489	321.50247	322.38306	322.49115	321.89321	50.7
3Bb	C_1	320.51782 (0)	321.45898	321.50658	322.38732	322.49574	--	50.6
3Ca	C_1	320.54121 (0)	321.48403	321.53107	322.40236	322.50557	321.91069	51.0
3Cb	C_1	320.53758 (0)	321.48152	321.52838	322.39907	322.50233	--	50.9
3Da	C_s	319.95544 (0)	320.90327	320.94546	321.82878	321.95437	321.36340	42.6
3Db	C_s	319.96034 (0)	320.90571	320.94803	321.83257	321.95785	321.36532	42.4
3E	C_1	320.44925 (1)	321.41821	321.45982	322.34729	322.45137	321.85219	47.8
3Ac (ts)	C_1	320.53368 (1)	321.47977	321.52674	322.39853	322.50137	--	50.4
3Aa (ts)	C_1	320.53372 (1)	321.47926	321.52630	322.39839	322.50109	--	50.3

[a] Values in parentheses are the number of imaginary frequencies.

[b] Using MP2/6-31G* geometries.

[c] Using B3LYP/6-31G* geometries.

d Zero point vibrational energies at HF/6-31G*, scaled by 0.8929

Table 4s. Summary of the MP2(full)/6-31G* Bond Critical Point Data for the Hydrogen Bonds of Nitroethylenes **1Aa** and **2Aa** and Their *aci*Nitro Tautomers, **1Ba** and **2Ba**.[a]

Compound	_	$\rho(r)$	$\nabla^2\rho(r)$	$H(r)$
1Aa	0.004	0.263	3.386	-0.008
2Aa	0.081	0.184	2.306	-0.003
1Ba	0.685	2.033	8.916	-3.126
2Ba	0.498	2.077	-4.582	-3.374

[a] $\rho(r)$ is in e.A^{-3}; $\nabla^2\rho(r)$ is in e.A^{-5}; $H(r)$ is in Hartree A^{-3}.

Table 5s. NPA group charges of $R\text{-}C^1(H)=C^2(H)\text{-}NO_2$ at MP2(full)/6-31G*.

Compound	R	Group Charges			
		R	C^1H	C^2H	NO_2
Nitroethylene	H	0.25	-0.15	0.14	-0.25
Cis-1-nitropropene, **3Aa**	CH_3	0.06	0.09	0.14	-0.28
Cis 2-nitrovinylamine, **2Aa**	NH_2	0.07	0.27	0.01	-0.35

Cis-2-nitrovinylalcohol, **1Aa** OH -0.14 0.44 0.0 -0.30

TABLE 1: Total(au) and Relative(kcal/mol)[a] Energies for B_2LiH.

Level[b]	Stucture/State	Energy(au)	NIF[c](cm^{-1})	$<S^2>$	Rel.En.
HF	$C_{\infty v}(^3\Sigma)$	-57.266157	0	2.019	0.0
MP2		-57.397730	0	2.019	0.0
CBS-Q		-57.483987	0(HF)		0.0
G2MP2		-57.483686	0(HF)		0.0
B3LYP	8.335373	-57.675801	0	2.007	0.0
CASSCF(9,12)	^{3}A	-57.325383	0		0.0
mcqdpt		-57.4166036924	ch		
HF	$C_{\infty v}$	-57.217293	0		30.8
MP2	Li-B-B-H	-57.362645	0		21.9
CBS-Q		-57.461227	0(HF)		14.3
G2MP2		-57.463978	0(HF)		12.4
B3LYP	8.199298	-57.643705	0		20.1
CASSCF(9,12)	^{1}A	-57.303652	0		13.5
mcqdpt		-57.384215	ch		20.3
HF	$C_s(^3A'')$	-57.185391	0	2.047	48.9
MP2		-57.334528	0	2.039	39.1
CBS-Q		-57.422794	1(148i)		38.4
G2MP2		-57.424131	0(HF)		37.4
B3LYP		-57.602676	0	2.01	44.6
CASSCF(9,12)		go to C2v			
mcqdpt					
HF	$C_s(^1A')$	-57.164347	0		61.8
MP2		-57.357129	0		25.2
CBS-Q		-57.469408	0(HF)		9.1
G2MP2		-57.473852	0(HF)		6.2
B3LYP	7.712383	-57.628291	0		28.7
CASSCF(9,12)	^{1}A'	-57.308169	0		10.8
mcqdpt		-57.399413	ch		10.8

TABLE 1: (Continued)

Level[b]	Sturcture/State	Energy(au)	NIF[c](cm^{-1})	<S^2>	Rel.En.
HF	C$_{2v}$(^{3}B$_1$)	-57.206580	0	2.163	36.0
MP2		-57.356321	1(94i)	2.158	24.4
CBS-Q		-57.453545	0(HF)		19.1
G2MP2		-57.453464	0(HF)		19.0
B3LYP	10.978532	-57.634043	0	2.018	24.9
CASSCF(9,12)		-57.289568	3824iA?		22.5
mcqdpt		-57.2710772352			-3.8
HF	C$_{2v}$(^{1}A$_1$)	-57.153198	0		70.8
MP2		-57.365801	0(bigFreq)		98.7
CBS-Q	?mo dif	-57.462604	0(HF)		13.4
G2MP2		-57.466735	0(HF)		10.6
B3LYP	7.763006	-57.622618	1(269i)		32.4
CASSCF(9,12)	^{1}A$_1$	-57.304593	1(205i)		12.5
mcqdpt		-57.395424	ch		13.3
HF	C$_{\sigma v}$	-57.135710	0	2.013	79.4
MP2		-57.244041	0	2.012	94.3
CBS-Q		-57.333539	0(HF)		94.4
G2MP2		-57.337903	0(HF)		91.5
B3LYP		-57.539187	0	2.003	83.7
CASSCF(9,12)	6.191775	-57.187277	0		84.5
HF	C$_{\infty v}$($^1\Sigma$)	-57.0878456	0		109.2
MP2	B-Li-B-H	-57.2096895	2(31i,31i)		114.9
CBS-Q		-57.315775	0(HF)		105.6
G2MP2	5.979394	-57.323576	0(HF)		100.5
B3LYP		-57.4920199	0		113.4
CASSCF(9,12)	^{1}A	-57.1867302314			

[a] Zero-point energies were added to the relative energies.
[b] The 6-31G** basis set were used in HF, MP2, and B3LYP calculation.
[c] NIF means number of imaginary frequencies.

TABLE 2: Total(au) and Relative (kcal/mol) energies for B_2LiH_2.

Struct.	Level	Energy	NIM(cm⁻¹)	<s²>	Rel.En.
$C_{2v}(^2A_1)$	HF	-57.858153	0	0.756	0.0
	MP2	-58.027510	2(274,122)	0.756(.751)	0.0
	CBS-Q	-58.116585	0(HF)		0.0
	G2MP2	-58.117822	0(HF)		0.0
	B3LYP	-58.314122	0	0.752	0.0
$C_{2v}(^2B_1)$	HF	-57.865645	0	0.757	-5.1
	MP2	-58.016144	0	0.757(.752)	8.0 (7.1)
	CBS-Q	-58.104402	0(HF)		7.6
	G2MP2	-58.106484	0(HF)		7.1
	B3LYP	-58.307128	0	0.752	4.0
$C_s(^2A'')$	HF	-57.851782	0	0.758	2.7
	MP2	-58.017382	0	0.752(.752)	6.9 (6.3)
	CBS-Q	collp. To 2	0		
	G2MP2	collp. To 2	0		
	B3LYP	-58.304521	0	0.753	5.2
$C_{2v}(^2A_1)$	HF	-57.808193	0	0.879	30.9
	MP2	-57.990290	0	0.875(.839)	24.3(19.9)
	CBS-Q	-58.086848	0(HF)		18.7
	G2MP2	-58.087999	0(HF)		18.7
	B3LYP	-58.277459	0	0.764	22.8
$C_s(^2A')$	HF	-57.810799	0	0.791	28.6
	MP2	-57.986073	0	0.782 (.77)	27.0(25.2)
	CBS-Q	-58.077639	0(HF)		24.4
	G2MP2	-58.079556	0(HF)		24.0
	B3LYP	-58.267535	0	0.755	28.4
$D_{\infty h}()$	HF	-57.742902	1(96)	0.753	70.3
	MP2	-57.742876	0	0.753 (.75)	91.8(92.1)
	CBS-Q	-57.974493	1(101)		89.2
	G2MP2	-57.978637	1(93)		87.3
	B3LYP	-58.191553	0	0.751	74.9
$C_{2v}(^2A_1)$	HF	-57.821127	1(305)	1.196	22.3
	MP2	-57.971247	1(267)	1.127(1.08)	36.0(30.3)
	CBS-Q	-58.076625	1(HF)		25.1
	G2MP2	-58.075720	1(HF)		26.4
	B3LYP	-58.264350	1(286)	0.772	30.6
$C_{2v}(^2A_1)$	HF	-57.781344	1(1011)	1.08	48.5
	MP2	-57.950996	1(1267)	1.001(.952)	50.5(43.0)
	CBS-Q	-58.049676	1(HF)		42.0
	G2MP2	-58.049674	1(HF)		42.8
	B3LYP	-58.237319	1(1106)	0.769	48.8

* "Collp" means both geometries and energies collapsed to another one but not including electronic state.

TABLE 3. Enthalpies (kcal/mol) of the Reaction $B_2Li + H_2 \rightarrow B_2LiH_2$.

Level	E(0K)			ΔH_{rxt}
	$B_2Li\ C_{2v}(^2B_1)$	H_2	$B_2LiH_2 C_{2v}(^2A_1)$	
HF	-56.565112	-1.120774	-57.834862	-93.5
MP2	-56.717697	-1.147150	-58.006621	-89.0
CBS-Q	-56.834633	-1.166085	-58.116585	-72.7
G2MP2	-56.838176	-1.166358	-58.117822	-71.1
B3LYP	-56.986658	-1.168369	-58.292057	-86.0

[a]   Zero-point energies were added to the relative energies. The 6-31G** basis set were used in HF, MP2, and B3LYP calculation.

TABLE 4: Geometrical Parameters of B$_2$LiH$_2$ system.

Structure		HF/6-31G**	MP2/6-31G**	B3LYP/6-31G**
C$_{2v}$(^{2}A$_1$)	r(BB)	1.483	1.496	1.490
	r(BLi)	2.199	2.181	2.151
	r(BH)	1.179	1.180	1.183
	α(BliB)	39.40	40.12	40.52
	α(liBB)	70.30	69.94	69.74
	α(HBLi)	107.1	106.4	106.0
C$_{2v}$(^{2}B$_1$)	r(BB)	1.618	1.603	1.600
	r(BLi)	2.171	2.174	2.147
	r(BH)	1.201	1.197	1.204
	α(HBB)	121.6	121.4	121.7
C$_s$(^{2}A'')	r(BB)	1.515	1.522	1.521
	r(BLi)	2.153	2.134	2.111
	r(B$_1$H$_3$)	1.453	1.374	1.408
	r(B$_2$H$_3$)	1.335	1.352	1.360
	r(B$_2$H$_4$)	1.177	1.178	1.182
	α(B$_1$B$_2$H$_3$)	60.93	56.74	58.18
	α(BHB)	65.64	67.89	66.63
	α(HBH)	119.0	117.6	117.9
	α(HBLi)	120.6	119.5	119.4
C$_2$(^{2}A)	r(BB)	1.574	1.551	1.556
	r(BLi)	2.237	2.231	2.188
	r(BH)	1.348	1.344	1.356
	α(BliB)	41.19	40.69	41.65
	α(LiBB)	69.40	69.66	69.17
	α(BHB)	71.43	70.50	70.01
	α(HBB)	54.28	54.75	55.00
	D(LiBBH)	123.5	124.1	124.5
C(^{2}A)	r(BB)	1.497	1.511	1.515
	r(BLi)	2.146	2.115	2.092
	r(B$_1$H)	1.333	1.375	1.395
	r(B$_2$H)	1.395	1.317	1.329
	α(BBH)	58.74	54.05	54.17
	α(BHB)	66.52	57.70	58.31
	α(HBLi)	123.1	127.6	129.4
	D(HBBH)	105.1	107.3	105.6
	D(BHHB)	94.28	97.61	95.65
D$_{∞h}$	r(BLi)	2.178	2.167	2.175
	r(B$_1$H)	1.199	1.200	1.209
C$_2$(^{2}A$_1$)	r(BB)	1.575	1.526	1.540
	r(BLi)	2.052	2.043	2.020
	r(BH)	1.221	1.213	1.218
	α(HBB)	120.4	119.3	119.1
	α(HBLi)	59.59	60.68	60.93
C$_{2v}$(^{2}A$_1$)	r(BB)	1.579	1.520	1.550
	r(BLi)	2.105	2.104	2.074
	r(B$_1$H)	1.247	1.242	1.254
	r(B$_2$H)	1.301	1.282	1.300
	α(BHB)	76.57	74.04	74.72
	α(HBLi)	129.8	128.2	128.7

**TABLE 5: Total and Relative energies for linear B_2LiH_2 with B-B bond.[a]**

Structure	Level	Energy (au)	NIM(cm^{-1})	$<s^2>$	Relative Energy
$C_{\infty v}$	HF	-58.2611427	2(1569,582)	0.758	0.0
	MP2	-57.9679097	1(816)	0.826	0.0
H-B-B-H-Li	CBS-Q	-58.065640	1(564,HF)		0.0
	G2MP2	-58.070521	2(1506,559)		0.0
	B3LYP	-58.2611427	2(870,644)	0.758	0.0
$C_{\infty v}$	HF	-57.7487143	0	1.756	29.9
	MP2	-57.8724013	1(124)	1.757	53.2
H-B-B-Li-H	CBS-Q	-57.987862	0(HF)		48.8
	G2MP2	-57.975744	0(HF)		59.5
	B3LYP	-58.1843678	2(88,72)	1.771	44.3
$C_{\infty v}$	HF	-57.7158007	0	0.875	48.9
	MP2	-57.8597814	1(10)	0.75	79.4
H-H-B-B-Li	CBS-Q	-57.961369	0(HF)		65.4
	G2MP2	-57.963155	0(HF)		67.4
	B3LYP	-58.1441268	1(21)	0.75	68.6

[a]   Zero-point energies were added to the relative energies. The 6-31G** basis set were used in HF, MP2, and B3LYP calculation. NIF means number of imaginary frequencies.

Relative Energies (RE) and Geometrical Parameters of
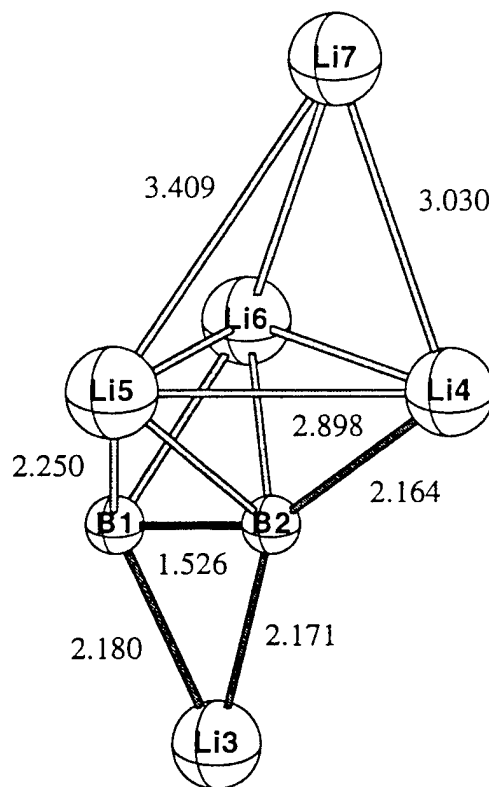B_2Li_5 structures at B3LYP/6-31G(d) level.
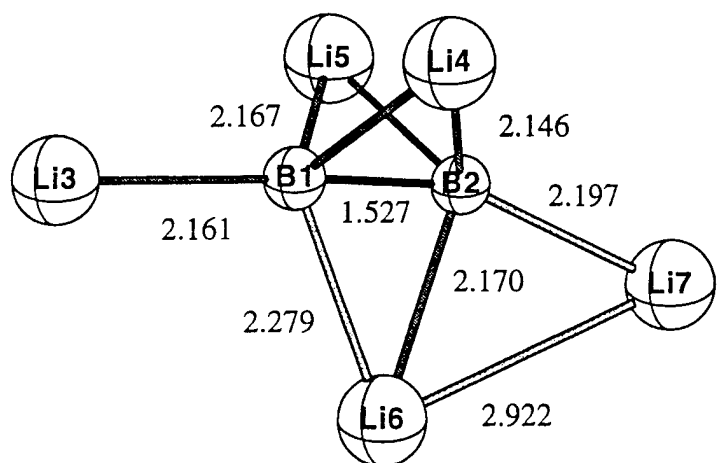
5a, C_S RE=0.0 kcal/mol
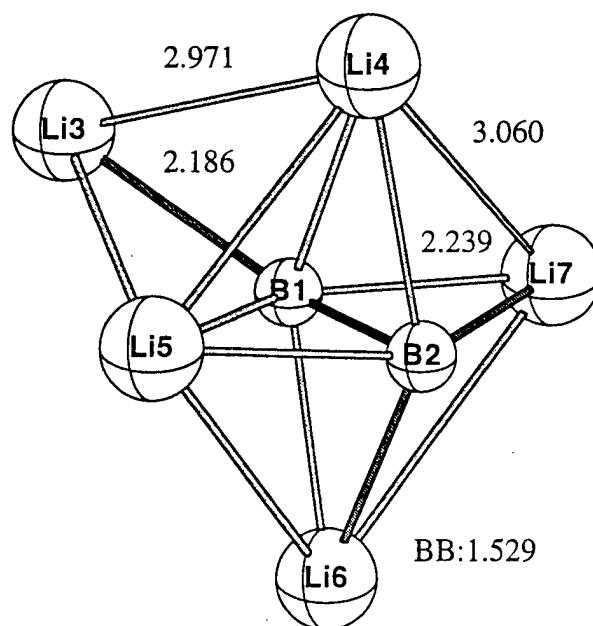
5b, C_S RE=0.4 kcal/mol
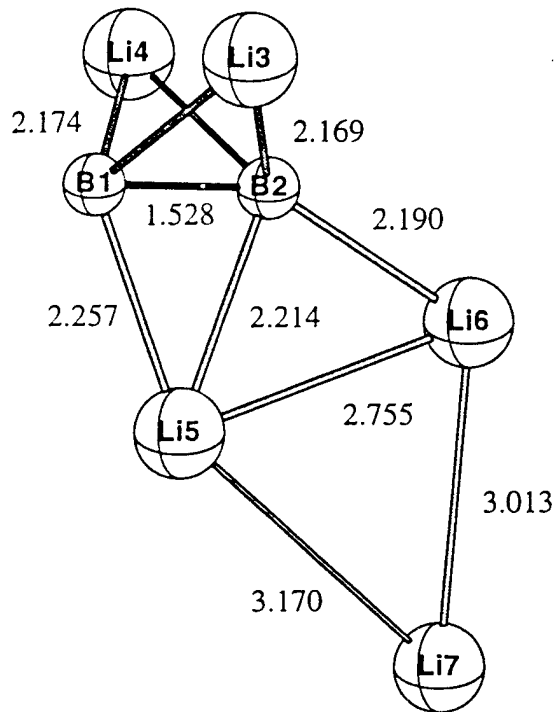
5c, C_S RE=15.7 kcal/mol

5d, C_S RE=16.8 kcal/mol

TABLE 1,2,3.

Total(au) and Relative (kcal/mol) energies for AlLi, $AlLi_2$, $AlLi_3$.

Structure	Level	Energy	NIM	$<s^2>$	Rel. En.
AlLi	HF	-249.290580	0		
	MP2	-249.340864	0		
	B3LYP	-249.891805	0		
$AlLi_2$C2v ($^2A_1$)	HF	-256.746147	1 (713i)	0.878	0
	MP2	-256.803146	0	0.77	0
	B3LYP	-257.418007	0	0.758	0
$AlLi_2$-linear	HF	-256.743504	1 (74i)	0.761	1.6
	MP2	-256.802731	1 (41i)	0.76	0.3
	B3LYP	-257.416803	1 (77i)	0.753	0.8
AlLi3-C2v $^1A_1$	HF	-264.193438	0		0
	MP2	-264.284623	0		0
	B3LYP	-264.958413	0		0
AlLi3-D3h	HF	-264.184476	0		5.6
	MP2	-264.271224	0		8.4
	B3LYP	-264.946824	0		7.3
AlLi3-Cs	nonplanar	goes to C2v			
AlLi3-C3v	nonplanar	goes to D3h			

[a] The 6-31G* basis set were used in HF, MP2, and B3LYP calculation.
[b] NIF means number of imaginary frequencies.
[c] Zero-point energies were added to the relative energies.

TABLE 4: Total(au) and Relative (kcal/mol) energies for AlLi4

Structure	Level	Energy	NIM	$<s^2>$	Rel. En.
C2v ^{2}B1 start from Td	HF MP2 B3LYP	-271.667700 -271.754185 -272.498444	0 0 0	1.923 1.825 0.759	0 0 0
C4v ^{2}A1	HF MP2 B3LYP	-271.654339 -271.755915 -272.489851	2(75i,75i) 0 0	1.283 0.773 0.76	8.3 -1.1 5.4
D4h ^{2}A2u	HF MP2 B3LYP	-271.645272 -271.755606 -272.485652	1(88i) 1(128i) 1(114i)	0.8 0.796 0.755	14.1 -0.9 8.0
C3v	HF MP2 B3LYP	-271.651390 mp2 run DM? -272.480882	2(179i,179i) 2(158i,158i)		
Td	HF MP2 B3LYP	-271.629971 -271.725590 -271.629971	5 3 5		
D2d	go to D4h				
Cs	go to C2v				

[a] The 6-31G** basis set were used in HF, MP2, and B3LYP calculation.
[b] NIF means number of imaginary frequencies.
[c] Zero-point energies were added to the relative energies.

TABLE 5: Total(au) and Relative (kcal/mol) energies for AlLi$_5$.

Structure	Level[a]	Energy at 0 K	NIM[b]	Rel.En.[c]
C4v ${}^1A_1$	HF MP2 B3LYP	-279.115106 -279.264268 -280.046746	0 0 0	0 0 0
D3h	HF MP2 B3LYP	-279.096987 -279.243662 -280.026633	2 (58i,58i) 2 (77i,77i) 2 (68i,68)	11.4 12.9 12.6
C5v	HF MP2 B3LYP	-279.089509 -279.235411 -280.022381	2 (94i,94i) 2 (105i,105i) 2 (94i,94i)	16.1 18.1 15.3
D5h	HF MP2 B3LYP	-279.066196 -279.217804 -280.001163	3 3 3	30.7 29.2 28.6
C3v		goes to D3h		
C2v		goes to C4v		
Cs		goes to C4v		

[a] The 6-31G** basis set were used in HF, MP2, and B3LYP calculation.
[b] NIF means number of imaginary frequencies.
[c] Zero-point energies were added to the relative energies.

TABLE 6: Total(au) and Relative (kcal/mol) energies for AlLi$_6$

Structure	Level	Energy(0K)	NIM	$<s^2>$	Rel. En.
C$_2$ (^{2}A)	HF MP2 B3LYP	-286.575630 -286.721397 -287.570868	0 0 0	2.082 1.047 0.773	0 0 0
C$_{5v}$	HF MP2 B3LYP	-286.559485 -286.718066 -287.568491	0 0 0	1.06 0.988 0.762	10.1 2.1 1.5
C$_{4v}$ (^{2}A1)	HF MP2 B3LYP	-286.569531 -286.721390 -287.567735	2 (59i,59i) 0 2 (75i,75i) f->2	1.939 1.047 0.763	3.8 0 1.9
O$_h$	HF MP2 B3LYP	-286.566558 -286.721391 -287.567457	6 0 3 (56i,56i,56i)	1.09 1.047 0.762	5.7 0 2.1
D$_{3h}$	HF MP2 B3LYP	-286.567293 -286.712980 -287.563971	2 (70i,15i) 1 (54i) 1 (47i)	1.49 1.102 0.77	5.2 5.3 4.3
D$_{6h}$	HF MP2 B3LYP	-286.503668 -286.669825 -287.517442	5 3 (133i,94i,94i) 3(131i,116i,116i)	0.78 0.775 0.754	45.1 32.4 33.5
D$_{3d}$		goes to Oh			
D$_{4h}$ short		goes to Oh			
D$_{4h}$-long		goes to Oh			

[a] The 6-31G** basis set were used in HF, MP2, and B3LYP calculation.
[b] NIF means number of imaginary frequencies.
[c] Zero-point energies were added to the relative energies.

Ground State Data

CuLi

	RHF	MCSCF	RHF-MP2	MCSCF-MP2	Exper.
Bond Length (A)	2.4796	2.4243	2.3409	2.202	2.26
Energy of State (H)	-.503961	-.657217	-.828332	-1.055627	
Harmonic Freq. (cm^{-1})	322.98	300.20	384.36	465.00	465.9
Dis-association Energy (cm^{-1})				15574	15727
Anharmonic Freq. (cm^{-1})				3.471	

Brock JCP 106(1997) 6268-6278

CuNa

	RHF	MCSCF	RHF-MP2	MCSCF-MP2	Exper.
Bond Length (A)	2.7289	2.6945	2.6301	2.5540	
Energy of State (H)	-.482796	-.634784	-.803162	-1.024433	
Harmonic Freq. (cm^{-1})	182.92	182.18	212.06	232.03	
Dis-association Energy (cm^{-1})				17757	
Anharmonic Freq. (cm^{-1})				.758	

CuK

	RHF	MCSCF	RHF-MP2	MCSCF-MP2	Exper.
Bond Length (A)	3.1913	3.1478	3.0622	2.9648	
Energy of State (H)	-.445799	-.597521	-.765774	-.988121	
Harmonic Freq. (cm^{-1})	120.38	120.45	139.94	149.90	
Dis-association Energy (cm^{-1})				20972	
Anharmonic Freq. (cm^{-1})				.268	

AgLi

	RHF	MCSCF	RHF-MP2	MCSCF-MP2	Exper.
Bond Length (A)	2.5653	2.5325	2.4790	2.3468	2.41[2]
Energy of State (H)	-.619967	-.678619	-.756477	-.942653	
Harmonic Freq. (cm^{-1})	316.01	327.61	351.35	450.57	389.0
Dis-association Energy (cm^{-1})				13969	16648[1] 15244[2] 14599[3]
Anharmonic Freq. (cm^{-1})				3.63	2.27[1]

1 Pilgrim CPL 232(1995) 335-340
2 Brock JCP 106(1997) 6268-6278
3 Thermochemical value cited by both papers

AgNa

	RHF	MCSCF	RHF-MP2	MCSCF-MP2	Exper.
Bond Length (A)	2.8196	2.7968	2.7561	2.6480	
Energy of State (H)	-.598694	-.656717	-.732693	-.915870	
Harmonic Freq. (cm^{-1})	171.29	177.81	187.06	233.9	210
Dis-association Energy (cm^{-1})				11781	12827
Anharmonic Freq. (cm^{-1})				1.16	

Strangassinger CPL 266(1997) 189-194

AgK

	RHF	MCSCF	RHF-MP2	MCSCF-MP2	Exper.
Bond Length (A)	3.2970	3.2657	3.2090	3.1036	2.40
Energy of State (H)	-.611343	-.619729	-.695659	-.877145	
Harmonic Freq. (cm^{-1})	105.96	109.24	116.51	124.8	
Dis-association Energy (cm^{-1})				13908	
Anharmonic Freq. (cm^{-1})				.280	

Yeh CPL 206(1993) 509-514

AuLi

	RHF	MCSCF	RHF-MP2	MCSCF-MP2	Exper.
Bond Length (A)	2.3952	2.3518	2.3618	2.3717	
Energy of State (H)	-.396754	-.45277	-.523645	-.594127	
Harmonic Freq. (cm^{-1})	409.19	442.60	437.15	459.4	
Dis-association Energy (cm^{-1})				20985	
Anharmonic Freq. (cm^{-1})				2.51	

AuNa

	RHF	MCSCF	RHF-MP2	MCSCF-MP2	Exper.
Bond Length (A)	2.6937	2.6671	2.6740	2.6819	
Energy of State (H)	-.370702	-.422505	-.494908	-.564503	
Harmonic Freq. (cm^{-1})	208.69	219.91	220.55	240.55	
Dis-association Energy (cm^{-1})				15034	21268
Anharmonic Freq. (cm^{-1})				.96	

AuK

	RHF	MCSCF	RHF-MP2	MCSCF-MP2	Exper.
Bond Length (A)	3.1265	3.0761	3.0933	3.0947	
Energy of State (H)	-.335015	-.388965	-.459889	-.530213	
Harmonic Freq. (cm^{-1})	129.81	136.57	138.31	134.33	
Dis-association Energy (cm^{-1})				18308	22168
Anharmonic Freq. (cm^{-1})				.25	

HF/6-31G*
B3LYP /6-31G*
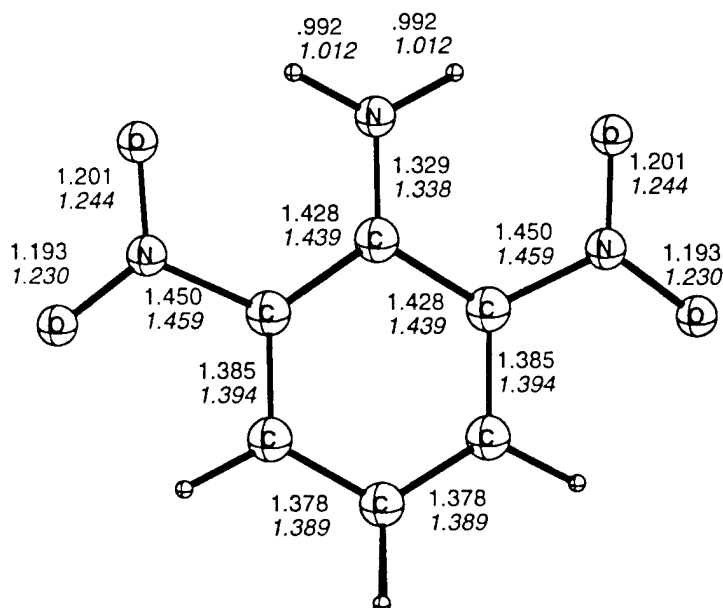Experimental
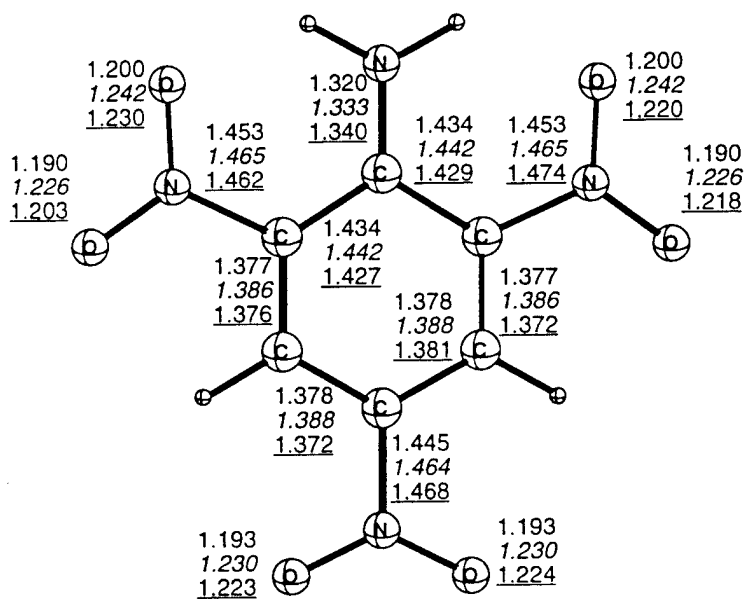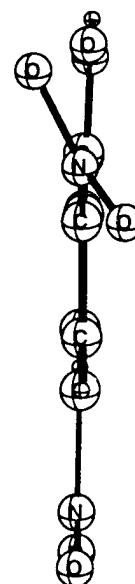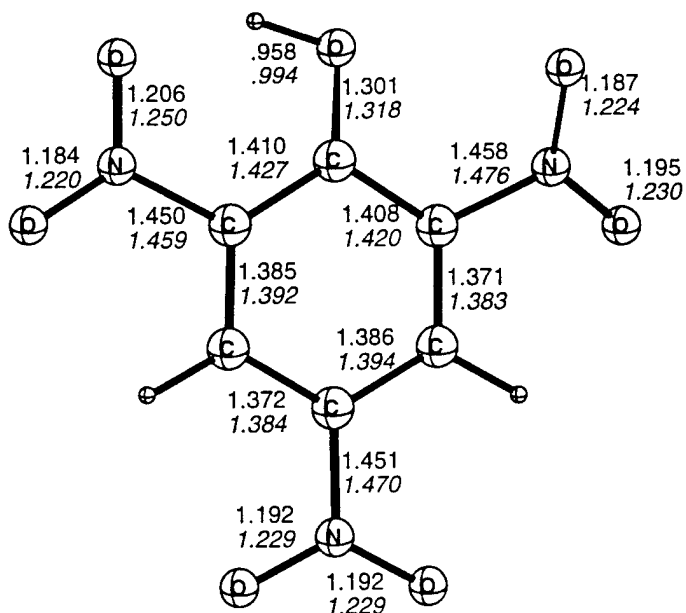
NO2 torsion: 29.7
36.4
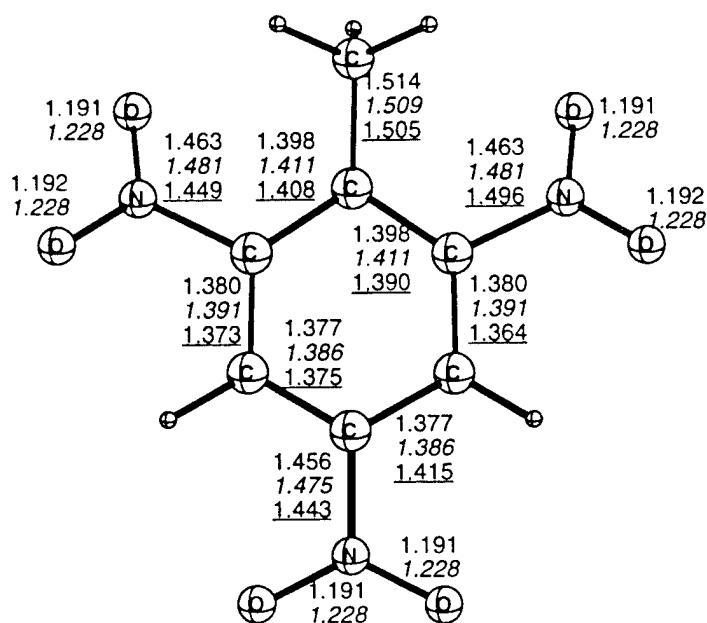
NO2 torsion   0
0
22.5

NO2 torsion: 33.8
35.8
43 & 51
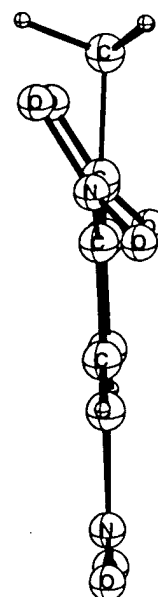
HF / 6-31G*
*B3LYP /6-31G**
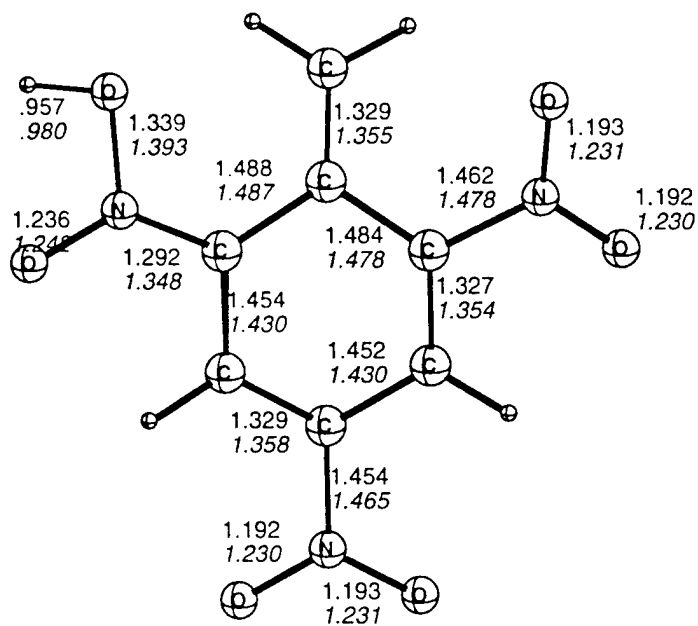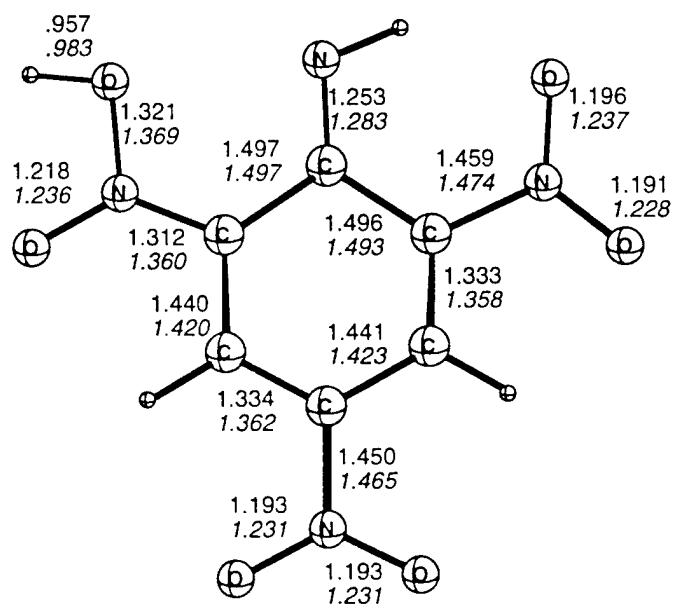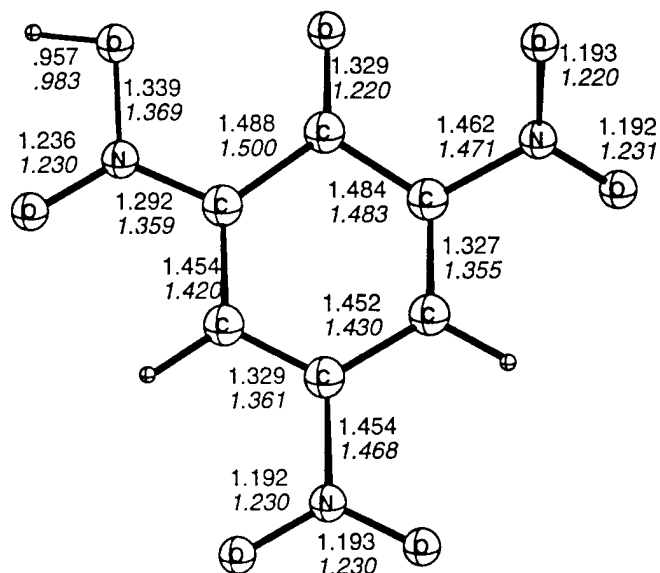
HF / 6-31G*
B3LYP /6-31G*
<u>Experimental</u>

NO2 torsion : 36.5
27.4

NO2 torsion: 0
0

NO2 torsion: 22.6
36.0

HF / 6-31G*
*B3LYP /6-31G**
Experimental
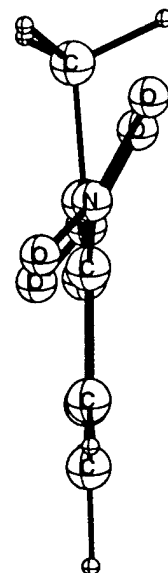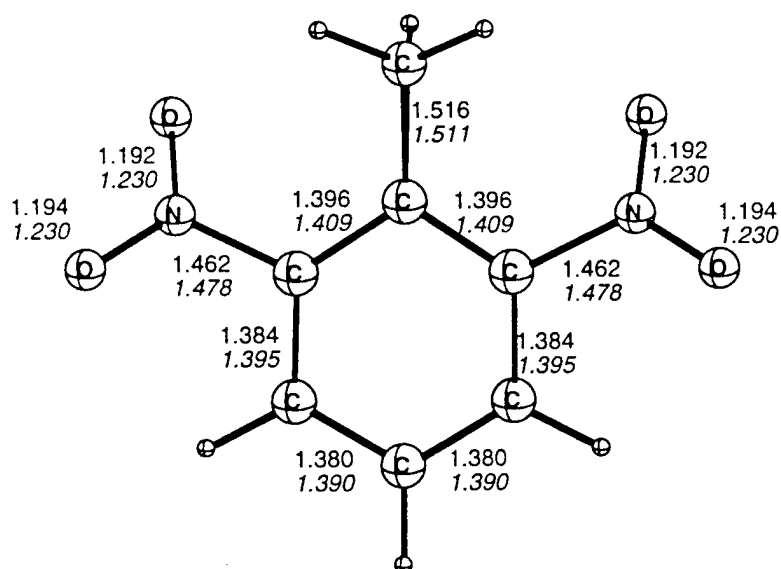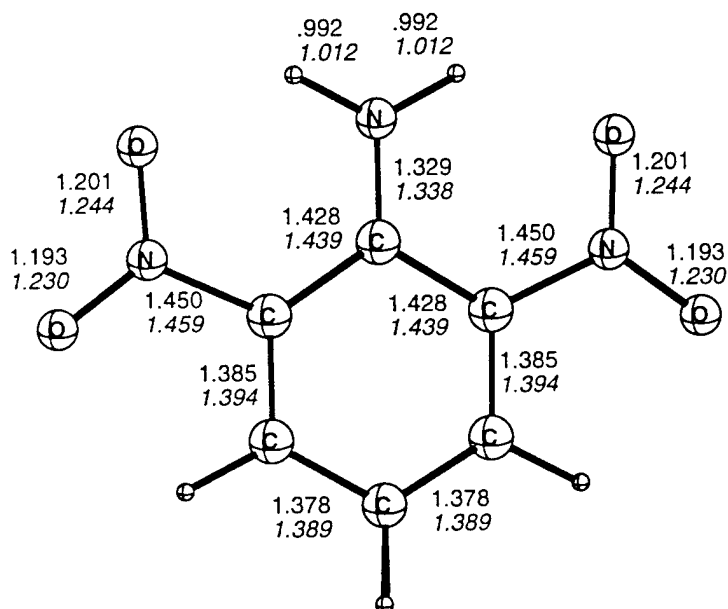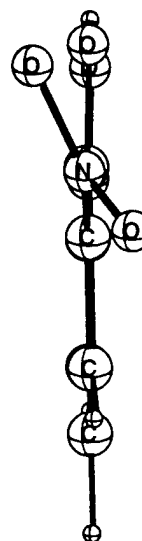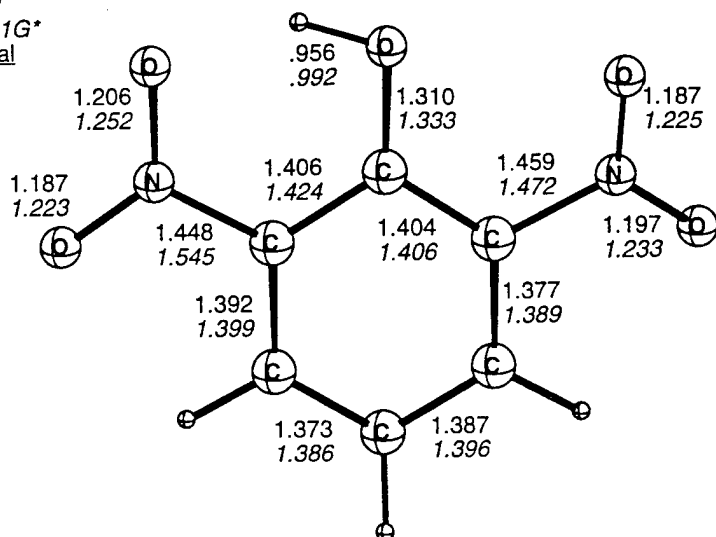
NO2 torsion : 36.5
27.4
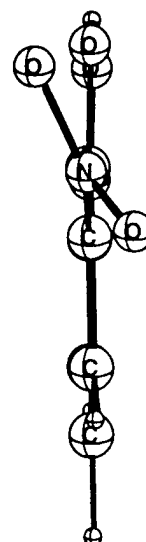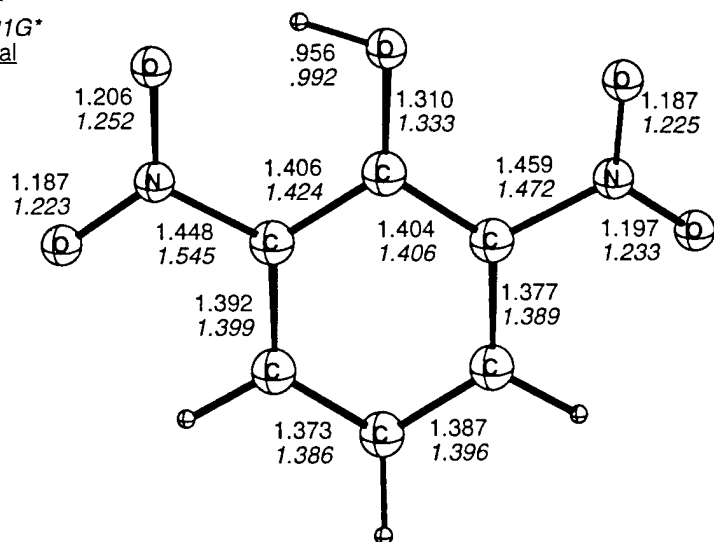
NO2 torsion: 0
0

NO2 torsion: 22.6
36.0
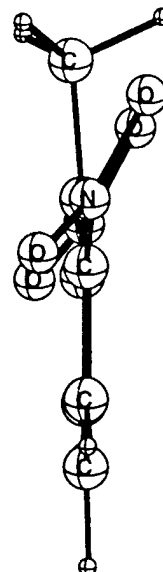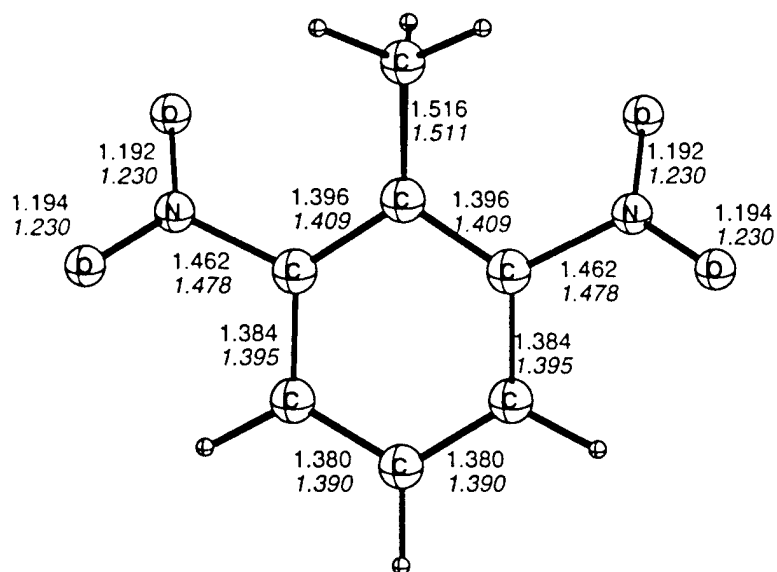
Compound	HF/3-21G	HG/6-31G*	B3LYP/6-31G*	B3LYP/6-311+G**	ZPVE
Benzene	-229.419445	-230.703137	-232.248660	-232.311134	67.56
Phenol	-303.860103	-305.558064	-307.464871	-307.558431	70.47
Toluene	-268.240213	-269.740165	-271.566650	-271.638692	85.91
Aniline	—	-285.730822	-287.601761	-287.687507	78.8
Nitrobenzene	-431.712161	-434.175232	-436.750585	-436.874445	70.11
Dinitro systems					
2,6-dinitrophenol	—	-712.488154	-716.461807	-716.675611	75.69
2,6-dinitroaniline	-688.737378	-692.670989	-696.610471	-696.816892	84.0
2,6-dintrotoluene	-672.807673	-676.664741	-680.553589	-680.749350	91.26
aci - tautomers of					
2,6-dinitrophenol	-708.397604	-712.4408432	-716.419780	-716.634637	75.09
2,6-dinitroaniline	-688.671000	-692.597487	-696.542554	-696.750666	83.70
2,6-dintrotoluene	-672.773438	-676.598539	-680.496703	-680.699932	90.94
Transition state for 1,5 hydride shift for					
2,6-dinitrophenol	—	-712.431942	-716.410903	-716.627394	74.33
2,6-dinitroaniline	-688.662713	-692.590788	-696.535192	-696.745378	82.99
2,6-dintrotoluene		-626.554206			87.58

Compound	HF/3-21G	HG/6-31G*	B3LYP/6-31G*	B3LYP/6-311+G**	ZPVE
Trinitro systems					
2,4,6-trinitrophenol	-910.716612	-915.949824	-920.954682	-921.229608	77.8
2,4,6-trinitroaniline	-891.023435	-896.136360	-901.105988	-901.979101	86.3
2,4,6,-trinitrotoluene	-875.088179	-880.125089	-885.045486	-885.302613	93.36
aci - tautomers of					
2,4,6-trinitrophenol	-910.678650	-915.903542	-920.914129	-921.189888	77.3
2,4,6-trinitroaniline	-890.953103	-896.060952	-901.037986	-901.306769	85.9
2,4,6,-trinitrotoluene	-875.054824	-880.061617	-884.992888	-885.256853	93.13